DEVELOPMENT OF A TIME DOMAIN (TD) NMR APPROACH BY USING THE RELATION BETWEEN MOLECULAR MOBILITY AND CRYSTALLIZATION BEHAVIOR TO QUANTIFY CAKING IN FOOD POWDERS

A THESIS SUBMITTED TO
THE GRADUATE SCHOOL OF NATURAL AND APPLIED SCIENCES
OF
MIDDLE EAST TECHNICAL UNIVERSITY

BY

SELEN GÜNER

IN PARTIAL FULFILLMENT OF THE REQUIREMENTS
FOR
THE DEGREE OF DOCTOR OF PHILOSOPHY
IN
FOOD ENGINEERING

DECEMBER 2022

Approval of the thesis:

DEVELOPMENT OF A TIME DOMAIN (TD) NMR APPROACH BY USING THE RELATION BETWEEN MOLECULAR MOBILITY AND CRYSTALLIZATION BEHAVIOR TO QUANTIFY CAKING IN FOOD POWDERS

submitted by **SELEN GÜNER** in partial fulfillment of the requirements for the degree of **Doctor of Philosophy** i**n Food Engineering, Middle East Technical University** by,

Prof. Dr. Halil Kalıpçılar
Dean, Graduate School of **Natural and Applied Sciences** _____

Prof. Dr. Hami Alpas
Head of the Department, **Food Engineering** _____

Assoc. Prof. Dr. Mecit Halil Öztop
Supervisor, **Food Engineering, METU** _____

Prof. Dr. Servet Gülüm Şümnü
Co-Supervisor, **Food Engineering, METU** _____

Examining Committee Members:

Prof. Dr. Serpil Şahin
Food Engineering, METU _____

Assoc. Prof. Dr. Mecit Halil Öztop
Food Engineering, METU _____

Prof. Dr. Behiç Mert
Food Engineering, METU _____

Assoc. Prof. Dr. Emin Burçin Özvural
Food Engineering, Çankırı Karatekin University _____

Assist. Prof. Dr. Elif Turabi Yolaçaner
Food Engineering, Hacettepe University _____

Date: 19.12.2022

I hereby declare that all information in this document has been obtained and presented in accordance with academic rules and ethical conduct. I also declare that, as required by these rules and conduct, I have fully cited and referenced all material and results that are not original to this work.

Name Last name : Selen Güner

Signature :

ABSTRACT

DEVELOPMENT OF A TIME DOMAIN (TD) NMR APPROACH BY USING THE RELATION BETWEEN MOLECULAR MOBILITY AND CRYSTALLIZATION BEHAVIOR TO QUANTIFY CAKING IN FOOD POWDERS

Güner, Selen
Doctor of Philosophy, Food Engineering
Supervisor : Assoc. Prof. Dr. Mecit Halil Öztop
Co-Supervisor: Prof. Dr. Servet Gülüm Şümnü

December 2022, 174 pages

Caking is one of the most important factors affecting fluidity and quality of powdered food samples by distorting the stability and functionality. Time-Domain Nuclear Magnetic Resonance (TD-NMR) techniques are frequently used in the polymer, drug and food industries since they require no initial sample preparation before the measurement and provide rapid results. The main goal of the study is to quantify crystallinity by using TD-NMR, Solid Echo (SE) and Magic Sandwich Echo (MSE) sequences. The method was first applied for the control and freeze dried sugar samples (glucose, sucrose and lactose) in powder form, and high correlation (>0.96) was found with the X-ray diffraction (XRD) and MSE crystallinity. In the second part, crystal growth in highly saturated sugar solutions were studied for glucose, fructose, allulose, lactose and sucrose equilibrated to 28°C from 50°C. Fitted kinetic model suggested that the crystallization rate was slowest for glucose and fructose, following allulose, lactose, and sucrose, respectively. In the last part, confirmed quantification method was applied to cheese and milk powders stored at different relative humidities (40, 50, 60, and 70%) and their crystallinities were related to caking tendency and fat content of the powders. Surface and total fat

content, moisture content, water activity analyses were also conducted complementary to NMR analyses. As a consequence of the study, it was found that molecular mobility could be modelled to calculate crystallinity by TD-NMR techniques, which gives information on physical changes such as crystal growth and caking tendency. The method could be a user friendly alternative to XRD.

Keywords: NMR, Caking, Crystallinity, Fat Content, Moisture Adsorption

ÖZ

TOZ GIDALARDA TOPAKLANMA MİKTARINI BELİRLEMEK İÇİN MOLEKÜLER MOBİLİTE VE KRİSTALİZASYON DAVRANIŞI ARASINDAKİ İLİŞKİDEN FAYDALANILARAK ZAMAN ALANDA (TD) NMR YAKLAŞIMININ GELİŞTİRİLMESİ

Güner, Selen
Doktora, Gıda Mühendisliği
Tez Yöneticisi: Doç. Dr. Mecit Halil Öztop
Ortak Tez Yöneticisi: Prof. Dr. Servet Gülüm Şümnü

Aralık 2022, 174 sayfa

Topaklanma, toz gıda numunelerinin stabilitesini ve fonksiyonelliğini bozarak akışkanlığını ve kalitesini etkileyen en önemli faktörlerden biridir. Zamansal Alanda Nükleer Manyetik Rezonans (TD-NMR) teknikleri, ölçüm öncesi herhangi bir ön numune hazırlığı gerektirmediği ve hızlı sonuç verdiği için polimer, ilaç ve gıda endüstrilerinde sıklıkla kullanılmaktadır. Çalışmanın asıl amacı, TD-NMR, Solid Eko (SE) ve Sihirli Sandviç Eko (MSE) sekanslarını kullanarak numunelerin kristalinitesini ölçmektir. Yöntem ilk olarak kontrol ve dondurularak kurutulmuş toz şeker numunelerine (glikoz, sukroz ve laktoz) uygulanmış ve X-ışını kırınımı (XRD) ve MSE kristalliği arasında yüksek korelasyon (>0,96) bulunmuştur. İkinci bölümde ise yöntem, kristal oranı kinetik olarak değişen örneklerde uygulanmıştır. Bu amaçla, 50°C'den alınarak 28°C'de dengeye bırakılan yüksek oranda doymuş şeker çözeltilerindeki (glikoz, fruktoz, alüloz, laktoz ve sukroz) sürekli kristal büyümesi takip edilmiştir. Uygulanan kinetik model, kristalleşme hızının, sırasıyla alüloz, laktoz, sükrozdan sonra fruktoz ve glikoz ikilisi için en yavaş olduğunu göstermiştir. Son bölümde, daha önceki çalışmalarda doğrulanan yöntem, farklı bağıl nemlerde

(%40, 50, 60 ve 70) depolanan peynir ve süt tozlarına uygulanmış ve numunelerin kristallikleri, topaklanma eğilimleri ve tozların yağ içerikleri ile ilişkilendirilmiştir. NMR analizlerini tamamlayıcı olarak yüzey ve toplam yağ içeriği, nem içeriği, su aktivitesi analizleri de yapılmıştır. Çalışma sonucunda, kristal büyümesi ve topaklanma eğilimi gibi fiziksel değişimler hakkında bilgi veren TD-NMR teknikleri ile moleküler mobilitenin kristalliği hesaplamak için modellenebileceği bulunmuştur. Yöntemin, XRD'ye kullanıcı dostu bir alternatif olarak kullanılabileceği öne sürülmüştür.

Anahtar Kelimeler: NMR, Topaklanma, Kristalinite, Yağ Miktarı, Nem Çekme

Dedicated to good people who has been a light to someone who is lost or confused at some point in their life

ACKNOWLEDGMENTS

The author wishes to express her deepest gratitude to his supervisor Assoc. Prof. Dr. Mecit Halil Öztop and co-supervisor Prof. Dr. Gülüm Şümnü for their guidance, advice, criticism, encouragements and insight throughout the research.

The author would also like to thank Dr. Leonid Grunin for his valuable suggestions, comments, and generous time. The support of Prof. Dr. Serpil Şahin, Prof. Dr. Behiç Mert, Doç. Dr. Emin Burçin Özvural, and Assist. Prof. Dr. Elif Turabi Yolaçaner are gratefully acknowledged.

I would like to thank Fulbright for giving me the opportunity to have a life time experience in the US, which also had valuable contribution to my thesis. Thanks to Assist. Prof. Dr. Nathalie Lavoine for being so active in solving problems and her involvement in our research. Prof. Dr. Lucian Lucia, thank you very much for always being positive and supportive. Prof. Dr. Jim Martin and Angela Shipman, your enthusiasm in science and your encouragement during our work always gave me strength, thank you so much for helping me for no reason. I learnt so much from Dr. Hanna Gracz and Dr. David Morgan, thank you for being so generous to teach me spectroscopy, which was a really hard job. Thanks to Dr. Josh Damron, my visit to Oak Ridge National Laboratories was fruitful and informative on TD-NMR and solid state NMR spectroscopy, contributing to my thesis.

Many thanks to Mukaddes Ünver, who managed all the paperwork of the thesis process. I also thank Hani Alam for his technical advice and Mehmet Çiftçi for helping me in whatever problem I have in the lab. Oztoplab members Eren Cantürk, Ayşe Sultan Kurt, Tayfun Şener, Esranur Kaya, Sena Kuzu, Umur Tuna, Zikrullah Bölükkaya, Gözde Özeşme Taylan, Eren Başdemir, and Şirvan Sultan Uğuz you have been my smiling face in the lab, thank you for your help and encouragement through this process. Thank you Eda Yıldız, for our interchanged stresses and mutual empathy.

I would also like express my deepest gratitude to my family; Esmanur İlhan, Özge Güven, Seren Oğuz, Kübra Ertan, Kubilay Uzuner, Esra Ceylan, Şinasi Güner, Zeynep Güner, Taner Güner and Halil İbrahim Şan for their continuous support, rehabilitation and patience through my thesis as well as my personal life. You were my hand when I could not reach, you were my medication when I had pain. Thank you for being there for me 7/24.

This work is partially funded by Scientific and Technological Research Council of Turkey under grant #217O089.

TABLE OF CONTENTS

ABSTRACT v

ÖZ vii

ACKNOWLEDGMENTS x

TABLE OF CONTENTS xii

LIST OF TABLES xv

LIST OF FIGURES xvi

CHAPTERS

1 INTRODUCTION 1

1.1 Mechanisms of Caking 2

1.1.1 Moisture Adsorption and Sorption Isotherm 4

1.1.2 Liquid bridge formation 9

1.1.3 Solid bridge formation 11

1.2 Primary Causes of Caking 12

1.2.1 Consolidation 12

1.2.2 Moisture 12

1.2.3 Temperature 13

1.2.4 Composition 15

1.3 Caking Studies in the Literature 18

1.4 Crystallization for Food Systems with High Sugar Content 21

1.5 Crystallinity Measurement in Food Systems 25

1.6 Time Domain NMR for Crystallinity Measurement in Food Systems 29

1.7 Objectives of the Study 36

2 MATERIALS AND METHODS 37
2.1 Applicability of the Method by the Crystallinity Analysis of Sugars 37
2.1.1 Sample Preparation 37
2.1.2 X-ray Diffraction (XRD) 37
2.1.3 Scanning Electron Microscopy (SEM) 38
2.1.4 TD-NMR Measurements 38
2.1.5 Statistical Analysis 39
2.2 Use of Crystallinity Measurement Approach on Model Food Systems 40
2.2.1 Sample Preparation 40
2.2.2 Determination of Crystal Mass Fraction (CMF) 41
2.2.3 X-ray Diffraction Analysis 42
2.2.4 TD-NMR Measurements 42
2.2.5 Statistical Analysis 42
2.2.6 Concentration-dependent Hydration Behavior of Sucrose studied by High Field NMR Spectroscopy 43
2.3 Use of Crystallinity Measurement Approach on Real Food Systems 44
2.3.1 Sample Preparation 44
2.3.2 Determination of Water Activity 44
2.3.3 Moisture Content Analysis 44
2.3.4 Surface and Total Fat Content Analyses 45
2.3.5 TD-NMR Measurements 45
2.3.6 Statistical Analysis 47
3 RESULTS AND DISCUSSION 49
3.1 Applicability of the Method by the Crystallinity Analysis of Sugars 51

3.2 Use of SE and MSE Sequences to Monitor Crystallization Kinetics of Model Systems 55
3.2.1 Comparison of Crystallization Rate of Different Sugar Types 55
3.2.2 Use of Low Field TD-NMR for Quantification of Crystallization in Samples with High Solid Content 63
3.2.3 Concentration-dependent Hydration Behavior of Sucrose studied by High Field NMR Spectroscopy 66
3.3 Use of Crystallinity Measurement Approach on Model Food Systems 72
3.3.1 Effect of Storage Condition on Surface Fat Content 73
3.3.2 Effect of Storage Condition on Moisture Content 75
3.3.3 Effect of Storage Condition on the Crystallinity 77
4 CONCLUSION 83
5 REFERENCES 87
6 APPENDICES 107
CURRICULUM VITAE (Only For Doctoral Thesis) 173

LIST OF TABLES

TABLES

Table 2.1 Theoretically calculated crystal mass fractions (CMFs) for sugar samples at process temperatures (50 °C and 28 °C). 41

Table 3.1. SE and MSE crystallinity values* of different sugars exposed to Freeze drying 54

Table 3.2. Model $SA = A1 - A2 * e\text{^}(-kt)$ parameters found for different sugar types and their significance denoted by capital letters for Tukey comparison test for 3 replicates conducted at 95% confidence interval. 56

Table 3.3. Calculated parameters to correlate with the constants found by the application of SE sequence. ICC denotes the initial crystal content while FCC is the final crystal content. 63

Table 3.4. Surface and total fat content results of powder food samples with different fat contents stored at different relative humidity*. 75

Table 3.5. Results of MSE crystallinity, water activity and moisture content of samples with different fat contents stored at different relative humidity (RH) environments*. 82

LIST OF FIGURES

FIGURES

Figure 1.1. Orientation of water in pendular (a), funicular (b) and capillary (c) states. Powder particles were represented by simple spheres. 5
Figure 1.2. Some examples to fully understand the adsorption behavior: the meniscus could be concave (a) or convex (b), geometry of the bridging could change (c, d, e) (Urso et al., 1999), and the smoothness of the particle surface (f). 6
Figure 1.3. Generalized forms of the typical adsorption isotherms..... 8
Figure 1.4. Typical sorption isotherm for a food product. 10
Figure 1.5. A representative DSC heating thermogram for a sucrose sample, showing glass transition step change around 150 °C. 14
Figure 1.6. Jenike cell design (M. Mathlouthi & Rogé, 2003). 19
Figure 1.7. Representative crystallization zones with changing concentration versus temperature. 22
Figure 1.8. Bragg diffraction (Britannica, n.d.). 27
Figure 1.9. Representative XRD patterns for crystalline (powder glucose, on the left) and amorphous behavior (commercial cooked sugar, on the right). 29
Figure 1.10. A representative FID decay collected after *a single* 90° pulse, *denot*ing fast decaying solid phase and slow decaying liquid phase. 32
Figure 1.11. Comparison of the overall signal taken from the application of FID, SE and MSE sequences (on the left) and their Fourier transform (on the right). 34
Figure 1.12. Representative curves for models used to describe signals. 35
Figure 2.1. Comparison of FID (a), SE (b) and MSE (c) sequences pulse diagram, signals acquired from application of those sequences (d) and the signals obtained from their Fourier transformation (e). 39
Figure 3.1. Calibration curves prepared for SE (left) and MSE (right) sequences.. 52
Figure 3.2. XRD spectra for sucrose control (left) and freeze-dried sucrose (right). 52

Figure 3.3. SEM images of glucose control (A), sucrose control (B), lactose control (C), freeze dried glucose (D), freeze dried sucrose (E), and spray dried sucrose (F). 53
Figure 3.4. XRD spectra for glucose control (1), freeze dried glucose (2), sucrose control (3), freeze dried sucrose (4), spray dried sucrose (5), lactose control (6) and freeze-dried lactose (7)..... 53
Figure 3.5. Solid amplitude measured by SE sequence as the samples crystallize when the temperature decreases from 50°C to 28°C and an example of one set data together with fitting results for sucrose (A), fructose (B), glucose (C), lactose (D) and allulose (E). 58
Figure 3.6. Optical microscope images of the original powder form of the sugars captured at x10 magnification; sucrose (A), fructose (B), glucose (C), lactose (D) and allulose (E). 60
Figure 3.7. XRD graph for the initial powder form of sucrose (A), lactose (B), glucose (C), fructose (D) and allulose (E). 65
Figure 3.8. Assignment of the hydrogen atoms on fructose ring (denoted by F) and glucose ring (denoted by G) of the sucrose structure. Large peak around 2.3-2.4 ppm belongs to water protons. 68
Figure 3.9. Change in the left shoulder of the water peak on the spectra of sucrose solutions overlapped by referencing the sugar peaks for samples at different concentrations at 28 °C. The area under the shoulder increases with concentration, shown by the direction of the arrow..... 69
Figure 3.10. A representative NMR Spectra for sucrose solution at 28 °C (—) and 5 °C (—). 70
Figure 3.11. Change in the shift of water protons peak by decreased concentration Figure at the bottom zooms at the relevant area where the trend was distorted, shown by a circle. 72
Figure 3.13. Moisture content of the samples at the studied relative humidity conditions. 77

Figure 3.14. Representative MSE signal for whole fat cheese powder at 40% relative humidity. The signal in region 1 reprents the solid signal while region 2 and 3 belonged to amorphous and long component (water), respectively. 78

CHAPTER 1

INTRODUCTION

Foods are commonly commercialized in powder form since this concise form is more conformable for transportation, storage, and handling. Caking is one of the challenges in powder handling, which could be induced by intrinsic factors like cohesion, elasticity, yield stress, amorphous content, hygroscopicity, particle size, amount of molten fat, amount of low molecular weight compounds (simple sugars, protein hydrolysates, amino acids…etc.) or the extrinsic factors such as temperature, humidity, stress, strain rate and vibration (Zafar et al., 2017). One of the problems encountered due to caking is poor product appearance, which decreases sensorial attractiveness and quality as it becomes less porous (Downton et al., 1982). On the other hand, the problem of caking ceases to be only an innocent quality parameter under industrial conditions where the powders should be handled in large quantities. Severe caking causes serious flow problems that reduce production rate and efficiency as they could be stuck in hoppers and silos prior to processing (J. J. Fitzpatrick, 2007; Michalski et al., 1997). Although caking is desirable in pelletization, dying, granulation, tablets, and similar processes, unintended caking could be very challenging to solve if develops after packaging and reaching to customer.

Understanding the stickiness phenomena is the first step to understand caking. The American Society for Testing and Materials (ASTM) designate a substance “sticky” (tacky) in case that it requires a noticeable strength to be apart after immediate contact (Gay & Leibler, 1999). Stickiness makes a free-flowing powder behave like a coherent mass with large cluster (Zafar et al., 2017). When it comes to the measurement of this strength, stickiness is measured and explained by a combination of *interparticle forces* (adhesion) and *particle-wall forces* (cohesion) (X. D. Chen & Özkan, 2007). The surface of touch is the key parameter to explain those forces, so

the properties of the two surfaces in contact is very determinant on the stickiness behavior. The strength of the adhesion force increases with the surface energy difference of the two surfaces. On the other hand, this separation force should also consider the properties of the bulk structure at molecular level, which should take into account the surface roughness.

1.1 Mechanisms of Caking

The caking process was classified into different categories by many researchers in the literature, depending on the particle interactions, external conditions and the mechanism of formation. Capes (1980) had a more compartmental point of view and approached the phenomenon by explaining *solid bridges, immobile liquids, mobile liquids, intermolecular and long-range forces, and mechanical interlocking*. Griffith (1991) made a broader classification and described the mechanical, chemical, electrical and plastic flow caking. In 2017, Zafar et al. described the process by categorizing particle interactions and explained the effect of van der Waals forces, electrostatic forces, liquid bridge formation, contact mechanics (elastic contact, plastic contact, and surface roughness), solid bridge formation (by sintering and solvent evaporation) and discussed the effect on amorphous materials. In their work, Afrassiabian et al. (2016) described different caking mechanisms with respect to parameters that trigger the process. They introduced four different concepts: 1) mechanical (dry) caking, 2) wet caking, 3) thermal and melt caking, 4) solid phase caking, which were induced by pressure, humidity, temperature, and crystallization, respectively.

Being dependent on the surface roughness and particle size, contact area is an important parameter, which promotes stickiness. While particle size is inversely correlated to cohesive/adhesive forces, surface roughness increases with cohesion or adhesion (X. D. Chen & Özkan, 2007). On the other hand, the consolidation stress exerted on the powder becomes really very important to understand the attraction since it becomes more effective when the interparticular space gets smaller during

storage and operation. When a material is deformed by either temperature change or consolidation, deformation of particles increases the contact area and caking. As an intrinsic parameter, van der Waals and Coulomb forces between particles of a bulk powder results in an attraction/repulsion between particles, which is referred as cohesive forces (Muller, 2017). When the atoms are ordered smoothly in the structure, the particles can come close and the interparticular forces like adhesion becomes comparable to Van der Waals forces, however it is not the case in food powders most of the time (Gay & Leibler, 1999). Muller (2017) explained the caking process by cohesive forces, liquid-solid bridging, and the plastic creep and sintering effects. Water can condense due to temperature drop or be absorbed from the surrounding environment on the surface of the particles (Peleg & Mannheim, 1977). Especially dried foods with high initial water content (such as fruits and vegetables) become very tacky with the increased water content since they contain a high number of soluble compounds that dissolve on the surface water. For the crystalline materials, M. Chen et al. (2018) emphasized the importance of environmental conditions on the process and narrowed down the topic by making a classification based on the sorption of different particles, which explained moisture adsorption, liquid bridging, and crystal bridge formation. One should consider all these forces in overall to fully understand caking phenomena.

As can be inferred from those various studies, many forces act on the interaction of the neighboring particles, and there is not only one way of explaining the mechanism and triggering factors.

Either as a plasticizer for an amorphous material or a solvent for crystalline powders, caking starts by capillary condensation (Afrassiabian et al., 2016). Thus, moisture dependent caking mechanism will be discussed here in three stages: 1) moisture adsorption, 2) liquid bridge formation, and 3) solid bridging (M. Chen et al., 2018).

1.1.1 Moisture Adsorption and Sorption Isotherm

One of the most frequent causes of caking is moisture absorption, which differs for deliquescent and non- deliquescent materials. Deliquescent particles adsorb water on all over their surfaces when the relative humidity of the environment exceeds a critical value. On the other hand, we see water accumulation at the contact point of the particles for non-deliquescent materials due to capillary condensation. Although the mechanism of caking is similar for both, one should also understand the difference of moisture between two different kinds of crystals to fully visualize the concept.

When a sample is placed in an environment having a higher equilibrium relative humidity, the capillaries of the powder start to fill with vapor, which initiates condensation at the contact point of the adjoining particles due to capillary pressure. Capillary pressure (P_c) is a phenomenon seen in the very small gap between two curved surfaces, which is enforced by increased vapor pressure of the environment between two powder particles. It has a positive relation with interfacial tension (σ) and contact angle (θ) while increasing pore radius (r) decreases capillary pressure, given by Equation 1.1 (Fanchi, 2002).

$$P_c = \frac{2\sigma \cos\theta}{r} \qquad \text{(Equation 1.1)}$$

Amount of condensed water at those contact points could also be calculated by Kelvin's equation for studied water activity conditions. When the Kelvin radius for a specific condition was calculated, one can infer if the capillaries were full of water or not. Detailed information of this approach could be found in other studies (Afrassiabian et al., 2016; Al-Muhtaseb et al., 2002; Billings et al., 2006; Butt &

Kappl, 2009; M. Chen et al., 2018; Yrö H. Roos, 1995; Torii et al., 1994; Xiao et al., 2019).

Condensed water at the free surface, which are in the shape of circular arcs (Urso et al., 1999) forms a meniscus between particles. This formation creates an additional gradient which forces the soluble matter to accumulate on the surface. This state of the condensed water at the particle intersections is known as *pendular state* (Figure 1.1). The saturation of the bulk material and the orientation of the water molecules may change depending on the diffusion behavior of water in the system and representative distribution of water inside a model particle system is shown in Figure 1.1. In funicular state, the liquid bridges that formed between two individual particles associate with each other and fuse. At the later stages, the blank spaces between particles fill with water and form capillary state or bulk state (M. Chen et al., 2018).

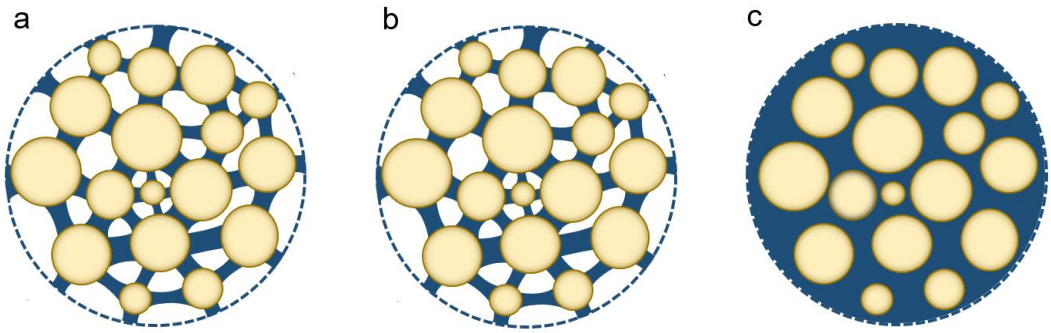

Figure 1.1. Orientation of water in pendular (a), funicular (b) and capillary (c) states. Powder particles were represented by simple spheres.

Moisture adsorption on the particle surface makes the molecules on the interphase between the particle core and air more mobile. The mobility may induce certain changes on the polymorphology or cause phase transition, may trigger chemical reactions…etc. (M. Chen et al., 2018). The position and the state of the water molecules described before also affect the overall system, which can make the

process more challenging to understand. Examples of the caking behavior due to moisture adsorption are shown in Figure 1.2.

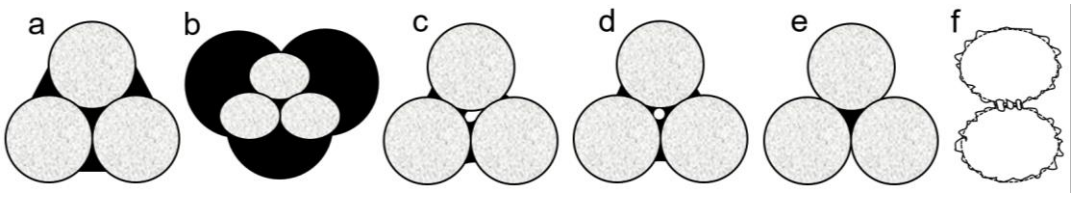

Figure 1.2. Some examples to fully understand the adsorption behavior: the meniscus could be concave (a) or convex (b), geometry of the bridging could change (c, d, e) (Urso et al., 1999), and the smoothness of the particle surface (f).

If we continue to look at the issue from the general perspective and continue with the affinity of particles to bind with water, looking at the sorption isotherms are known to be indicative and very helpful.

A moisture sorption isotherm provides the relation between total moisture content and the water activity of a sample. There are a couple of forms that water can be present in the system. Free water sits on the surface, while bound water is physically (electrostatically) or chemically engaged in the particles (Khalfaoui et al., 2003; Muller, 2017). As the moisture content of the sample increases, the state and the strength of the (bound/unbound) water change depending on the presence of hydroxyl groups, amine, and carbonyl groups in the food structure. In such cases, water chemically incorporates into the structure rather than being a solvent. This behavior is explained by the sorption isotherm (Al-Muhtaseb et al., 2002; Chiou & Langrish, 2007; FDA, 2014; Harnkarnsujarit & Charoenrein, 2011; Kelly et al., 2015; Laine et al., 2008; D. S. Lee & Robertson, 2022; Zouari et al., 2020).

An isotherm could be drawn either by adsorption or desorption methods. The adsorption method refers to recording water uptake of initially dry material at an increased relative humidity. On the other hand, desorption isotherms are prepared by

measuring the weight loss of an initially wet material equilibrated at decreasing relative humidities.

The moisture sorption isotherms were defined by the famous BET (Brunauer-Emmett-Teller) method, which is also frequently used to measure the specific surface area and pore volume by nitrogen adsorption. There have been defined five generalized adsorption isotherm types in the literature (Figure 1.3) (Al-Muhtaseb et al., 2002; Khalfaoui et al., 2003; M. Mathlouthi & Rogé, 2003). Type I is known as Langmuir isotherm and shows characteristic monomolecular adsorption until saturation which is followed by a plateau after a certain relative humidity (Khalfaoui et al., 2003; M. Mathlouthi & Rogé, 2003).It is characteristic to microporous materials with small external surface (such as activated carbon) (Sing et al., 1985). Type II is also called sigmoid isotherm and represents soluble materials (Mathlouthi & Rogé, 2003). Unlike Type I isotherm, Type II isotherm does not show a saturation behavior and represents macro-porous systems with different range of pore sizes. Those materials first experience monolayer adsorption then multilayer adsorption. That is why the sorption isotherm shows a variant behavior after a relatively steep increase at the beginning of the curve, which will be followed a linear like trend at the moderate relative humidity (Sing et al., 1985). After a certain limit at higher relative humidity, condensation is observed and those processes are reversible (Khalfaoui et al., 2003). Type III is the Flory-Huggins isotherm. The curve represents the adsorption behavior of samples with continuous adsorption ability. Plasticizers like glycerol above glass transition temperature could be an example of this behavior (M. Mathlouthi & Rogé, 2003). There are also common examples to this behavior in food systems, for which the transition between monolayer to multilayer adsorption is indistinct. Type IV isotherm is rather like Type I isotherm, only having differences at the low relative humidity environment (Khalfaoui et al., 2003). Those are hydrophilic, mesoporous materials that can swell (forming mono- and multilayers). The isotherm is representative for industrial adsorbents and related to capillary condensation. Although it is like Type II and Type III isotherms, Type V is not seen very frequently. It represents some industrial adsorbents like charcoal (M.

Mathlouthi & Rogé, 2003; Sing et al., 1985). Type IV and Type V isotherms show significant hysteresis, which means the history of adsorption or the amount of moisture uptake affects the present behavior of the samples upon dehumidification. Those materials follow different paths of sorption when their moisture was decreased and increased. IUPAC classification also involves a Type 6 isotherm, which shows stepwise increase representing layer by layer adsorption (Sing et al., 1985). Food materials are generally classified under Type II and Type III isotherms. Starch gels, potato, tomato, carrot, hazelnut, cocoa beans, lentil seeds, onion are some examples of the samples showing a Type II isotherm. Sugar alcohol, sugars, apple, pineapple, banana, apricot, raisins, and sucrose-starch samples are some food examples showing the behavior of Type III isotherm (Al-Muhtaseb et al., 2002).

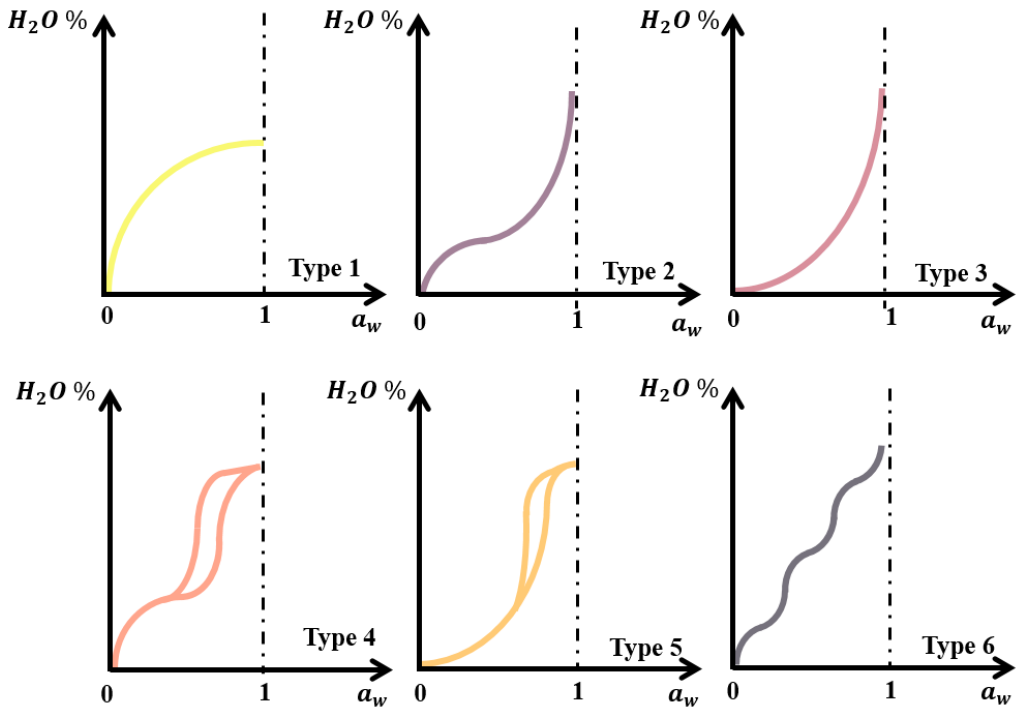

Figure 1.3. Generalized forms of the typical adsorption isotherms.

1.1.2 Liquid bridge formation

Dissolution, wetting, melting, and liquid component release from inside to the surface of the particles may result in liquid bridging (B. R. Bhandari, 2007). Moisture adsorption and possible water states in the structure was explained in Section 1.1.1. In this section, the effects of the adsorption stages on the liquid bridge formation will be explained.

Typical adsorption of a food powder could be defined by three representative sections (Figure 1.4). At the very dry state, at low relative humidities, powder surface is covered with a water layer first (monolayer). This initial connection of the particle surface with moisture linearly increases with relative humidity (Muller, 2017). At this stage, there is no significant caking or bridging occuring between particles. As the moisture uptake continues, the number of layers on the surface starts to increase (multilayer), which corresponds to the second section on a moisture isotherm (Figure 1.4). At this level, hydrogen bonds are formed over the particle surfaces and depending on the nature of the particle, it may get solubilized, and the surface may become more viscous. This morphology change, which is a kind of deformation on the surface of the particles is the first sign of caking since it creates a suitable environment for bridging. Although bridging is initiated, it may not be measurable by mechanical techniques since it does not cause a significant decrease in porosity or the bridge strength may not be enough to overcome the flow at the beginning (Aguilera et al., 1995). The number, distance, surface morphology and shape of the particles as well as the amount of water in the environment significantly affect the degree of liquid bridging. Although there are attempts to formulize the effect of each parameter on overall caking phenomena, the real system normally becomes more complicated than formulations (M. Chen et al., 2018).

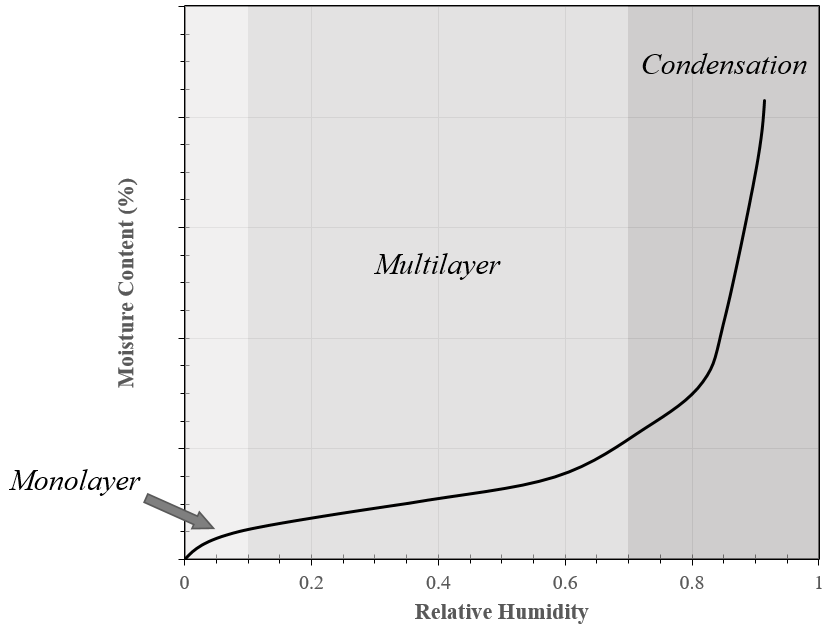

Figure 1.4. Typical sorption isotherm for a food product.

If we continue analyzing the sorption isotherm, the governing adsorption mechanism in the last portion (Figure 1.4) is driven by capillary condensation, which causes a characteristic sharp increase in moisture content (Muller, 2017). The limit where the condensation, thus immense increase in moisture content is observed is called ***critical relative humidity***.

After the critical water activity, capillary condensation and mobility in the interparticular area result in liquid bridge formation (M. Chen et al., 2018). The moisture could be absorbed or condensed from the air, or it can be externally to the system for a specific purpose such as binding or shaping like in the case of sugar cubes production. Extensive condensation is seen after the critical relative humidity limit at the contact point of particles, which form liquid bridges, the main reason of a caked food powder in most of the cases.

After the water bridges form, the soluble compounds on the surface diffuse to the condensed water bridge, or the material could recrystallize directly (Nestl et al., 2011). Although the dissolution of the small molecules through the bridge has a

slight effect on the viscosity, its transformation to solid bridges makes it crucial for detection for the quality control purposes.

1.1.3 Solid bridge formation

Environmental factors have a dramatic effect on caking. When those conditions change to evaporate the water of the liquid bridges, the solubilized material within those water pools becomes viscous. Recrystallization or mass transfer from the liquid bridges promotes the solidification of the bridges and results in solid bridges. Caking is the word that describes the phenomena occurring due to this viscous bridge formation. At the end of these processes, there would no longer be single bridges in the system but enlarged entities of irregular shape and organization. Those solid bridges are seen in most severe caking cases since the strength of the bonds are the largest. The strength of the interactions caused by other mechanisms decrease for liquid bridging, van der Waals forces, electrostatic interactions, magnetic/interlocking forces, respectively (Afrassiabian et al., 2016; Zafar et al., 2017). However, those forces hardly cause caking even though they increase particle interaction. For food powders that are originally in a free-flowing state, an increase in the number and duration of liquid/solid bridges are indications of poor quality.

Caking is the main problem for hygroscopic materials with low glass transition temperature, spray dried sugar and acid rich products, salts, meat extracts, powdered vegetables, flavor compounds, any kind of material that contain amorphous compounds (such as amorphous lactose containing dairy powders, hydrolyzed fish proteins, starch hydrolyzates…etc.) (Muzaffar et al., 2015; Nestl et al., 2011).

1.2 Primary Causes of Caking

1.2.1 Consolidation

Consolidation is the process of compressing a material to form a stronger, rigid structure. By the effect of consolidation, particles get close to each other and tend to stick together. This consolidation stress does not necessarily have to be applied externally. When used in large quantities like in silos and tanks, caking could simultaneously develop due to consolidation effect of powder mass. Since the pressure may not be uniformly distributed in the container, it gets very difficult to predict local caking tendency.

1.2.2 Moisture

The initial moisture content as well as moisture adsorption during handling and storage is one of the main causes of caking (please see Section 1.1.1). Beside the water inside the sample, migration of moisture to/from the environment may also induce changes in the structure. The moisture that occupies the empty spaces between particles, which is easily manipulated by the environmental conditions is called interstitial moisture (Muller, 2017). For the crystalline powders, the structure is modified by this interstitial moisture upon condensation at the interparticular area.

One of the most important positions that water is in the structure is the inherent moisture, which is contained in crystals or micropores of randomly ordered amorphous compounds (Muller, 2017). Upon recrystallization, this inherent moisture release on the surface becomes the main issue in amorphous caking. Moreover, one of the effects of moisture uptake is to trigger anomerization of compounds in the food powder content. Since caking is one of the main problems in dairy powder industry, the effect of lactose crystals on the stickiness and processing parameters were investigated in the literature (Altamimi et al., 2017; Foster et al., 2005; Paterson et al., 2005; Willart et al., 2004). In those studies, it was suggested

that the particles got softer, and the stickiness increased since the anomeric ratio of lactose is significantly affected from relative humidity of the environment.

The ability to agglomerate by moisture uptake of the particles is not always considered as a disadvantage. Assembling the individual particles into a larger structure is a mean to improve the flow behavior, shape, appearance and the solubility characteristics in related processes (Aguilera et al., 1995).

1.2.3 Temperature

Fluctuation in temperature is one of the main issues in transportation to long distances and different climate conditions. When the equilibrium conditions were manipulated, the distribution of the water inside the sample adjust itself to compensate the change. Especially for amorphous powders, temperature is a critical issue since the physical properties (such as viscosity and elasticity) and the amount of enclosed water completely change below/above glass transition temperature (T_g). The rigidity of a plastic or polymer is greatly influenced by temperature and T_g is one of the best indicators that describe the transition. High viscosity of an amorphous material keeps the structure stable in the glassy state if it is kept in a dry environment below T_g. When the temperature is increased, the material deforms and lose its glassy structure. The reason behind this behavior could be explained by surface energy change with temperature (B. Bhandari & Howes, 2005). When a sample has a low surface energy, it is less likely to stick to another low energy surface. Converting into rubbery state, surface energy of the sample increase and the increased mobility causes a sudden decrease is seen in the viscosity of polymer and the material tends to deform and flow (Aguilera et al., 1995), which has a significant influence on caking. More detail on the amorphous structure will be given in Section 1.2.4.1. T_g could be easily determined by thermal analyses and characterized by a step change in the Differential Scanning Calorimetry (DSC) curve, due to the significant change in the sample's heat capacity. A representative DSC heating thermogram for a

sucrose sample, showing glass transition step change around 150 °C was shown in Figure 1.5.

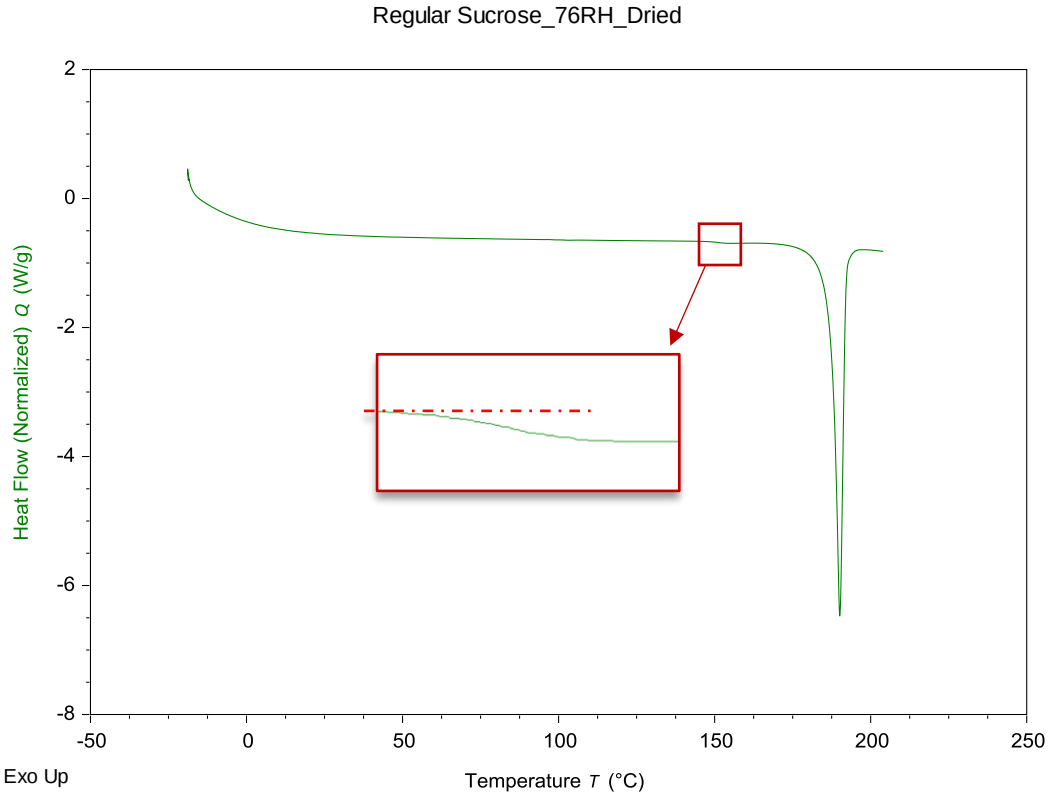

Figure 1.5. A representative DSC heating thermogram for a sucrose sample, showing glass transition step change around 150 °C.

Accumulation of the condensed or evaporated water on the surface or on the container becomes another issue that will trigger caking upon cooling or heating (Muller, 2017). Since the temperature change affects physical properties and result in plastic creep, the compaction, which is referred as sintering in the caking literature, also increases. On the other hand, the composition of the food powder is also very determinant on the effect of temperature to the system, since the individual compounds in a multicomponent sample will melt considerably at different

temperatures (such as water and fat), which will affect the stickiness of the structure (X. D. Chen & Özkan, 2007).

The surface composition of particles in bulk powder is one of the most important aspects to consider in terms of caking (Huppertz & Gazi, 2016; Kelly et al., 2015).

1.2.4 Composition

1.2.4.1 Amorphous Structure

A crystalline state of a compound is energetically favored over an amorphous structure (B. R. Bhandari, 2007). Since the entropy of amorphous compounds is higher, the system acts to decrease its energy with time to reach an equilibrium state. When the water hold within the structure was released due to recrystallization, the transfer of water between the compound, the food matrix, and the surrounding (Christakis et al., 2006) becomes the main reason for caking in amorphous materials.

Water soluble amorphous materials can associate considerable amount of water. As the asssociated water content increases, the mobility of the molecules increases, resulting in a decrease in viscosity (Nestl et al., 2011), which interferes with the flow behavior by the increased adhesion/cohesive forces.

Dry, crystalline materials are expected to be flowable unless the particles are not deformed by physical intervention such as grinding which will cause crystal surface to transform into amorphous state (X. D. Chen & Özkan, 2007).

Amorphous structure is seen very frequently in the drying industry for food products since the nature of the process require transformation of the product from liquid or rubbery state into glassy state by removal of the plasticizer (mainly water). As long as the food material is not exposed to drying temperatures higher than T_g, it remains in a high-energy (sticky) state (B. Bhandari & Howes, 2005). For the milk powders, there are two main issues that basically trigger caking: *fat content and the amount of the amorphous lactose*. When the effect of those two components were compared, it

is reported in the literature that fat bridges on the surface of the particles make looser bonds than lactose bridges, which are much stronger (B. Bhandari & Howes, 2005).

1.2.4.2 Fat Content

The amount of fat on the surface of the particles is another parameter that affect caking since it changes physical properties like dispersibility and hydrophobicity (Kim et al., 2005). High surface fat content is typically viewed as a drawback since the sample can also get oxidized easier, expedite phase separation and becomes sticky (Buma, 1971).

As mentioned before, the amount of hygroscopic amorphous lactose is the major concern for milk powder caking. However, flow problems associated to whole fat milk powder were also encountered for the conditions where lactose is in stable crystalline state (Foster et al., 2005). Another hygroscopic compound found in milk powder is milk proteins, so their effect on development of stickiness was also considered and the results showed that they did not significantly increased stickiness tendency (Özkan et al., 2002). Combining both facts, the reason of stickiness for milk powders was explained by the presence of fat in the formulation, having a considerable influence on the powder rheology by softening the structure. Depending on the environmental conditions (generally followed by a temperature increase), fatty components in the food matrix gets looser, increase in surface area and cause liquid bridge formation (B. Adhikari et al., 2001). Several studies have identified milk fat as the source of caking and verified that viscous liquid bridges could impair the flow of those powders (Foster et al., 2005). Especially in the production of cream powders, stickiness is a significant concern due to clogging and smearing over the chamber walls, causing huge product loss (B. Bhandari & Howes, 2005; X. D. Chen & Özkan, 2007).

1.2.4.3 Small molecular compounds

For the food powders, sugars and organic acids are the main reason of caking due to small molecular compounds. Although the physical state (amorphous/crystalline) is also determinant on the stickiness behavior, intense binding of those hygroscopic compounds with water in the continuous phase of the bulk solution makes the structure sticky (X. D. Chen & Özkan, 2007).

In confectionary industry where high concentration of sugars are boiled and further processed, glassy state of the sugar could be spoiled by moisture uptake easily which is highly undesirable (B. Adhikari et al., 2001). In drying processes, the amount of those low molecular sugars (mainly glucose, fructose) and acids (such as citric and malic acids) makes it very difficult to recover the product (Nestl et al., 2011).
In real life conditions, triggering factors of caking are mostly tangled together. The main problems with low molecular compounds are their thermoplastic properties as well as high hygroscopicity and low T_g values. Especially for fruit powder production, high molecular weight aids are required to prevent collapse and stickiness to manufacture powders of high quality (Muzaffar et al., 2015).

1.2.4.4 Particle Size

Particle size is conceived to be inversely related to caking in general. As the particle size gets smaller, particles come closer to each other, and the contact area increases. However, for sensitive materials with a mixture of particles with broad size distribution, available surface area for contact between coarse and fine fragments increases, which in turn may induce caking (Muller, 2017). Increased Van der Waals forces as the particles get closer increase their tendency for stickiness. It is known that the cohesion of particles increases significantly for non-dairy powders with the particle size (Buma, 1971). On the other hand, the properties of the fragments are also important to determine caking tendency. If the smaller particles are in nanosize and not sticky enough to the main structure, it may indeed prevent caking (Muller,

2017) or increased amount of fat on the surface of the particles does not significantly affect the flow after a certain concentration (X. D. Chen & Özkan, 2007).

1.3 Caking Studies in the Literature

Shear testing method is generally preferred over other methods to quantify caking. The flow function of the powder is measured at different consolidation stresses, which mimics possible operating conditions. Detailed information regarding test methods and related procedures could be found in different studies (Aguilera et al., 1995; Billings et al., 2006; M. Chen et al., 2015, 2018; J. J. Fitzpatrick et al., 2007, 2017; John J. Fitzpatrick & Ahrné, 2005; Freeman et al., 2015; Shenoy et al., 2015; Zafar et al., 2017).

However, there is no standard quantification method to determine caking degree. There are theories and mechanical/morphological approaches that were applied in the literature. To understand the interaction between two surfaces, in general, surface energy-based methods are used to describe the mechanism to estimate adhesion and cohesion forces. For this purpose, contact angle measurement, wetting and surface energy measurements are done (B. Bhandari & Howes, 2005). However, when it comes to caking, environmental conditions and the surface characteristics change as the particles adsorb water or the temperature is increased. One of the most important parameters is the interparticular space. Although it should inevitably be related to the surface energy, the surfaces are not smooth and the solid powder samples have a porous structure, which also changes as the caking develops in the structure and make it very difficult to estimate the change in the surface energy. That is why food related studies in the literature mainly focuses on the flow behavior and moisture sorption isotherms when it comes to powder samples in terms of characterization of the stickiness behavior.

In their paper, Mathlouthi & Rogé (2003) studied the effect of particle size and shape of the microcrystals on caking properties of sucrose. They plotted the sorption isotherm for those samples and deducted the conclusion that the caking tendency is

conversely related to particle size. The results were also confirmed by using a Jenike cell (shown in Figure 1.6), which is recognized as the most reliable technique valid within the current options to understand caking behavior. Jenike cell works under a range of load stress and enables shear stress recording. Flowability of the powder is estimated from the cohesion and internal resistance of the powder.

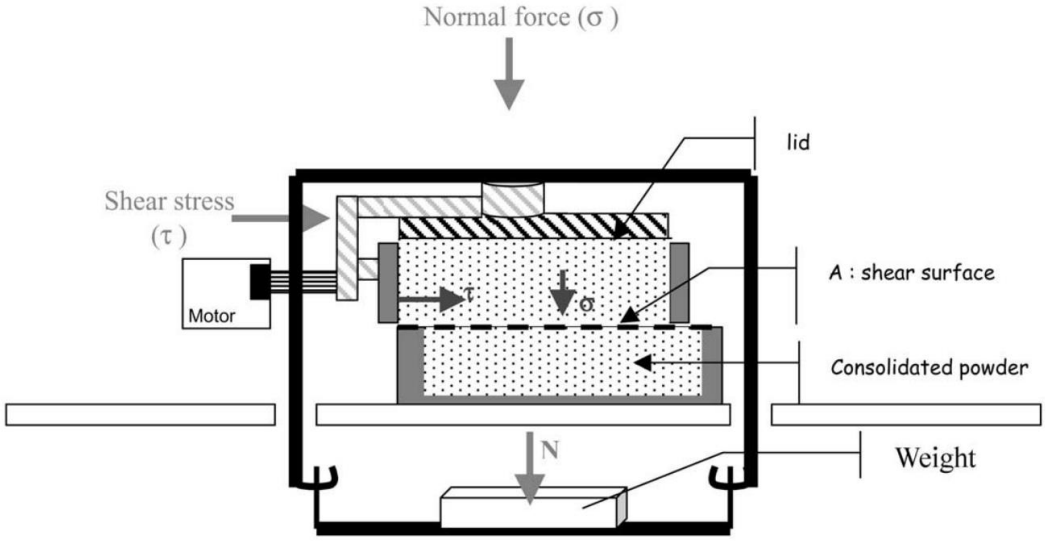

Figure 1.6. Jenike cell design (M. Mathlouthi & Rogé, 2003).

In another study, Lipasek et al. (2012) investigated the effect of moisture sorption on the flow characteristics of some deliquescent ingredients and their binary mixtures. The effect of anticaking agents on the flowability characteristics at different relative humidity were measured by a powder analyzer, referencing *avalanche* power and *avalanche* angle, which are characterized by the sudden fall of the powder after a certain angle or power. Sieve analysis was also used as an indicator of caking. They found out that one should consider the complexity of the sample before choosing a suitable anti-caking agent to prevent caking (Lipasek et al., 2012). Another study focused on the effect of anticaking agents on the flowability of dried honey powder

with amorphous fraction and employed flow tester with multiple consolidation stress together with sorption isotherm (Nurhadi & Roos, 2017). Calcium stearate as an anti-caking agent gave better results on the flowability of the honey powders while calcium silicate did not show any difference on the sorption isotherm (Nurhadi & Roos, 2017). Freeman et al. (2015) demonstrated a different approach and studied on the samples that display homogeneous versus inhomogeneous caking behavior when exposed to moisture. The group analyzed the caking degree by using a powder rheometer, which was specially designed for the experiment with its twisted blades that allow only a specific volume of the powder to flow through the predefined path. They showed that the interaction of the particles, the caking may or may not be homogeneous and the strength of the interactions were reversible for homogeneous type caking while nonhomogeneous caking was severe in their case (Freeman et al., 2015). Wang & Hartel (2020) considered rheological properties and glass transition temperature. Texture analyzer with the tack test was used to explain the stickiness behavior. In their formulations with different starch hydrolysate and sugar content, they found that maltodextrin increased the stickiness while allulose acted as a plasticizer (Wang & Hartel, 2020). On the other hand, statistically interpreted visual assessment of caked particles are also preferred to understand caking since mechanical tests are rather difficult. Fitzpatrick et al. (2017) measured cake strength by a texture analyzer and tracked the bridging on binary mixtures of sticking and non-sticking food powders by using a light microscope. Sieving is also widely applied in the industry due to convenience (J. J. Fitzpatrick et al., 2017).

In the year 2000, Chung et al. used NMR to understand caking. They built up T_2 curves at 20-100°C temperature range and through storage time. The results indicated a strong analogy between caking behavior and molecular mobility (Chung et al., 2000). In the year 2008, same group also studied on dosing the ingredients of the soup recipe to decrease caking in the soup powder. There were again used a low field NMR instrument by calculating T_2 from the signal acquired by single 90° pulse Free Induction Decay (FID). Construction of spin-spin relaxation (T_2) time vs temperature curves enabled interpretation of the caking tendency (Chung et al.,

2008). The results also verified the idea that the molecular mobility information taken from the NMR instrument could be used to understand physical changes and interpret caking behavior of the food products.

1.4 Crystallization for Food Systems with High Sugar Content

Crystallization is one of the most essential and complicated processes since the balance between transferred phases, density and diffusion of solute, dissolution, free energy, heat transfer, and physical properties simultaneously change during operation (Sander & Kardum, 2012).

For the food systems, there are two defined cases where crystallization would be a significant process to be controlled. The first one is 'crystallization as a separation process' and the other one is 'crystallization as a property of the system' affecting the overall structure (Hartel, 2002). In either case, understanding and controlling of crystallization is important since it empowers one to manipulate final product characteristics such as texture, flavor, purity, polymorph, appearance, shape and size distribution of the crystals (Hartel, 2002; Sander & Kardum, 2012). In both cases, the effect of driving forces and the triggering factors could be explained by the same thermodynamic rules, which require a deeper knowledge of crystal formation theory. In its most simple form, crystallization initiates with nucleation and continues with the phenomenon known as crystal growth. The driving force-supersaturation-energetically requires particles to affiliate with each other to form clusters, which causes concentration inconsistencies in the solution (Schwartz & Myerson, 2002). If the sizes of those clusters are small, they dissociate back in the solution since forming a surface will not help to decrease the energy of the system. However, if the sizes of those associating particles exceed a critical value, Gibbs free energy becomes negative, and the clusters will automatically start to grow (Schwartz & Myerson, 2002). The occurrence of this new phase (nuclei), which will be the center of further growth, is called nucleation (Khvorova et al., 2018). Nucleation could be homogeneous or heterogeneous, as well as primary and secondary. To have a good

control over crystallization, industrial applications are usually performed in the metastable zone, which enable crystal growth without nucleation and seed particles are used for this purpose to achieve a bigger and homogeneous particle size distribution (Earle, 2004). Seeding prevents random nucleation and provides sufficient area for crystal growth (Chianese & Kramer, 2012). This type of crystallization is an example of heterogeneous crystallization, where a crystal particle is added to the solution externally. On the other hand, homogeneous nucleation is an example of primary nucleation, which takes place when there is no crystal surface present to grow in the solution initially. Metastable zone is normally slightly above solubility curve, and its width could change from sample to sample. A representative concentration vs temperature curve is shown in Figure 1.7.

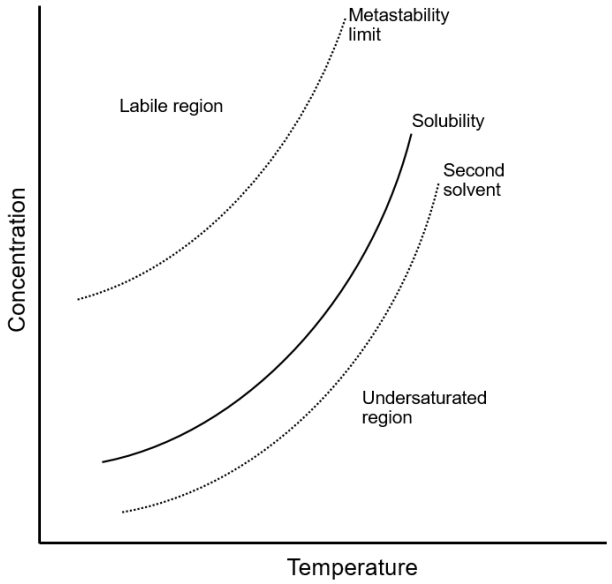

Figure 1.7. Representative crystallization zones with changing concentration versus temperature.

Following nucleation, nuclei should diffuse to a crystal surface (crystal-solution interphase) to grow and this stage is known as crystal growth (Erdemir et al., 2009).

On the crystal surface, further integration of nuclei into the crystal lattice requires time. At this point, either diffusion rate or growth energy could be the limiting factor for crystallization rate (*Kinetics and Mass Transfer in Crystallization*, n.d.). Although thermodynamics explain the mechanism and equilibrium conditions, it does not give information on the rate of crystallization (Schwartz & Myerson, 2002). Crystallization rate is studied by isothermal and non-isothermal DSC procedures by measuring the latent heat due to transformation of nuclei and growth, polarized optical microscopy, or dielectric spectroscopy (which is effective for materials with slow nucleation rates) (Shalu, 2018).

Solidification, which refers to a phase change due to temperature decrease of the target compound, is a widely used technique in the food industry to manufacture frozen foods, crystalline candies, polymorph modification of fat compounds (Atsukawa et al., 2020; Moraga & Barraza, 2003; Widlak et al., 2001) and crystallization of molten sugar is a solidification technique used to produce crystal candies or fondant. The solidification ratio is an indicator of better quality for candies and to maintain high quality standards, sugars are cooled as quickly as possible to prevent crystals to diffuse each other and enlarge to form separate entities within the food matrix. The period where desirable and undesirable crystals are present at the same time is shortened and the desirable texture is achieved quickly by a quick process (Atsukawa et al., 2020).

Sugars are crucial to meet the energy requirement of body cells but they are not only regarded as energy sources but also used for a variety of reasons in food industry due to their strong water binding, contribution to texture, glass forming abilities (Simperler et al., 2006), thickening, stabilization effects and contribution to food preservation. They are also important contributors to crystallization in various foods.

Crystallization is an important operation for the manufacture of sugars in the food industry. Known as table sugar, sucrose is the most widely consumed and produced sugar type in the world. The main natural carbohydrate source of all milk varieties, disaccharide lactose, is important for the food industry since it is utilized by the

bacteria in fermentation, acts as prebiotic in human digestive system, prebiotic in human digestive system, enhance flavor and color (reducing) characteristics as well as being used to decrease the intense taste of confectionery products due to its low contribution to sweetness (30% of sucrose).

Sucrose has a long history of research so there is an abundant of information in the literature due to its significance in human diet, availability, modelling of non-ideal solute systems, reformulation and storage of products as well as the variety of applications over a century. It is produced in large quantities to supply the demand so its thermal and physical properties, water interactions via sorption isotherms, hygroscopicity due to crystalline and amorphous fractions, morphological changes resulting from the sugar source, deliquescence, de-structuring and plasticizing effects, cryo-protection, effects of dilution and concentration, hydrophobic bonding were all studied in the literature (Bock & Lemieux, 1982; Branca et al., 1999; Bressan et al., 1994; Lans, 2016; S. L. Lee et al., 2005; Lu et al., 2017; Olsson & Swenson, 2020; Yrjö H. Roos et al., 2013; Starzak et al., 2000).

As it is already a self-defining word, rare sugars are simple monosaccharides and their derivatives naturally found in some kinds of foods but only in trace amounts. A rare sugar, allulose, is C3 epimer of fructose and announced “generally recognized as safe” (GRAS) by US Food and Drug Administration in 2017 (FDA, 2017). Although the amount is really scarce; allulose could be naturally present in wheat, commercial mixtures of D-glucose and D-fructose, steam-treated coffee, processed cane and beet molasses, fruit juice with a long-term heating process and some fruits (Jiang et al., 2020; Zhang et al., 2016). Since its quantity is too low to be extracted, they are produced by either fermentation or enzymatic treatments. Being a low-calorie sugar, allulose mimics 70% relative sweetness of sucrose while exhibiting 0.2 kcal/g, which corresponds to a very low energy value when compared with sucrose, giving 4 kcal/g. Other than calorie reduction, allulose also contributes to overall health that makes it a value-added compound to be used in food formulations (Jiang et al., 2020). In that regard, many studies have been conducted to explain the physical, chemical and nutritional characteristics of allulose (Fukada et al., 2010;

Ikeda et al., 2014; Ilhan et al., 2020; Jiang et al., 2020; Keda et al., 2011; A. Li et al., 2017; Maeng et al., 2019; Shintani et al., 2017; Zhang et al., 2018, 2016, 2017) since it was started to be commercially available in 2009.

Rare sugars are naturally found in foods but their quantity is too low to be extracted. For this purpose, they are produced by either fermentation or enzymatic treatments. One of the most important attributes of a rare sugar, namely D-allulose, is that it is low in calorie it is also an ideal substitute for sucrose with its clean taste, desirable rheological properties, antioxidative effect and health benefits (Ilhan et al., 2020).

On the other hand, crystallization becomes one of the challenges during shelf life of foods and it could easily develop due to improper storage. In foods, storage related quality deterioration could be seen due to crystallization. Sugar crystallization in honey; graining in hard candies; ice crystallization in the case of frozen foods (most likely in ice cream); lipid crystallization like polymorph switch in margarines or chocolate and starch crystallization that stales the bread are just some examples (Hartel, 2002).

1.5 Crystallinity Measurement in Food Systems

There are different approaches to calculate crystal content and monitor crystallization process in the literature. Some of them are microscopic techniques (Martins et al., 2005), which have restrictions such as transparency and concentration of the sample. Furthermore, it does not detect 3D crystal development (Dejong & Hartel, 2016). On the other hand, differential scanning calorimetry (DSC) is used to detect the changes in thermal properties (T_g, melting point or enthalpy) of the samples, which are related to crystallinity. Fourier transfer infrared spectroscopy (FTIR) is another method, which is rather fast and nondestructive (when compared to DSC), however the identification of different phases on the bands are rather difficult (Partini & Pantani, 2007).

The most widely used method for estimation of crystallinity to compare alternative approaches is wide angle X-ray Diffraction (XRD) (French & Santiago Cintrón, 2013). The method allows for accurate calculation of the crystallinity up to a certain moisture content, however the interpretation of the peaks and calculation totally depends on the human judgement (Dejong & Hartel, 2016).

XRD working principle relies on sending x-ray beams to the sample and collection of the diffracted beams of the same angle, theta. Both the sample and detectors are in a fixed position in the equipment design. The intensity maxima are collected from the sample at that certain angle gives information on the distance between atoms as well as their amount and the geometry since the wavelength of the x-ray beams are close to the distance between atoms (Garvey et al., 2005; Kidder & Lyu, 2020). From the acquired signals, the spacing between planes (d) could be calculated by using Bragg's law:

$$n\lambda = 2d \sin\theta \qquad \text{(Equation 1.2)}$$

where n is an integer (order of reflection), λ is x-ray wavelength, and θ is the angle between reflected beams. "n" represent the extra distance that a wave will travel with respect to another parallel beam. From the intensity of the waves that is recorded at the detector for each position, the distributions are drawn (Figure 1.8). XRD analyses could be done for both thin films and powders.

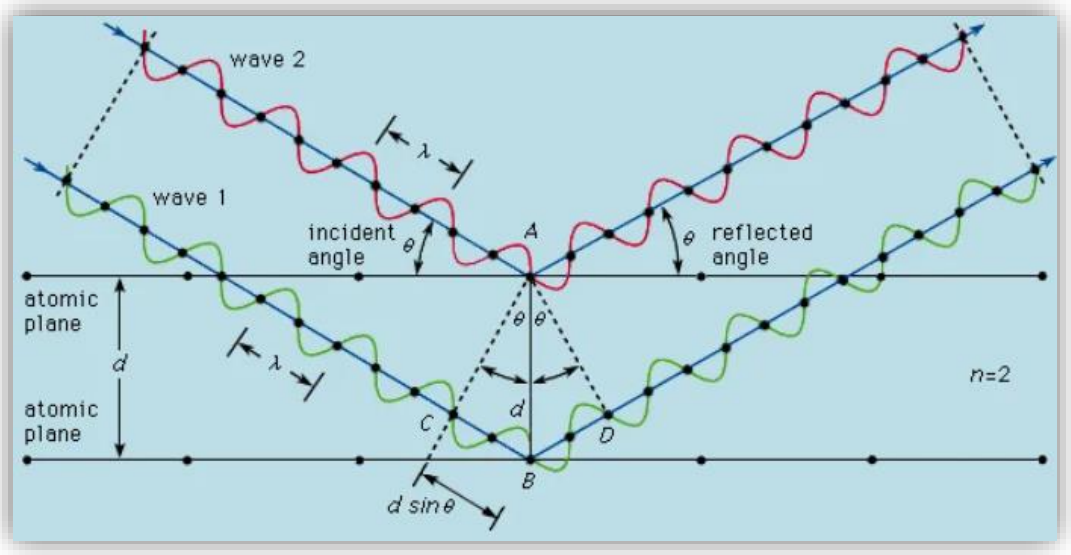

Figure 1.8. Bragg diffraction (Britannica, n.d.).

When it comes to analyzing XRD pattern, the procedure starts with removal of the background signal. After the signal was collected, corresponding peaks for amorphous proportions are picked up. While making the selection, the portion of the diffraction pattern that cannot be marked as a crystal peak are referred as the amorphous part (Minor & Murthy, 1989). Amorphous materials do not have a consistent, long-range order in their molecular arrangement that is why no crystalline peaks but dispersed bands with "halo" patterns (Serrano Nava et al., 2022) are observed in their XRD spectra. An example to crystalline and amorphous behavior could be seen in Figure 1.9.

There are many approaches to analyze an XRD spectrum, such as Segal method, XRD deconvolution, peak area or amorphous subtraction (French & Santiago Cintrón, 2013; Nam et al., 2016). Segal index is used as a quick method and gives a rough estimation of the crystalline fraction. It references the maximum intensity of one specifically assigned peak and the minimum intensity of the diffraction height between two significant peaks as crystalline and amorphous parts to calculate crystallinity (French & Santiago Cintrón, 2013). Since the method is not accurate, it

is not preferred over the other methods (Nam et al., 2016). Deconvolution method is a more accurate technique, in which the peak profiles are fitted to several patterns defined by modified Lorentzian or Gaussian distributions, or in combination (Minor & Murthy, 1989; Partini & Pantani, 2007). Crystallinity index was then calculated by the fraction of area under crystal peak and total peak area (Rotaru et al., 2018). Amorphous subtraction method based on subtraction of the signal of an externally measured standard from the original x-ray diffractogram. The main issue with that method is the selection of the reference material that represents the real sample (Park et al., 2010).

Another approach is to directly use the area under curves, assuming that the area beneath each XRD peak is proportional to the weight fraction of the corresponding crystalline entity (Belcourt & Labuza, 2007). The crystal fraction could be calculated by dividing the area under the curves of crystalline peaks (chosen manually by means of a specific software) over total area (crystalline + amorphous).

Those distributions revisit corresponding intensity values by taking into account the full-width at half maximum of each peak, which is an important parameter for the XRD analysis. Peak width and crystal size have an inverse relationship. Larger crystals would give thinner patterns (Kidder & Lyu, 2020).

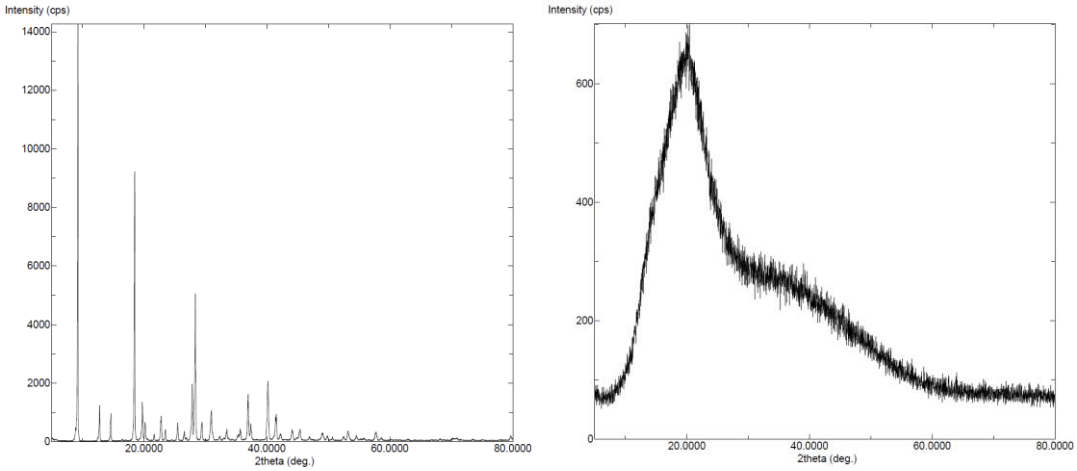

Figure 1.9. Representative XRD patterns for crystalline (powder glucose, on the left) and amorphous behavior (commercial cooked sugar, on the right).

1.6 Time Domain NMR for Crystallinity Measurement in Food Systems

Time Domain NMR has a wide range of applications for all kind of materials in macroscopic scale. When the scope of information taken from the NMR analyses was considered, modest requirement of space and technical knowledge makes it very desirable for particular industries such as cosmetics, pharmaceutical, composites, adhesives, plastics, and food industries (Besghini et al., 2019).

In mechanism, NMR is used to detect the changes in proton alignment, produced by radiofrequency (RF) pulses. The samples are placed in magnets and exposed to a magnetic field, through which protons align themselves. By distortion of this orientation by pulse sequences, the energy exchange between ^{1}H spins (spin-spin) and with the surrounding environment (spin-lattice) could be recorded, which are referred as and T_2 and T_1 relaxation times, respectively. Those two are the most common parameters to interpret time domain NMR signals, which are also typically applied to calculate crystallinity as well.

By solid-state NMR studies, one can get information on the structure, explain internal motions and understand the phase transitions in the samples (Goc, 1998a). Selectivity of the analysis method is the most prominent advantage (Schmidt-Rohr

& Spiess, 1994). It does not give chemical information like spectroscopy does. However, it provides detailed information on the dynamics of the system both in overall and in component base (localized), thus, domain size and morphological information of heterogeneous materials are also easily studied by *NMR relaxometry* (Buda et al., 2003). However, the signal to noise ratio, field inhomogeneity, and the dead time of the LF-NMR instrument are the main issues of low field NMR to optimize the signal yield and the measurement efficiency (Besghini et al., 2019; L. Grunin et al., 2019).

In NMR measurements, the resulting signal is obtained from the entire sample regardless of orientation, although it enables the detection of separate entities (Kirtil & Oztop, 2015). The non-invasive, non-destructive low resolution time domain NMR method have been proven effective in determination of solid fat and water content, degree of crystallinity, particle size distributions as well as polymer gelation and aggregation at various systems.

There has been many studies in the literature to understand crystallization of molecules in different scenarios. Le Botlan et al. (1998) investigated the mobility of different solid states to understand sugar polymorphism by using T_1 relaxation time of TD-NMR spectroscopy. The caking of commercial cooked sugar was attributed to (re)crystallization of sugar in the structure since the samples did not have any crystalline phase (Le Botlan et al., 1998).

The decaying trend of the T_2 curve is also very important to understand the current properties of the sample. Felix da Silva et al. (2018) used low field ^{1}H NMR equipped with a T_2 CPMG pulse sequence to identify and quantify components of water populations in spray dried cheese powder. The group also utilized ^{13}C cross-polarization *magic angle spinning NMR spectroscopy* to identify the polymorphs of crystalline lactose as well as the amorphous lactose in the structure (Felix da Silva et al., 2018). In another study, the effect of lactose and sodium chloride on crystallization of freeze-dried sucrose solution was investigated and 1 dimensional ^{1}H NMR spectroscopy was employed for the identification of components (Jawad et al., 2018). Baranowska et al., (2012) studied starch-colloid binary gels and explained

retrogradation (recrystallization) of starch molecules by low field, time domain (TD) NMR, inversion recovery sequence (T_1 relaxation time measurement). T_1, which is also known as spin–lattice relaxation time or longitudinal relaxation time, denotes the time necessary for the spins to reach their equilibrium state after excitation with the radio frequency pulse. It is known that that T_1 measurement could give information on the moisture distribution of the samples since it is affected from the presence of water protons and their mobility.

Solid fat content (SFC) measurement is an official technique that was universally approved for analysis. The procedure relies on the differentiation of solid and liquid signals form a single FID decay curve. The idea comes from the fact that solid signal decays much faster than liquid signal (*Determination of Solid Fat Content (SFC) in Oils and Fats by Pulsed- NMR Analyzer [Brochure]*, 2017). Since the solid molecules interaction is higher for a crystalline matrix due to close packing, they relax faster than liquid molecules (Porter & Hartel, 2013). The amplitude of the corresponding signals ("S" for solid signal amplitude, "L" for liquid signal amplitude) and a correction factor (f) are used to mathematically calculate SFC (Figure 1.10). Point "S" should ideally be at the maximum of the signal, however, inevitable dead time of the equipment and the time for sending the complete pulse delay the measurement that is why the point is drawn at a representative point. The time passes until the signal is applied and the echo is recorded is called "dead time", which is one of the main challenges of the relaxation measurements. The factor "f" is determined by a calibration curve to estimate the delay coming from the dead time.

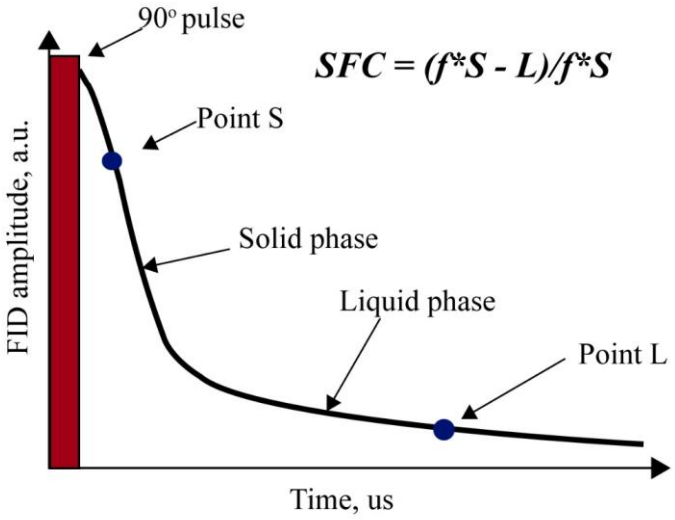

Figure 1.10. A representative FID decay collected after *a single* 90° pulse, *denot*ing fast decaying solid phase and slow decaying liquid phase.

Porter & Hartel (2013) developed a procedure to quantify sucrose crystal content of fondant, a confectionary product prepared by cooling supersaturated sucrose syrup mixture under intense agitation. They proposed that crystallinity could also be calculated similar to SFC procedure. Their results suggested the method to provide a good understanding of the crystalline fraction of different high sugar systems (Porter & Hartel, 2013). In 2016, Dejong & Hartel took the study one step further, and applied this modified SFC approach to determine crystallization rate of a sugar-free sweetener, sorbitol, at different temperature and moisture contents. An empirical model was utilized to explain time dependent increase in crystal content, which succeeded to represent data set with high correlations (Dejong & Hartel, 2016).

As can be inferred from those examples, food scientist approach to TD-NMR crystallinity mainly focuses on relaxation parameters, or relies on spectroscopy. On the other hand, polymer scientists' approach is mainly based on the second moment to quantify and explain the crystallinity, which is one of the most important characterization tools to have an idea of the quality of a polymer. Although simple

relaxation parameters (FID, T_1, and T_2) give accurate information on the internal motion, they are not sufficient to explain and quantify the crystallinity of samples with restricted molecular mobility. For those powder samples with low moisture and high solid content, widely used FID sequence could not be sufficient to collect signal of the solid fraction due to equipment and methodology constraints mentioned before (dead time problem). One way to overcome this problem is having a specific equipment with a dead time of 1-2 μs (Maus et al., 2006), which may not be the case at the present technical conditions. For this purpose, Solid Echo, a.k.a. "quadrupole-echo", (SE) and Magic Sandwich Echo (MSE) sequences were developed to be used to refocus the signal (at low frequencies) to recover the information of the solid fraction (Boutis & Kausik, 2017; L. Grunin et al., 2019). SE is a modified form of the FID signal (single 90° pulse), followed by another 90° pulse. By performing a back extrapolation over a series of experiments with different echo delays, SE could be used to quantify the degree of crystallization (L. Grunin et al., 2019; L. Y. Grunin et al., 2017). On the other hand, MSE is an advanced form of SE, which dramatically increases measurement time but also increase the signal due to refocusing of the initial fast decaying component (Figure 1.11). The increase of the signal amplitude (Figure 1.11, on the left) and the area of the Fourier transformed data (Figure 1.11, on the right) is an indication of more signal collection. The sequence is adaptable to any NMR equipment (both at low and high field) to yield similar crystallinity results (Maus et al., 2006).

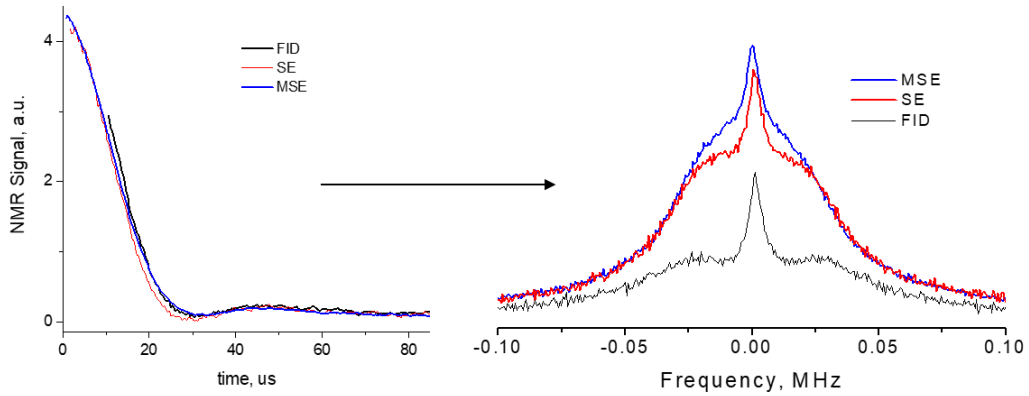

Figure 1.11. Comparison of the overall signal taken from the application of FID, SE and MSE sequences (on the left) and their Fourier transform (on the right).

After the signal is collected, the interpretation method mostly used for polymers depends on the individual system. While simple exponential formulas could be sufficient to explain liquid systems where there is significant mobility, magnetization decays become more difficult to model for solid systems with restricted mobilities. Once the decaying signal is collected by either methods, fitting of the curve by using second moment gives information on the mobility of different phases in the structure (L. Grunin et al., 2019; Uehara et al., 2000). Although famous Abragamian function $\left[exp\left(-\frac{1}{2}a^2t^2\right)\sin(bt)/bt\right]$ is frequently used in the literature to model crystallites, it did not fit very well to model cellulose samples. Thus, L. Y. Grunin et al., (2017) used Anderson-Weiss approximation, which is the Gaussian function $\left[exp\left(-\frac{1}{(T_2^{am})^2}t^2\right)\right]$ to model cellulose behavior in their study (L. Y. Grunin et al., 2017).

Depending on the trend of the decaying line, one can choose a typical model that best describes their system for characterization. *Gaussian, Lorentzian, Abragamian*, stretched exponential or compressed exponential functions are some of those models. Representative curves for typical trends were shown in Figure 1.12. For highly crystalline materials, *Abragamian* function is generally used, which has a typical bump following the initial fast decaying line. The fluctuation represents strong

second dipolar moment and described by a combination of sinc and exponential functions in the equation (Besghini et al., 2019; Hansen et al., 1998). One can simply fit the data to Gaussian model for the solid part and Weibullian for the more mobile part, the latter being an indication of phase separation (Uehara et al., 2000). Mixed systems generally require to use a combination of those models, such as the semi-crystalline model for samples with both crystalline and amorphous components, amorphous part being represented by either Weibullian, exponential, stretched exponential or a combination of these models (Litvinov & Penning, 2004).

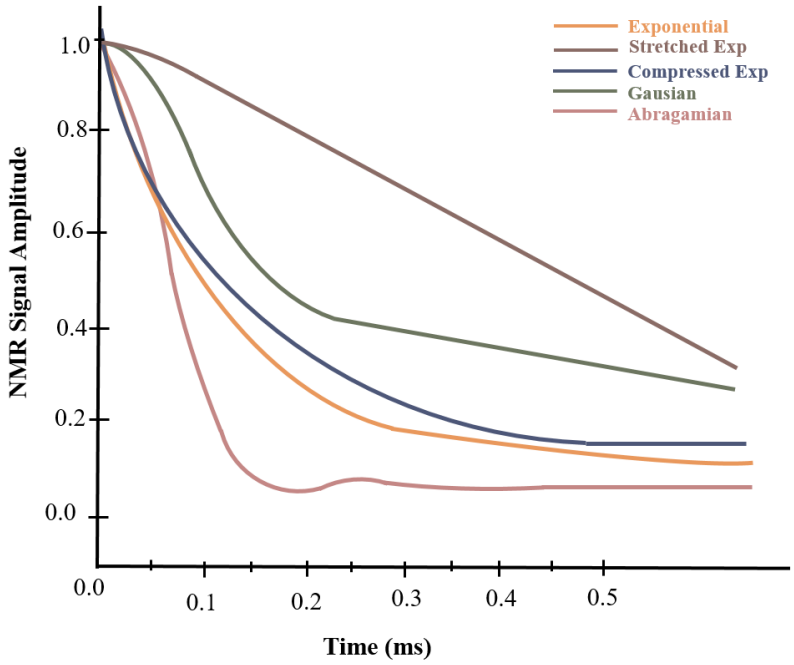

Figure 1.12. Representative curves for models used to describe signals.

1.7 Objectives of the Study

In this thesis, the main goal is to measure crystallinity by using bench-top TD-NMR method as an easy to use, nondestructive, rapid tool. Quantification of the crystallinity in the structure by this method can expand the use of crystallinity as a quality control tool and will not require specially trained staff for the analysis and significanly decrease the result interpretation time. Validation of the method by the application on food powders will give information on the physical changes induced by environmental changes, which enable prediction of storage characteristics. Correlation of the results with the caking behavior will give an idea on the combined effect of food ingredients and environmental factors change on any sample of concern.

Minor goals of the study are:

- To quantify the crystalline and amorphous fractions of different sugars modified by freeze drying, since their amorphous fraction cause significant problems during manufacturing of new and existing products.
- To compare the applicability and effectiveness of SE and MSE sequences for crystal content quantification on solid food systems.
- To quantify crystal formation of different sugars on crystal growth stage by kinetic analysis, which is typically monitored by microscopic analyses, which only provides 2D data and may not be reproducible.
- To have an attempt to understand the relation between sucrose and water, on the perspective of hydration shells by NMR spectroscopy.
- To understand the moisture uptake at the presence of high and low surface fat content on the powder particles.
- To relate the crystallinity degree with the mobility of the enclosed components and have an idea of the caking tendency of food powders at different relative humidity and fat contents to verify that multiple factors could also be detected by the proposed method.

CHAPTER 2

MATERIALS AND METHODS

2.1 Applicability of the Method by the Crystallinity Analysis of Sugars

2.1.1 Sample Preparation

Glucose, and lactose were purchased from Smart Kimya (Turkey) and LAB M (United Kingdom), respectively. Commercial crystal sucrose was purchased from a local market with the brand name Altın Küp (Turkey). Sugars were intentionally processed through freeze drying to make them more hygroscopic and amorphous (Ergun et al., 2010) so that crystallinity would decrease.

Freeze drying (FD) of glucose, sucrose (50% w/v) and lactose (10% w/v) were carried out using a vacuum freeze dryer (LGJ-10, Beijing Songyuan Humxing Tech. Co. Ltd., Beijing, China).

2.1.2 X-ray Diffraction (XRD)

XRD experiments were conducted to explain the structural behavior of the powder samples to support NMR data. All the samples were analyzed by using Rigaku Ultima-IV X-Ray Diffractometer equipment at METU Central Laboratory. The sampling width, scan axis, scan range, and scan speed were 0.02°, 2θ, 5-80°, and 1°/min, respectively. To quantify the crystallinity, the smooth area under the XRD curve was calculated and assumed as the amorphous fraction while the area under thin distinct peaks represented crystalline fraction (Belcourt & Labuza, 2007).

2.1.3 Scanning Electron Microscopy (SEM)

SEM *with* FEI Nova NanoSEM 430 equipment was used for the investigation of surface morphology of the samples. Measurement voltage was kept at 5 kV to prevent sample damage and the images were taken at different magnifications for all of the studied sugar samples.

2.1.4 TD-NMR Measurements

Solid Echo (SE) experiments were conducted using a 20.34 MHz system (Spin Track, Resonance Systems GmbH, Kirchheim/Teck, Germany) equipped with a 10 mm r.f coil. 90^{o} r.f pulse duration was 2.4 μs. As mentioned previously, the *Solid Echo* sequence was chosen to rapid up the measurement process. We have observed considerable decrease of the SE after interpulse time (τ, Fig. 2.1 b) exceeded 14 microseconds, so it was set up at 10 μs while the probe ringing time was 9 μs. Repetition delay was set to 10 s for all samples. 4 scans were acquired for each measurement. Three replicates were used for each sugar and mean values were reported.

For the MSE experiments the sequence was constructed according to Figure 2.1c and 4 phase cycling steps were applied similar to a previous study (Cucinelli Neto et al., 2018). Three replicates were used for each sample and mean values were reported. Crystallinity analysis was done using the special module on the Relax8 (Resonance Systems GmBH, Kirchheim/Teck, Germany) software that was able to calculate values of the spectral line second moment M_2.

A calibration curve was established using mixtures of dry sucrose (assuming as pure crystalline) and FD sucrose (assuming as pure amorphous) at different ratios (20%, 40%, 60%, 80% w/w).

The details of the analysis procedure could be reached from the study of Grunin et al. (2019).

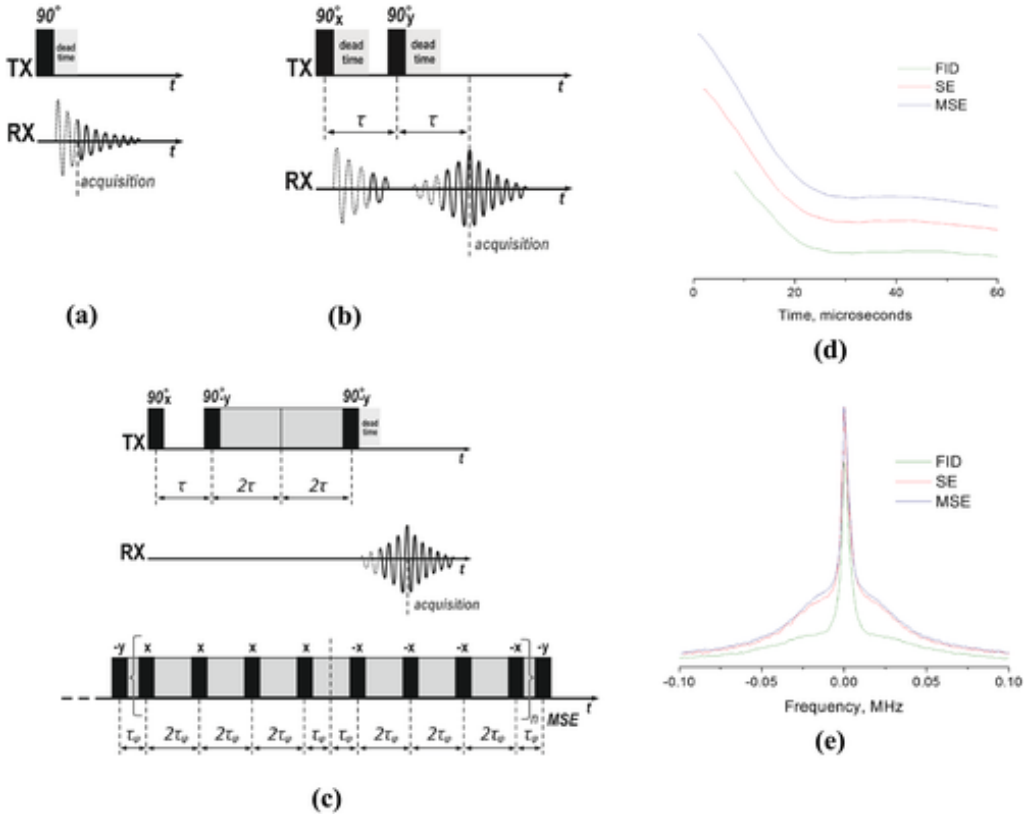

Figure 2.1. Comparison of FID (a), SE (b) and MSE (c) sequences pulse diagram, signals acquired from application of those sequences (d) and the signals obtained from their Fourier transformation (e).

2.1.5 Statistical Analysis

The results were analyzed by 1-way ANOVA and correlation tools of Minitab (ver.16.2.0.0, Minitab Inc., State College, USA) at 5% significance level. Tukey's comparison test was used at 95% confidence interval to determine the statistical significance between results. Origin 9 was used for modelling the data (OriginPro 9.0, Origin Lab Corporation, Northampton, USA).

2.2 Use of Crystallinity Measurement Approach on Model Food Systems

2.2.1 Sample Preparation

Glucose, fructose, sucrose, lactose and allulose sugars were used. Sucrose and allulose were supplied from a local grocery store (Altınküp, Ankara, Turkey) and Santiva Inc. (All-u-lose, Downers Grove, IL, USA), respectively. Fructose, glucose and lactose were purchased from Smart Kimya Trade. Co. Ltd. (Tito, Izmir, Turkey).

To prepare the sugar samples, the method of Dejong and Hartel (2016) was used. Saturated sugar solutions at 50°C were prepared in distilled water. The solubility at 50°C were 69.43, 83.02, 49.00, 86.58 and 18.72% (w/w) for sucrose, allulose (Fukada et al., 2010), glucose (Jackson & Silsbee, 1922), fructose (Fukada et al., 2010) and lactose (Belitz et al., 2009), respectively. Each saturated solution was mixed with its powder form to achieve 60% (w/w) powder concentration and mixed until homogeneity. Samples were filled in 10 mm NMR tubes and equilibrated to 50 °C in water bath. For the measurements, samples were taken from water bath (50°C) and inserted in the NMR sampling space, which was held constant at a temperature of 28 °C.

A calibration curve was also prepared for each sugar by mixing saturated sugar solution (at 28°C) with 35, 50, 65 and 80% (w/w) powder form. Samples were prepared in triplicate.

The solubility of the samples at 50°C were assumed as 72.25% (2.6036 g sucrose/water), and 30.07% (0.4370 g lactose/water), 83% (4.89 g D-allulose/water). Later on, the saturated solution was packed with powder form of the sugar to achieve 60% (w/w) powder concentration and mixed until homogeneity. Samples were filled in 10 mm NMR tubes and equilibrated to 50 °C in water bath.

For the measurements, samples were taken from water bath (50°C) and inserted in the NMR sampling space (Spin Track, Resonance Systems GmBH, Kirschheim/Teck, Germany) with constant temperature of 28 °C.

2.2.2 Determination of Crystal Mass Fraction (CMF)

Supersaturation is the driving force that enable crystallization in all systems that is why it is important to predict the crystallization behavior. As the crystals grow out the solution, the driving force in the solution decreases or when the supersaturation ratio is too high, it becomes really challenging to control crystal type, formation rate or size. In this study, supersaturation ratio was expressed as the mass fraction of crystals according to the given formula:

$$CMF = \frac{(S_T - S_S)}{(W_T - W_w)} \times 100 \qquad \text{(Equation 2.1)}$$

where S_T, S_S , W_T and W_w are the total sucrose in the finished product on a 100 g water basis, solubility of sucrose at a given temperature on a 100 g water basis, total solids in the formulation on a 100 g water basis and the weight of the water portion or 100 g, respectively (Miller & Hartel, 2015). Calculated results were given in Table 2.1 for the studied processing temperatures.

Table 2.1 Theoretically calculated crystal mass fractions (CMFs) for sugar samples at process temperatures (50 °C and 28 °C).

Sugar Type	CMF at 50°C	CMF at 28°C
Glucose	1.01	1.17
Fructose	0.67	0.78
Sucrose	0.82	0.87
Lactose	1.66	1.75
Allulose	0.69	0.83

2.2.3 X-ray Diffraction Analysis

X-ray Diffraction (XRD) experiments were conducted to explain the structural behavior of the powder sugar samples to complement the NMR data. All the samples were analyzed by using Rigaku Ultima-IV X-Ray Diffractometer equipment (The Woodlands, USA) at METU Central Laboratory. The sampling width, scan axis, scan range, and scan speed were 0.02°, 2θ, 5-50°, and 1°/min, respectively.

2.2.4 TD-NMR Measurements

For the kinetic measurements, samples were allowed to crystallize as their temperature decreased gradually from 50 to 28 °C at the r.f coil inside the magnet and this change was monitored by Solid Echo (SE) sequence. (1H) NMR experiments were conducted on a 20.34 MHz system (Spin Track, Resonance Systems GmbH, Kirchheim/Teck, Germany) that was equipped with a 10 mm radio frequency (r.f) probe. 90° r.f pulse duration was 3.4 μs. Inter-pulse time was set up at 10 μs whereas the probe ringing time was 9 μs. Four scans were acquired for each measurement.

Crystallinities were calculated by using the approach in the study of Berk, Grunin, and Oztop (2021) using MATLAB (Mathworks, 2019a). Three replicates were measured for each sugar and mean values were reported.

2.2.5 Statistical Analysis

The results were analyzed using appropriate tools of Minitab (ver.16.2.0.0, Minitab Inc., United Kingdom) at 5% significance level. Tukey's comparison test was used at 95% confidence interval to determine the statistical significance between results.

Interpretation for the modeling of the data was made by using Origin (OriginPro 9.0, OriginLab Corporation, Northampton, US).

2.2.6 Concentration-dependent Hydration Behavior of Sucrose studied by High Field NMR Spectroscopy

2.2.6.1 Preparation of saturated aqueous solutions of sucrose

High purity sucrose (≥99.5%) was purchased from Sigma-Aldrich (Merck KGaA, Darmstadt, Germany) and used as received HPLC grade MilliQ water was used to prepare the aqueous solutions. The concentration of those 20 solutions changed from 5 to 2000 mole of water/mole of sucrose. This unit, which corresponds to the amount of water molecules per solute will be reffered as "R" value through the text.

2.2.6.2 Nuclear Magnetic Resonance (NMR) Spectroscopy

The samples for NMR analysis were prepared by inserting 3 mm tube filled with deuterated toluene into a 5 mm NMR tube, filled with sample. Proton spectra of the supernatants of the saturated sucrose solutions prepared according to the procedure explained above were acquired at a set temperature of 28 °C using a liquid state proton NMR Bruker Avance 500 MHz spectrometer (Bruker, Billerica, MA, USA) with a 5-mm Broadband Observe (BBO) probe. A similar set of experiments was also conducted at 5 °C using a Bruker Avance NEO 600 MHz NMR equipped with RT BBO Smart Probe.

Deuterated toluene was filled in 3 mm NMR tube and used as the lock sample. The lock sample was placed inside the sample of interest (which was taken from the supernatant of supersaturated solution and placed in 5 mm tube) before each measurement.

The recorded spectra were analyzed using the TopSpin 4.1.1 software. Peak assignment was confirmed using additional data collected on one concentrated sucrose solution by Carbon-13 (13C), 2D, heteronuclear single quantum coherence (HSQC) and total correlation spectroscopy (TOCSY).

2.3 Use of Crystallinity Measurement Approach on Real Food Systems

2.3.1 Sample Preparation

To monitor the effect of fat content on the crystallization behavior of food samples; milk powders (low fat (LF) and whole fat (WF)) and cheese powders (WF and Light feta cheese) (Mis Süt Sanayi, İstanbul, Turkey) were used. While milk powders were kindly supplied by Sütaş (Sütaş Süt Ürünleri), cheeses were bought from a local grocery store and freeze dried. For this purpose, a lyophilizator (LGJ 10, Beijing Songyuan Humxing Tech. Co. Ltd., Beijing, China) was operated for 48 hours.

Powder samples were spread as a thin layer on the glass petri dish, covered and kept for 1 hour in the oven at 90 °C. After the temperature history of fat was reset with that procedure, the samples were kept in the desiccator until they reach room temperature, and then they were placed in TK120 climate chamber (Nüve Industrial Materials Manufacturing and Trade Inc., Ankara, Turkey) adjusted to 40, 50, 60 and 70% relative humidity at 21 °C until they reached equilibrium (confirmed by water activity measurements).

2.3.2 Determination of Water Activity

Equilibrium relative humidity of the samples were confirmed by water activity measurements. AquaLab water activity meter (Decagon, Model 4TE, Pullman, Washington), which operates based on dew point principle was used for the measurements.

2.3.3 Moisture Content Analysis

Moisture content analysis was conducted by using Radwag MA 50.R infrared moisture analyzer (Radwag Balances and Scales, Poland). The samples were set to

105 °C and the temperature was kept the same for 4 minutes until they reach constant weight. The results were presented as the average of 3 samples in weight percent.

2.3.4 Surface and Total Fat Content Analyses

Surface and total fat contents were measured for the samples experiencing crystallization changes due to changing relative humidity environments (at 40, 50, 60 and 70 % relative humidity). The method of Foster et al. (2005) was used for surface fat content analysis. 4 grams of powder sample was weighed and washed with 50 ml of petroleum ether (Isolab Laborgerate GmbH, Eschau, Germany) with a boiling range of 40-60 °C. The powder and petroleum ether were then passed through Whatman No: 1 (125 mm) filter paper and the residues washed with 25 ml of ether. The filtered sample was dried in an oven at 105 °C and weighed until it reached constant weight. The amount of surface fat was calculated by subtracting the tare from the total weight and presented as the amount of surface fat in 1 gram of sample. Reported results were given in grams per dry basis.

The Soxhlet method was applied to measure the total fat content of powder food samples with different fat contents. For this purpose, 3-5 grams of the samples were weighed and wrapped in filter paper. Soxhlet set up a run for 5 hours and hexane (Merck KgaA, Darmstadt, Germany) was used as the solvent. After extraction, hexane was evaporated and the fat content was calculated by subtracting the tare from the total weight and presented as the amount of % fat in 1 gram of dry sample. The terms surface fat and free fat content were used interchangeably throughout the text.

2.3.5 TD-NMR Measurements

Powder samples at different relative humidity were directly filled into NMR tubes (diameter of 10 mm) after reaching equilibrium relative humidity. (^{1}H) NMR experiments were conducted on a 20.34 MHz system (Spin Track, Resonance

Systems GmbH, Kirchheim/Teck, Germany) that was equipped with a 10 mm radio frequency (rf) probe. 90° rf pulse duration was 3.4 µs. Inter-pulse time was set up at 10 µs whereas the probe ringing time was 9 µs. Results were analyzed by using Relax 8 (Resonance Systems GmBH, Kirchheim/Teck, Germany) software using semi crystalline model (Equation 1). 16 scans were applied and the mean value of three replicates were reported. (diameter of 10 mm) after reaching equilibrium relative humidity. (^{1}H) NMR experiments were conducted on a 20.34 MHz system (Spin Track, Resonance Systems GmbH, Kirchheim/Teck, Germany) that was equipped with a 10 mm radio frequency (rf) probe. 90° rf pulse duration was 3.4 µs. Inter-pulse time was set up at 10 µs whereas the probe ringing time was 9 µs. In addition to SE and MSE measurements, T_1 relaxation time was also measured for powdered samples. 4 and 16 scans were applied for T1 measurements and crystallinity measurements, respectively. Results were analyzed by using Relax 8 (Resonance Systems GmBH, Kirchheim/Teck, Germany) software using semi crystalline model (Equation 2.2). Mean value of three replicates were reported.

$$s(t) = A_{cr}\exp(-\frac{1}{2}a^2t^2)\cos\frac{1}{2}bt + A_{am}\exp(-\frac{1}{2}M_2^{am}t^2) + A_w\exp\left(-(t/T_2^{*w})^2\right.$$

(Equation 2.2)

where “s” denotes the signal, “A" is the amplitude, “M_2” is the second moment, “T_2” is the spin-spin relaxation time, “t” is time, “a” and “b” are constants. “cr”, “am”, and “w” represents the crystalline, amorphous and water fractions, respectively.

This function (cosine) was initially developed for cellulose and selected instead of classical Abragamian (sinc) due to better fitting match with experimental data of relaxation decays in our samples.

Considering that "A_{cr}" and "A_{am}" show the population of protons of ordered and amorphous domains in the structure (L. Y. Grunin et al., 2017), crystallinity values were calculated by:

$$\frac{A_{cr}}{A_{cr}+A_{am}} \quad \text{(Equation 2.3)}$$

2.3.6 Statistical Analysis

The results were analyzed by 1-way ANOVA and correlation tools of Minitab (ver.19, Minitab Inc., State College, USA) at 5% significance level. Tukey's comparison test was used at 95% confidence interval to determine the statistical significance between results. Origin 9 was used for modelling the data (OriginPro 9.0, Origin Lab Corporation, Northampton, USA).

	Factors	Levels	Characterization Techniques
#1 APPLICABILITY	Sugar type	Glucose Lactose Sucrose	SEM XRD NMR (SE & MSE sequences)
	Drying method	Control Freeze drying	
#2 MODEL SYSTEM	Sugar type	Glucose Lactose Sucrose Allulose Fructose	XRD NMR (SE sequence)
	Cooling	50°C to 28°C	
#3 REAL SYSTEM	Sample Type	Milk Powder Cheese Powder	Moisture Content Water Activity Surface Fat Content Total Fat Content NMR (MSE sequence)
	Fat Content	Low fat Whole fat	
	Storage condition (Relative Humidity)	40% 50% 60% 70%	

CHAPTER 3

RESULTS AND DISCUSSION

Crystallinity degree of the food samples could be affected from extrinsic factors like temperature and relative humidity of the environment as well as intrinsic factors like water activity, sugar content and the presence of solid fat in the mixture. That is why shelf life of the confectionary products depends on storage temperature and the hygroscopicity of the confection and the necessary precautions should be taken during transportation or storage especially for the exported goods. Characterization of the crystallization behavior for sugar derivatives is a very important quality aspect in confectionary industry as it may result in graining or hardening depending on the nature of the product. Sugar content, amount of melting fat, water activity, amorphous fraction, storage temperature and relative humidity (RH) trigger stickiness and result in caking, which is an important factor affecting fluidity and quality of powdered food samples during production and storage. Monitoring and detection of stickiness as the indicator of caking is important for the stability and functionality of powdered foods.

The main objective of this study is to develop a reliable quality control method, which will enable quantification of crystallinity for food powders. To achieve this goal, three consecutive research were made to confirm the applicability first, then the approach was used on model systems and finally applied on real food systems.

First step, confirmation of the applicability of (^{1}H) NMR (SE/MSE sequence) as a means to quantify crystallinity degree was tested on simple sugars. XRD was used as the control analysis. Simple sugar samples (glucose, sucrose, and lactose) were freeze dried to interfere their crystallinities. Calibration curves were prepared by using amorphous and fully crystalline sucrose at different proportions. Following calibration, the correlation of XRD with SE and MSE results were really high (0.94

and 0.96, respectively). High correlations confirmed that the integration of the FFT of the solid signal was sufficient to calculate the second moment, and the idea of its linear dependence with the crystallinity was confirmed. Our approach was sufficient to explain the crystallinity of the sugar powders. As the second step, different sugars were put in a dynamic system in a solution where their crystallinity were intentionally altered by changing the temperature. Crystalline fraction of the supersaturated sugar samples was kinetically quantified by the proposed SE and MSE sequences as an alternative to Free Induction Decay (FID) based Solid Fat Content (SFC) sequences, which have been traditionally used in the literature.

After recording the signal, back extrapolation on successive experiments with varying echo delays gave the quantity of the crystal content (%). MSE is a modified version and it was derived from SE sequence. In fact, it enables refocusing of the nearly all the signal to provide more detailed information than SE. However, the measurement time for MSE is longer than SE due to the requirement of four phase cycling steps, which was the main drawback at the beginning of the crystallization stage where the nucleation was fastest. In this study; crystallization of lactose, sucrose, glucose, fructose, and a rare sugar (D-allulose) were kinetically monitored. As the elevated temperature (50 °C) of the supersaturated solution was cooling down to room temperature, crystallinity increase was successfully monitored by the applied SE sequence. R-square values for the applied models changed between 0.929-0.996. Since MSE analysis took much longer than both SE and FID, it was not appropriate for a kinetic analysis, as suspected at the beginning. On the other hand, simple FID analysis results were not as accurate as the results of SE analysis. Calculated kinetic constants showed that sucrose crystallizes much faster (4 fold) than lactose while the crystallization process was the slowest for glucose and fructose, which was explained by the conversion of different forms of more stable forms in aqueous solution. Mutarotation rate had a competent effect on the crystallization of those sugar types. Since D-allulose enantiomers were naturally present in comparable amount in the solution, mutarotation was not restrictive on its crystallization rate.

As the final step of the research, crystallinity calculation was applied on the real food powders. To understand the effect of moisture adsorption on the crystallinity; cheese powders (whole fat and light) and milk powders (low fat and whole fat) were stored at different relative humidity. Crystallinity values calculated from the signal that was acquired by MSE sequence were fitted to a semi-crystalline model. Crystallinity of the samples decreased as the relative humidity or moisture content of the samples increased. The exceptions to this trend were explained by the change in free fat content on the particle surfaces and moisture content. In general, moisture adsorption was the prominent variable in our experkimental design, however the effect of fat and salt content was also defined and the underlying mechanism were explained to understand caking phenomenon.

3.1 Applicability of the Method by the Crystallinity Analysis of Sugars

To obtain quantitative measurement on crystalline and more mobile amorphous fractions, alternative sequences to the classical FID were proposed to be used. SE and MSE sequences perform the relaxation decay refocusing excluding the dead time problem and allow detection of the signal from the solid fraction. At the previous study, knowledge of amorphous/crystal fraction, which is obtained through SE and MSE has been explored on powder sugar samples for the purpose of developing a groundwork for a reliable quality control method. Calibration curves had been prepared by using amorphous and fully crystalline sucrose at different proportions (Figure 3.1). The crystallinity of calibration materials were justified by XRD (Figure 3.2).

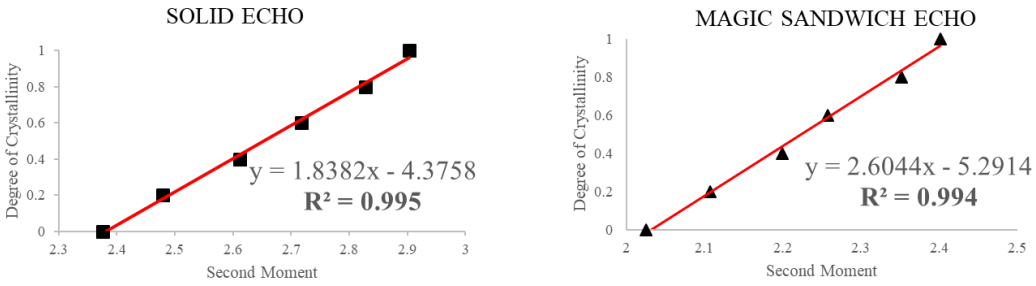

Figure 3.1. Calibration curves prepared for SE (left) and MSE (right) sequences.

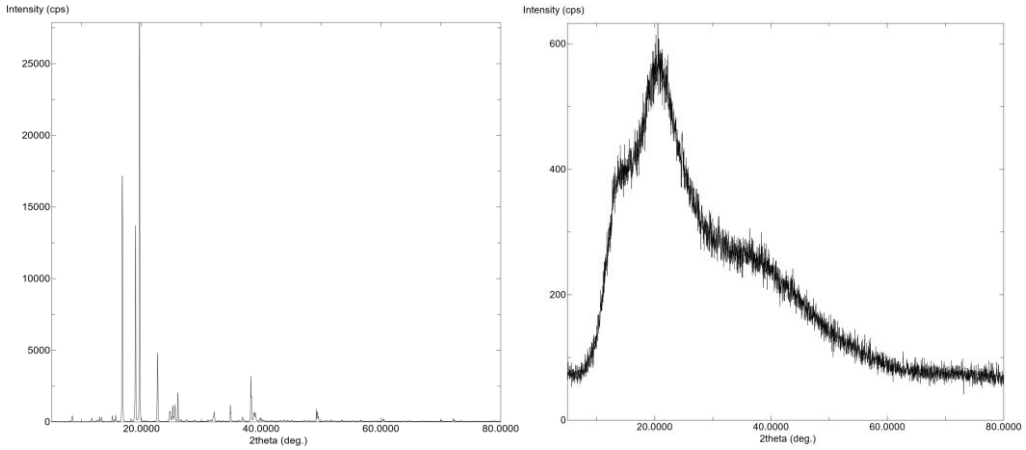

Figure 3.2. XRD spectra for sucrose control (left) and freeze-dried sucrose (right).

For the studied sugar samples (control and freeze dried forms of lactose, sucrose and glucose), SE and MSE analysis were conducted and the results were given in Table 3.1 and Table 3.2. Samples were also visualized by SEM (Figure 3.3) and the crystallinity values were verified by XRD (Figure 3.4).

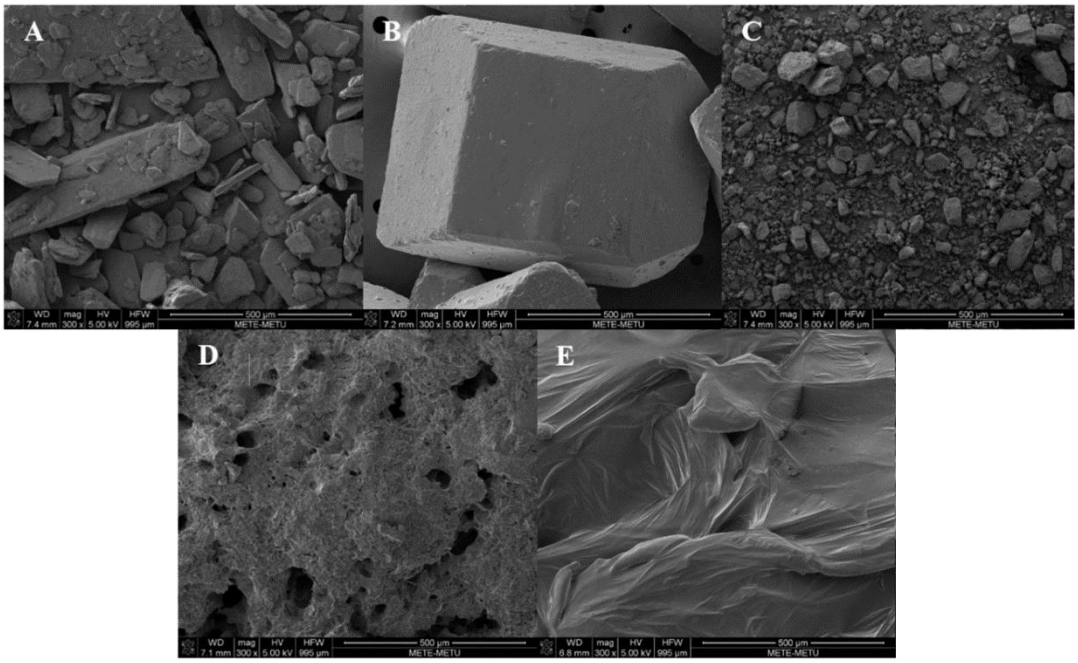

Figure 3.3. SEM images of glucose control (A), sucrose control (B), lactose control (C), freeze dried glucose (D), and freeze dried sucrose (E).

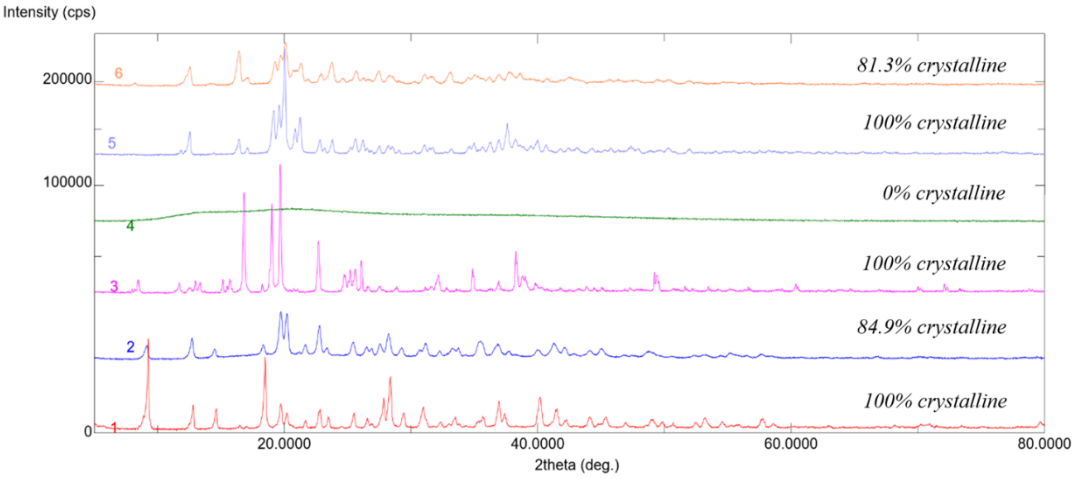

Figure 3.4. XRD spectra for glucose control (1), freeze dried glucose (2), sucrose control (3), freeze dried sucrose (4), lactose control (5) and freeze-dried lactose (6).

The method proposed did not involve multiparameter fitting of the signal that normally suffers from ambiguity; just the integration of the FFT of the solid echo was needed to calculate the second moment, (M_2). Applicability of the proposed method had been verified on the simple sugar systems.

Table 3.1. SE and MSE crystallinity values* of different sugars exposed to Freeze drying

	Control	Freeze Dried	Control	Freeze Dried
	SE		MSE	
Glucose	$105.93^{AB} \pm 10.18$	$116.01^{A} \pm 1.33$	$113.68^{b} \pm 3.56$	$114.16^{b} \pm 4.41$
Lactose	$90.53^{C} \pm 0.96$	$88.94^{C} \pm 4.75$	$88.06^{d} \pm 2.55$	$98.36^{c} \pm 6.07$
Sucrose	$100.72^{BC} \pm 5.13$	$-14.53^{E} \pm 3.99$	$127.00^{a} \pm 1.12$	$-9.57^{f} \pm 3.61$

*Data represent mean values of at least 3 replicates and their corresponding standard deviations
*Lower case letters denote significance difference at 95 % CI between all samples for MSE analyses.
*Upper case letters denote significance difference at 95 % CI between all samples for SE analyses.

As the result of those analysis:

- The correlation of XRD crystallinity with SE and MSE crystallinities were found as 0.944 and 0.964, respectively. MSE was much better at predicting the crystallinity values.
- Integration of the FFT of the solid is sufficient to calculate the second moment, and the idea of its linear dependence on the crystallinity was confirmed. Our approach was sufficient to explain the crystallinity of the sugar powders.

3.2 Use of SE and MSE Sequences to Monitor Crystallization Kinetics of Model Systems

3.2.1 Comparison of Crystallization Rate of Different Sugar Types

For the fitting of time-dependent crystallization data, nonlinear fitting tool of Origin software was used. Phase transformation of solids are normally explained by the *Johnson-Mehl-Avrami* equation (also known as Avrami equation) which is in the form of:

$$y = 1 - e^{-kt^n} \qquad \text{(Equation 3.1)}$$

However, one of the assumptions to use Avrami equation is to conduct the measurement at a constant temperature. In the experiment setup of this study, the period of the most drastic crystallization change was observed at the initial stages where temperature decreased to come to equilibrium with the equipment temperature (28 °C). This temperature change was monitored manually and the equilibrium was seen to be reached in approximately 16 minutes. Most probably due to the fact that the crystallinity change in our experiment design is driven by the temperature difference, our data did not fit Avrami equation. Since the temperature equilibrium is reached in a relatively much shorter time (16 min) than complete crystallization, temperature itself was not included in the governing equation and assumed to be negligible. cc was applied which was in the form of:

$$SA = A_1 - A_2 * e^{-kt} \qquad \text{(Equation 3.2)}$$

where "SA" was Solid Amplitude (%), "t" was time (min), "k" was the kinetic rate constant while "A_1", "A_2" and "$A_1 - A_2$" were equilibrium crystal content (%), pre-exponential factor and initial crystal content (%), respectively.

To obtain a quantitatively interpretable data from the crystallinity curves, the measurements were conducted in triplicate and one example for each analysis with the fitting curves were given in Figure 3.5 and obtained constants were presented in Table 3.2. When the comparison was made between sugar types for the kinetic constant (k), it was seen that crystallization rate was the highest for sucrose, lasting less than 2 hours to achieve 99% of equilibrium crystallization. Order of crystallization rate decreased for lactose and allulose, respectively while glucose and fructose had the lowest crystallization, being significant (p<0.05) (Table 3.2). Fructose is already known with its high water binding capacity and it has been used to retard crystallization for decades in high sugar products (Brown, 2008), so the low kinetic constant of fructose was expected. What is prominent was the crystallization rate of glucose, being prominently lower than the others, even being 77 times slower than another monosaccharide, allulose.

Table 3.2. Model $SA = A_1 - A_2 * e^{-kt}$ parameters found for different sugar types and their significance denoted by capital letters for Tukey comparison test for 3 replicates conducted at 95% confidence interval.

Sample	**k (1/min)**	**A_1**	**A_2**	**(A_1-A_2)**
Allulose	0.00665 ± 0.00092^{C}	49.625 ± 0.946^{B}	12.121 ± 0.450^{A}	37.504 ± 0.840^{C}
Glucose	0.00009 ± 0.00002^{D}	48.694 ± 1.713^{B}	9.502 ± 0.699^{B}	39.192 ± 2.261^{C}
Fructose	0.00011 ± 0.00002^{D}	61.341 ± 3.254^{A}	7.132 ± 0.247^{C}	54.209 ± 3.230^{A}
Lactose	0.00943 ± 0.00141^{B}	36.760 ± 0.186^{C}	2.228 ± 0.134^{D}	34.533 ± 0.165^{C}
Sucrose	0.03651 ± 0.00673^{A}	50.203 ± 1.402^{B}	1.932 ± 0.257^{D}	48.271 ± 1.596^{B}

Possessing sharp angles in crystalline form, sucrose is prone to form fracture spots in the continuous network, that is why it is not singly used in products that require elongation, for example in the case of caramel (Miller & Hartel, 2015). Forming extra area due to sharp angles could be indicated as one of the reasons that speeds up crystallization for sucrose. Another reason of rapid crystallization could also be attributed to glass transition temperature at the studied concentration for sucrose and lactose samples (89% and 68%, respectively), which was reported to be result in rapid crystallization at the studied concentration in the literature (Y. Roos, 1993). Being a non-reducing sugar, the lack of mutarotation is another factor that encouraged fast crystallization, unlike other sugars, which already have a reducing end.

In theory, sugar molecule in the liquid should diffuse on the surface of sugar crystals first, to nucleate and grow. In our system where there is no impurity, pH change or agitation, change in Gibbs free energy to initiate nucleation was supposed to be due to the supersaturation ratio (B. M. Adhikari et al., 2018), which was represented with crystal mass fraction (CMF) in this study.

Furthermore, the energy of the system was high due to heating (to 50 °C), so the system tried to release its energy to reach chemical equilibrium when placed in a cooler environment (28 °C). Considering that the temperature change was same for all samples; the initial moisture content, seed size, solubility and nature of the sugar samples were varying independent factors that eventually caused the differences between crystallinity behaviors of sugars. On the other hand, CMF (concentration gradient) was the dependent factor to be focused on as it changed with respect to aforementioned independent factors, so it was one of the most important factors that affected the crystallization parameters in our system.

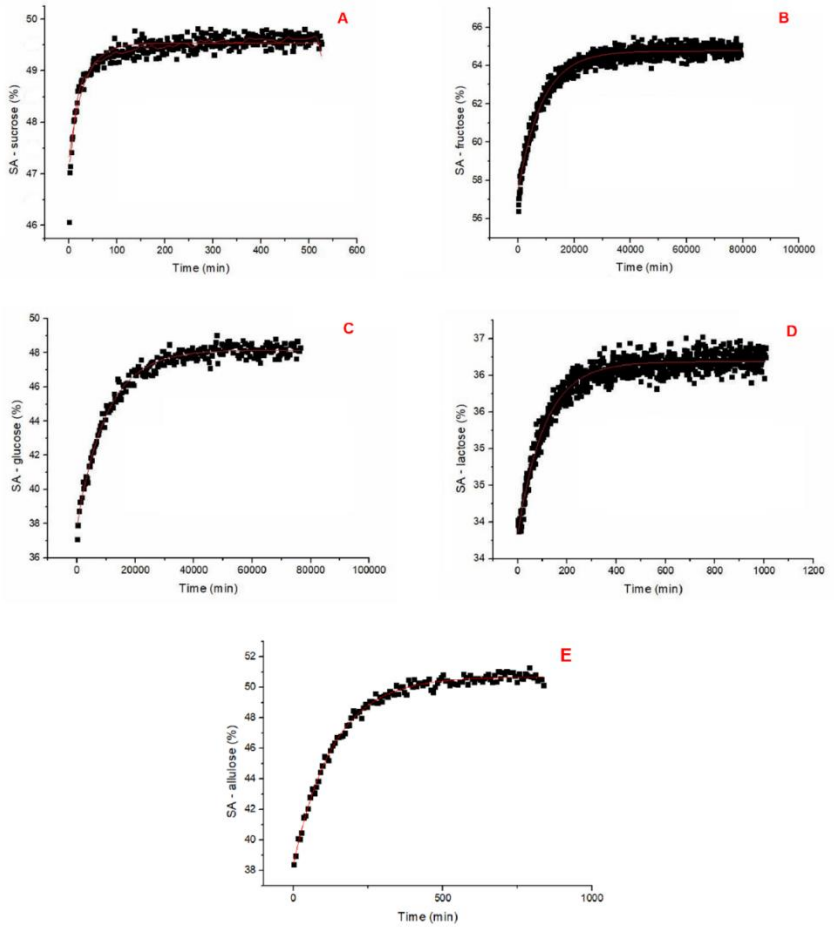

Figure 3.5. Solid amplitude measured by SE sequence as the samples crystallize when the temperature decreases from 50°C to 28°C and an example of one set data together with fitting results for sucrose (A), fructose (B), glucose (C), lactose (D) and allulose (E).

In the crystallization studies, the supersaturation zone is particularly important to control the process and the studied concentration is generally arranged to coincide with the metastable zone, which is slightly above the saturation line while the labile zone is avoided since it results in random nucleation and makes it difficult to monitor the system. Within the metastable zone, increase in supersaturation decreases metastability of the solution and results in an increase in crystallization rate (Schwartz & Myerson, 2002). In a heterogeneous solution with seeds like in our case, supersaturation was expected to increase crystallization rate, which was really high

at the studied concentration (Table 2.1). Due to its low solubility, the CMF of lactose samples were significantly higher when compared to other samples. Referencing the previous data on lactose stability zone (Teixeira et al., 2013), we could say that the concentration of the lactose samples coincided the labile zone, which could promote random nucleation. The images obtained from native powder form of the lactose crystals was spherical and small in size (Figure 3.6). However, again due to high saturation ratio, which drastically increased the driving force, the shape of the crystals could have transformed into a rough shape rather than smooth, as was proposed in the study of Cubillas & Anderson (2010). The rough edges of the present crystals were probably another factor that speeded up the crystallization rate for lactose.

Fluctuation in concentration and formation of new crystals could only be possible in an attempt to reach equilibrium state, so our system was a no equilibrium case (Erdemir et al., 2009), which means that the thermodynamics and kinetic of the system was also unsteady. We have seen large variations within the replicates of the samples and this is known to be one of the challenges of monitoring crystallization (Nagy et al., 2013). Monitoring an unsteady system is rather difficult and a sensitive process like crystallization could also be affected from many extrinsic and intrinsic factors as mentioned before. Such a hurdle was also cited in the literature for the solidification case, where high sugar content solutions were casted on molds, which is analogous to our case (Atsukawa et al., 2020). Although the samples are casted simultaneously, solidification was different for two sugar solutions and the state of the solid had a significant effect on this result (Atsukawa et al., 2020). Considering that the time scale to reach equilibrium is relatively long and the time dependent changes were attempted to be explained in such small sizes, individual variations are expected due to random motion and homogeneity of the replicates.

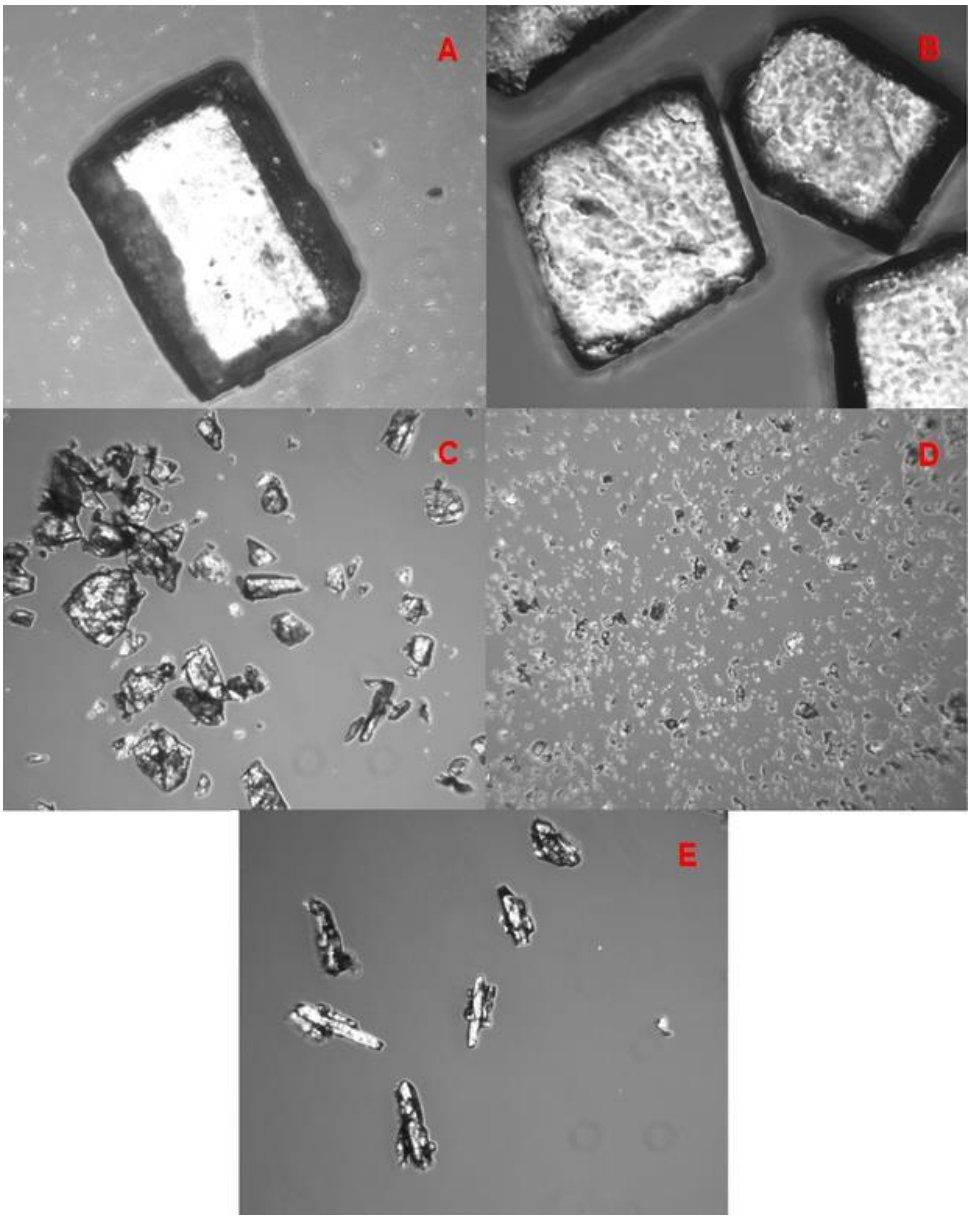

Figure 3.6. Optical microscope images of the original powder form of the sugars captured at x10 magnification; sucrose (A), fructose (B), glucose (C), lactose (D) and allulose (E).

As the disaccharides were explained to crystallize faster, comparison of the crystallization rate of the monosaccharides could be explained by their mutarotation vs crystallization reaction rates. Having at least one reducing end, all of the studied

sugars except sucrose have mutarotation ability in the solution form. In the case of crystallization, mutarotation is an important contributing factor on the crystallization rate since the aqueous form of the solution should always have its own balance of exchanging anomers. If the crystallization rate is relatively faster than the mutarotation rate, depletion of the crystallizing anomers results in a decrease on the crystallization rate (Srisa-nga & Flood, 2004).

In aqueous solution at 20 °C, D-glucose is known to exist in α-pyranose (31.1-37.4%) and β-pyranose (64-67.9%) forms while D-fructose is in α-pyranose (≈ 4%), β-pyranose (68.4-76.0%) and β-furanose (28.0-31.6%) forms (Shallenberger & Birch, 1975). On the other hand for D-allulose, four different forms could be found in the solution at 27 °C, which are α-furanose (39%), β-furanose (15%), α-pyranose (22%), and β-pyranose (24%) (Fukada et al., 2010). This type of equilibrium could compete with crystallization as one of the anomers starts to crystallize and the reversible mutarotation reaction is triggered to compensate the depletion. If the mutarotation rate was the restrictive reaction, crystallization is directly retarded. In their study on detection of mutarotation products of fructose in water at different temperatures and sucrose inversion, Cockman et al. (1987) mentioned a lagging time for glucose samples, which delayed the equilibrium state of anomers. This delaying also fits to our results as we have seen that glucose samples crystallized much slower than other monosaccharides. For glucose, the α:β ratio is around 1.5 at equilibrium conditions and this ratio is not affected from temperature or overall solution concentration (Srisa-Nga et al., 2006). However, fructose mutarotation was affected from temperature and the concentration of furanose form increased as the temperature was increased from 10 to 55 °C, decreasing the amount of pyranose form from 76.31% to 66.43% (Cockman et al., 1987). The tendency of glucose and fructose that significantly took longer to crystallize has also been reported in the literature (Srisa-Nga et al., 2006). To fully understand the reasoning behind this behavior, it is important to identify the crystal types in our samples. We know that as a native property, D-allulose and D-fructose have only one crystal form (β-pyranose) (Cockman et al., 1987; Fukada et al., 2010) while the stable crystal form

of D-glucose below 50 °C is the α-pyranose form (Horton, 2004; Srisa-nga & Flood, 2004). It is a known fact that conversion between pyranoses is slower than pyranose to furanose conversion (Bates, 1942) and the β forms are generally more stable when compared to α forms, which have higher bond energy. These properties are related to position of the hydroxyl group attached to the anomeric carbon and being in equatorial or axial position in the chair conformation determines the stability and energy barrier required for the crystal formation. Being in the axial position, overlapping of electrons of the neighboring hydroxyl groups result in an increase in the energy intensity. When we compare the number of hydroxyl groups positioned in equatorial direction, β-pyranose form of D-allulose had only C4 carbon while D-fructose had both C3 and C4 in equatorial position (Fukada et al., 2010). This fact enables comparison of the stability of the crystal form (β-pyranose) of the two ketoses. We could hypothesize that being in a lower energy state and in a more stable condition, crystal form of the D-fructose developed much later than D-allulose. Furthermore, crystallization of β-fructopyranose could have altered the equilibrium and the mutarotation kinetic of the furanose was forced to shift towards pyranose form, which is also known to be a fast reaction, so the mutarotation rate was not a restriction for crystallization of D-fructose. When the state of glucose was considered, the situation was just the opposite. As mentioned before, glucose is present as only in pyranose form and the crystallization forces interconversion between pyranose forms, which is known to be much slower than furanose-pyranose conversion (Shallenberger & Birch, 1975). That was why the crystallization of glucose was hypothesized to be restricted by mutarotation kinetics.

Considering that the conversion between pyranoses is slower than pyranose to furanose conversion, it was reasonable to have a higher mutarotation rate for fructose, which directly affects the amount of crystallization. For the allulose samples, it could be stated that presenting comparable amounts of all furanose anomers in the solution, mutarotation was quick enough to provide the crystal form and the reaction was favored that was why its crystallization was faster than the other studied monosaccharides, glucose and fructose.

It should also be noted that the equilibrium condition before and after the measurements were assumed to be achieved due to experimental preparation step at resting at the water bath prior to measurement for 1 h and the extended measurement time until equilibrium.

3.2.2 Use of Low Field TD-NMR for Quantification of Crystallization in Samples with High Solid Content

The degree of crystallinity changes between different sugar samples have already been discussed and the results provided a comparison between crystallinity rates. Now, quantification approach by the used SE sequence will be explained.

Initial solid (crystal) content of the samples was calculated theoretically to provide a comparable reference to our findings by using the SE pulse sequence (Table 3.3). Initial moisture content of the powders was also considered in the final solid content calculation, which were measured as 0.122, 8.000, 0.080, 5.093 and 0.031 for allulose, glucose, fructose, lactose and sucrose, respectively.

Table 3.3. Calculated parameters to correlate with the constants found by the application of SE sequence. ICC denotes the initial crystal content while FCC is the final crystal content.

Sample	Expected ICC (%)	Expected FCC (%)	Quantified ICC (%)	Quantified FCC (%)	Measured ICC (%)	Measured FCC (%)
Allulose	59.34	71.87	58.97 ± 0.68	71.96 ± 0.34	36.67 ± 0.67	49.33 ± 0.33
Glucose	65.44	73.05	67.90 ± 0.76	73.88 ± 0.62	38.33 ± 1.33	48.83 ± 1.09
Fructose	59.51	69.49	69.79 ± 1.49	75.96 ± 1.35	52.57 ± 2.08	61.17 ± 1.88
Lactose	61.23	64.86	63.69 ± 0.16	65.83 ± 0.12	34.73 ± 0.15	36.72 ± 0.11
Sucrose	63.60	67.91	65.85 ± 0.96	68.88 ± 0.89	47.00 ± 1.00	50.17 ± 0.93

A_1 value, which physically denotes the crystal content at the equilibrium, had a negative correlation with moisture content, as expected (Dejong and Hartel, 2016). When focused on the dependent variables, there were two parameters that could be interpreted as the indicator of the appropriateness of the results for quantification purposes. The first one was the initial crystallinity which corresponds to y axis intercept of the SE curves ($A_1 - A_2$) while the second one was the difference between initial and final crystallinities (A_2). Results for the kinetic model constants had been presented in Table 3.2.

Pearson correlation between A_2 and theoretically calculated solid content difference (due to supersaturation and cooling) was found to be 0.966 and it was significant (p<0.05). This is one of the strong indications that the method is successful to detect changes in molecular alignments.

When the initial solid amplitudes were compared, measured values showed two group of results. One group was significantly higher (consisting sucrose and fructose) than the rest of the samples, lactose, allulose and glucose samples (Table 3.3). To begin with, the initial state of the fructose and sucrose powders were particularly different from the others and their particle sizes were clearly larger. Although the particle size is not the exact cursor of the crystallinity, due to homogeneity of the distinct, regular shape of their particles, powder form of fructose and sucrose sugars were expected to be initially more crystalline. Microscopic images shown in Figure 3.6 distinctly reveal the structures. Fructose and sucrose particles were much bigger with sharp edges. Furthermore, the similarity of particles was more apparent, composing a more homogeneous composition while the similarity between particles as well as their sizes are much lower for the rest of the samples, namely lactose, allulose and glucose. To support this observation, XRD data were analyzed (Figure 3.7). While interpreting the XRD spectrum, one could expect wider peaks for amorphous samples while narrow peaks with no bottom enlargement are the sign of regular crystalline arrangement. The powder (initial) form of the samples were mostly crystalline however the peaks of fructose and

sucrose samples were higher in intensity and noticeably narrower. When the average of FWHM (full width at half maximum) was examined, we have obtained 0.117, 0.155, 0.152, 0.105 and 0.248 for sucrose, lactose, glucose, fructose and allulose samples, respectively. The width of fructose and sucrose peaks were much narrower than the rest of the samples, which was a strong basis for our initial crystal content hypothesis. So, it was concluded that having initially more noncrystalline fractions differentiated the initial results, which was also promising to show that this method could be a precise tool for quantification of specific samples.

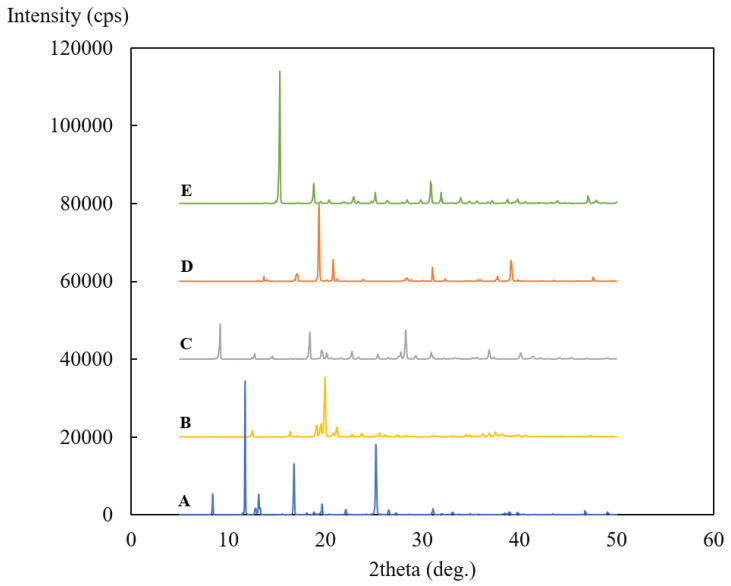

Figure 3.7. XRD graph for the initial powder form of sucrose (A), lactose (B), glucose (C), fructose (D) and allulose (E).

When it comes to the calculation of crystallinity difference or final crystallization, no correlation was found between theoretically calculated crystal contents and NMR solid amplitude results. To provide a quantified initial and final crystallization data for the process which will not be affected from the individual characteristics of the sugar types like particle size or shape, calibration curves were prepared for each

sugar type and the results were presented in Table 3.3. The correlation between the difference of expected and quantified crystallinities were found as 0.913 ($p<0.05$). The temperature driven crystallization rate was initially much faster than the rest of the process so it was expected to have higher initial crystal content when compared to the expected initial crystal content due to insertion of sample and measurement delay. The quantified results were found to be really close to the expected values except fructose samples. The reason was related with the unexpectedly high solubility of the studied fructose, which could not be correlated with any data from the literature.

The main focus of this study was on modelling the crystallization behavior for sugar systems at high concentration. The aim was to provide a quantitatively comparable data for crystallization rate of simple sugars and to explain the underlying chemistry behind their well-known behavior in the applications. Results showed that although the structure of the sugars were identical (glucose, fructose and allulose), crystallization rate could be drastically different. The competence of the anomers in the solution and the relative comparison between different isomers was explained by the conformation and equilibrium concentration of different anomers. To be specific, glucose mutarotation rate restricted the crystallization rate while for fructose, crystallization at the stable beta form was hypothesized to be the reason for retarding crystallization. On the other hand, another isomer of fructose, popular rare sugar of the last decade, allulose, had neither of those restrictions and enabled easy conversion for both mutarotation and crystallization reactions by possessing all four isomers at the comparable concentration at the same time in the solution.

3.2.3 Concentration-dependent Hydration Behavior of Sucrose studied by High Field NMR Spectroscopy

Over centuries and generations, sucrose has played a major role in our everyday life, whether it has been used for cooking, baking, or formulation and storage of food products.

Research on sucrose, spanning from studies on its physicochemical and structure/morphological properties at different temperatures/relative humidity conditions to its properties when combined with other food materials or dispersed/dissolved in different media, is grandly available, as it covers decades of investigations (Bock & Lemieux, 1982; Branca et al., 1999; Bressan et al., 1994; Lans, 2016; S. L. Lee et al., 2005; Lu et al., 2017; Olsson & Swenson, 2020; Yrjö H. Roos et al., 2013; Starzak et al., 2000). However, the hydration behavior of sucrose at the molecular level still lacks understanding, especially when we consider that even the bulk water itself is considered as state of equilibrium between a collection of clumps in different sizes (Starzak & Mathlouthi, 2002). The identification of hydration behavior, meaning the water shells that surround the sucrose molecules could be very helpful to understand their behavior. For this purpose, first the sucrose peaks in the proton spectra were assigned for each H^+ in the samples (Figure 3.8).

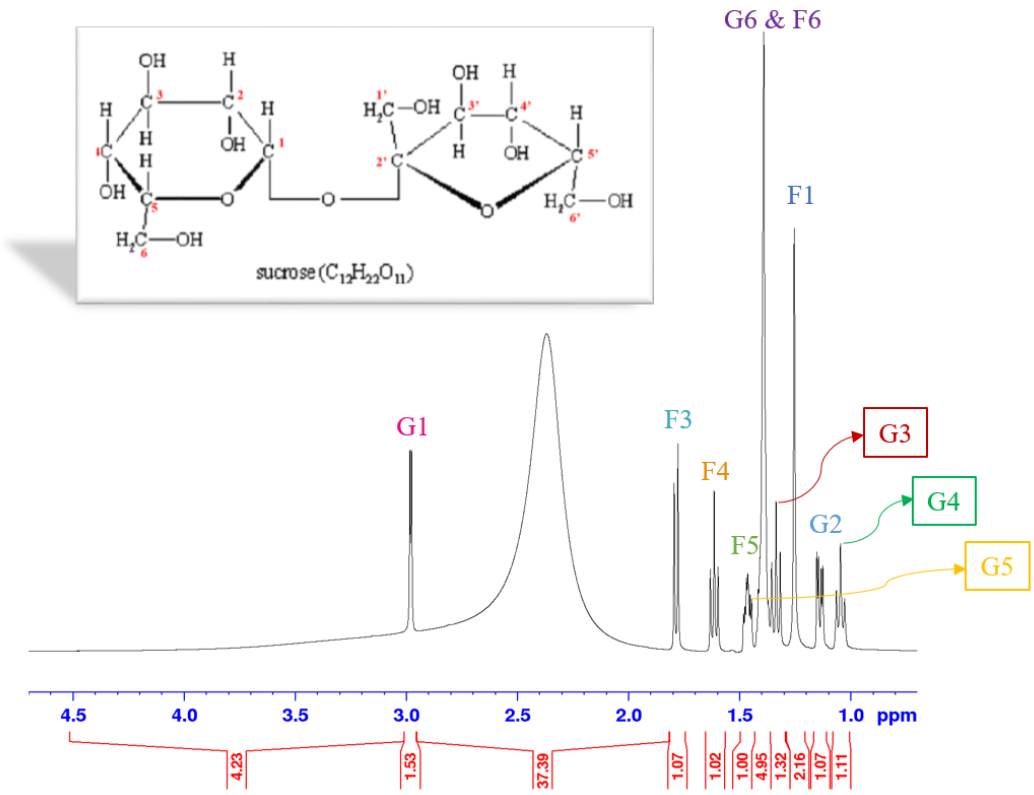

Figure 3.8. Assignment of the hydrogen atoms on fructose ring (denoted by F) and glucose ring (denoted by G) of the sucrose structure. Large peak around 2.3-2.4 ppm belongs to water protons.

In aqueous solution, interactions between sucrose and water molecules can occur but also water-water and sucrose-sucrose interactions (Starzak et al., 2000). Sucrose is known to interact with water through its eight hydroxyl groups (OH–) and can additionally form three weaker hydrogen bonds through its hydrophilic oxygen atoms (Starzak & Mathlouthi, 2002). However, the formation of aggregates due to the interaction between those sucrose-water and sucrose-sucrose entities should also be taken into consideration to fully understand the hydration concept (Gharsallaoui et al., 2008).

Providing information on the water mobility in the solution, NMR is widely used to investigate molecular dynamics of carbohydrates and water in the literature (Engelsen et al., 2001; Hartel & Shastry, 1991). ^{2}H NMR is widely used to prevent

interference of 1H on the spectra. However, the rotational dynamics of the water associated systems present a rather complicated pattern but provides inside on the effect concentration as well as temperature on the system (Girlich & Lüdemann, 1994). Indeed, in our case, the left shoulder of the curve of water protons were the starting point of this study (Figure 3.9).

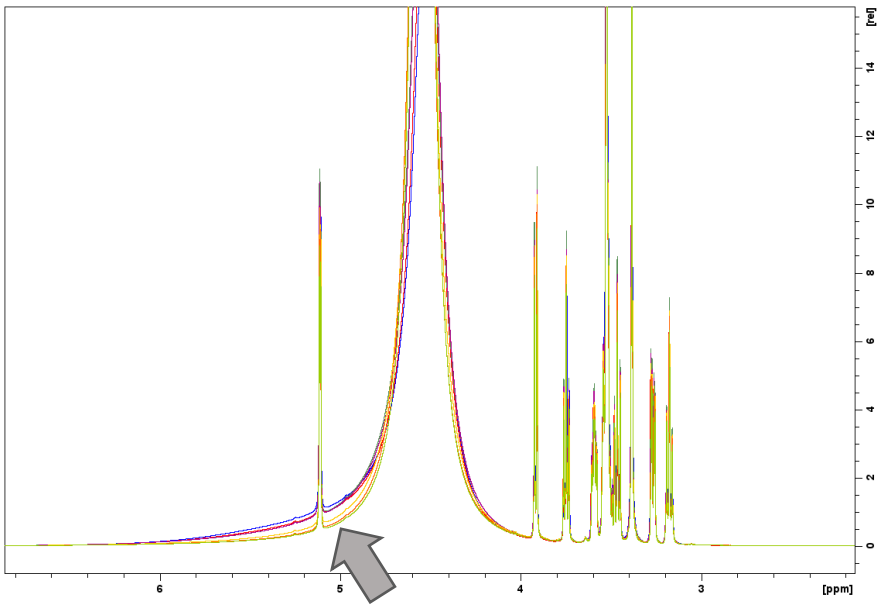

Figure 3.9. Change in the left shoulder of the water peak on the spectra of sucrose solutions overlapped by referencing the sugar peaks for samples at different concentrations at 28 °C. The area under the shoulder increases with concentration, shown by the direction of the arrow.

Increasing the solid content concentration shifted the water peak through down field (to the left on the spectra, higher energy). To resolve this shoulder, temperature of the solutions were lowered to 5 °C and the measurements were repeated. The results comparing the spectra at 5 °C and 28 °C was shown in Figure 3.10.

When the temperature is lowered, rotational dynamics slow down and the overlapping mobility of the components at the high temperature starts to separate. As one can see, there has emerged a couple of peaks at down field of the spectra

(Figure 3.10). As the concentration increased, proton movements were restricted and it slowed down the exchange explaining why the peaks were resolved better in high concentration. When those peaks were individually investigated, it was found that their contribution is due to hydroxyl groups in the solution. Even though they are difficult to identify, their assignment could be very useful to understand the bonding scheme in the structures.

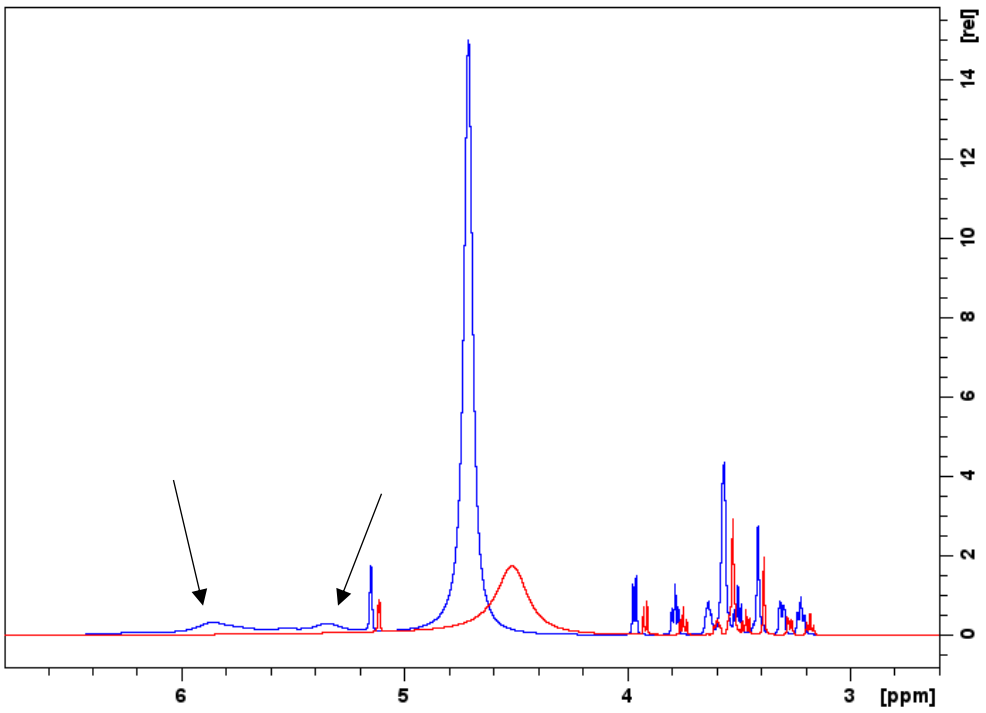

Figure 3.10. A representative NMR Spectra for sucrose solution at 28 °C (—) and 5 °C (—).

In dilute concentrations, sucrose does not make hydrogen bonds with itself (Mathlouthi & Genotelle, 1998). However, as the concentration of the sucrose increases, sucrose-sucrose interactions are promoted and the sucrose molecules tend to form intermolecular bonds with each other, sacrificing one hydrogen bond. Those interactions significantly increases after reaching a sucrose concentration of 65%

(w/w) at 25°C (Hartel & Shastry, 1991; Mohamed Mathlouthi, 1981). Richardson et al. (1987) reported that in the region of 5-40% (w/w), water molecules are exchanged rapidly while both water-sucrose and sucrose-sucrose were present in the region of 40-60% (w/w). This intramolecular bonding conformation in high solid concentrations of aqueous solution is also seen in sucrose's crystal form (Yrjö H. Roos et al., 2013).

To understand the effect of concentration on the sucrose-water interactions, the water peak shifts of the samples at different concentrations were drawn Figure 3.11. The trend showed an usual decrease around 600R to 700R, which corresponds to the 6th layer of the possible hydration cells around sucrose molecules. Being aware of the hydration layer and the importance of the hydrodynamic radius, at which the particles move together with the solvent, the study could reveal further properties of sucrose-water relationship.

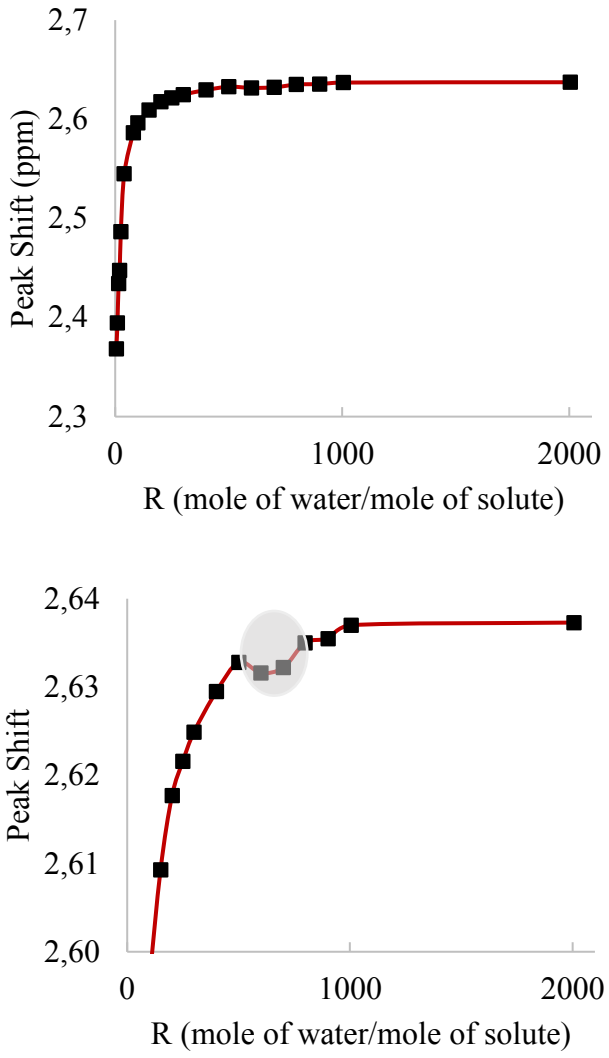

Figure 3.11. Change in the shift of water protons peak by decreased concentration Figure at the bottom zooms at the relevant area where the trend was distorted, shown by a circle.

3.3 Use of Crystallinity Measurement Approach on Model Food Systems

Caking in powdered foods is one of the factors that are not welcomed by the consumer and seriously affect the quality perception of the product. In addition to the liquid bridges formed on the particle surface due to moisture absorption; the freezing following the melting of the oil also causes the formation of liquid bridges

for high fat content samples to form solid bridges afterwards. This liquid bridge formation, which is invisible to the powder sample, is known as "sticking" in the literature and is considered to be the indicator of caking.

In this part of the study, samples of low and high fat milk powder, and cheese powder (whole fat/light) were heated to 90 °C to erase thermal history and allowed to cool to the studied temperature, 21 °C (in dessiccator). As the hypothesis of this study, measured crystallinities of those samples were associated with the caking properties such that adhesion and moisture absorption tendency will be less affected by external factors such as moisture in high-crystalline matrices where molecules form regular and stable bonds.

3.3.1 Effect of Storage Condition on Surface Fat Content

Storage quality of powder milk products are determined by their water activity and glass transition temperature (Schuck et al., 2007). Total and surface fat content measurement results were given in Table 3.4. As the moisture absorption of the powders increased with the relative humidity of their storage environment, the surface fat content of the samples showed a decreasing trend. Powders usually have pores and cracks in their structures due to drying. When those pores fill with water, the accessible amount of free fat on their surface is supposed to decrease. The correlation between moisture content vs surface fat content for light cheese, WF cheese, LF milk, and WF milk were -0.90, -0.83, -0.68, and -0.47, respectively ($p<0.05$). As the numbers suggest, the analogy between moisture and surface fat were distorted for the milk powders. Since the surface fat as well as total fat content for light cheese powder is really low, the surface fat was not expected to have a considerable effect on the moisture absorption of those samples. However, the correlation was supposed to decrease by its higher surface fat content alternative, WF cheese, which was not the case. The correlation remained too high (-0.83), which showed the ineffectiveness of surface fat content on the moisture absorption of WF cheese powder. When we look at the literature, there are studies stating that the

surface fat content dominates over the cohesion of the particles when it is below 20% (Buma, 1971; Pyne, 1961). In our samples, the surface fat content changed between 34% and 26%, which was in the range where the fat content did not affect the powder particles' cohesion for dairy products.

The effect of storage condition (relative humidity of 40, 50, 60, and 70%) on the surface fat content of each sample was also analyzed statistically. In general, the surface fat content decreased as the relative humidity increased for all samples, however milk powders had some exceptions. For WF milk sample, surface content first decreased from 40% RH to 50% RH, but it suddenly reached a maximum at 60% RH, following a minimum at 70% RH (Table 3.4). A similar behavior was also seen for LF milk. The surface fat content trend was distorted around 50-60% RH. In milk powders, one of the main parameters that significantly affect the surface fat content is lactose crystallization. As the lactose absorbs water and crystallize, it results in a sudden increase in free fat content (Buma, 1971). Because lactose rearrangement release water and breaks the structure, forming cracks and open the door for fat migration (Saxena et al., 2020). In their study, Buma (1971) reported that this moisture content range that we see lactose crystallization was around 9-10%, which was in correlation with WF milk powder sample at 60% RH. On the contrary, mentioned behavior was seen at 50% RH range for LF milk, which corresponds to a moisture content of 6.5%. In their study, Choi et al. (1951) referred to a critical moisture content between 6.0 to 7.5%, after which lactose crystallization becomes significant for spray dried milk powder. The crystallization process is also dependent on the movement and transfer of the molecules within the powder matrix. The presence of cracks enable penetration while the amount semisolid fat soothes the surface. That was why whole fat milk powder samples' moisture absorption were not perfectly correlated to their free fat content and the lactose crystallization required more moisture uptake than LF milk powder .

Total fat content of the samples decreased in order for whole fat cheese powder, whole fat milk powder, low fat milk powder, and light cheese powder, respectively

(Table 3.4). Since the total fat content of the light cheese was already very low, the surface fat content measurement was not accurate enough to detect the small fat migration on the surface for that sample.

Table 3.4. Surface and total fat content results of powder food samples with different fat contents stored at different relative humidity*.

Sample	Totat Fat (g/g)	Surface Fat (g/g)							
		40% RH		50% RH		60% RH		70% RH	
LF Milk	0.169 ± 0.002	0.152 ± 0.004	A	0.146 ± 0.003	AB	0.147 ± 0.011	A	0.130 ± 0.002	B
WF Milk	0.220 ± 0.000	0.180 ± 0.004	B	0.174 ± 0.002	B	0.193 ± 0.002	A	0.161 ± 0.002	C
Light Cheese	0.020 ± 0.001	0.015 ± 0.000	A	0.014 ± 0.001	A	0.011 ± 0.002	B	0.008 ± 0.001	C
WF Cheese	0.418 ± 0.002	0.362 ± 0.005	A	0.355 ± 0.011	A	0.358 ± 0.012	A	0.322 ± 0.015	B

*Results were analyzed by using Tukey's multiple comparison test at 5% confidence interval, average of 3 replicates were reported with standard deviations. Comparison tests were made separately for each sample type.

3.3.2 Effect of Storage Condition on Moisture Content

The change in moisture content of the powders stored at different relative humidity environments are given in Figure 3.12. Initial moisture content and water activity of the samples were also measured and given by single points in the figure. Moisture content of the whole fat samples were close to each other (around 8%) while light cheese and LF milk powders' were around 6%.

When Figure 3.12 is examined, the first impression was that the water adsorbed on the milk powders increased in a linear way while the cheese powders showed a more different trend, having a sharp jump in water adsorption after 60% relative humidity. When milk powders were compared, a similar behavior was seen for those two samples of the same origin with different fat contents (high fat alternative adsorbs significantly more water after 60% RH). However, moisture content of the milk powders were comparable unlike the light and whole fat cheese powders at the lowest

RH. At 40% RH, moisture content of the light cheese powder was significantly higher than its high fat equivalent ($p < 0.05$).

Water adsorption trend of two types of cheese powders were similar, however the increase in moisture content on the whole fat cheese powder was noticeably large after 60% relative humidity.

In the overall picture, cheese powders tend to absorb more water at different relative humidities. In the process of cheese making, hydrophobic casein molecules are denatured and the hydrated inner cores are exposed out. Casein protein is sensitive to pH (decreased in cheese production) rather than temperature (drying of milk) (Post et al., 2012). As the integrity of the casein micelle structure, which constitutes appx. 80% of the source milk, are preserved in the milk powders, hygroscopicity is expected to be lower than cheese powders. On the other hand, the most hygroscopic behavior was seen for light cheese, which includes much more salt and calcium than WF cheese, also given on the nutrition label of the producer. Calcium chloride is readily used as a green absorbent for desiccation purposes (Zhang et al., 2016). The amount of excess salt was another significant parameter that contributed to the hygroscopicity of cheese powders.

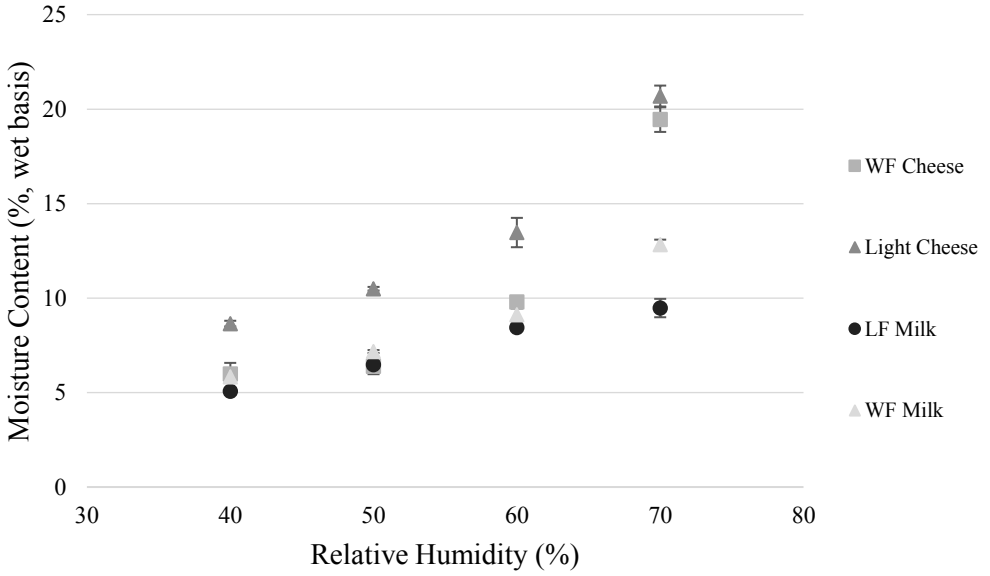

Figure 3.12. Moisture content of the samples at the studied relative humidity conditions.

3.3.3 Effect of Storage Condition on the Crystallinity

Caking problem is encountered due many variables in the powdered food systems, which may be mainly related to environmental conditions like temperature and humidity or it could totally be attributed to the nature of the individual components of the food system when it includes small molecular components or fat. The presence of fat in the recipe is one of the main issues in dairy powder caking beside from the amorphous lactose. To understand the combined effect of lactose and fat content on the caking behavior of dairy powders, low field time domain NMR was employed in this study.

Since the essence of our experimental setup include moisture adsorption, samples were expected have free water, as well as crystalline and partially amorphous portions. A representative NMR signal acquired by MSE sequence is given in Figure

3.13. To focus on the solid fraction of the samples only, liquid portion were filtered and removed from each signal.

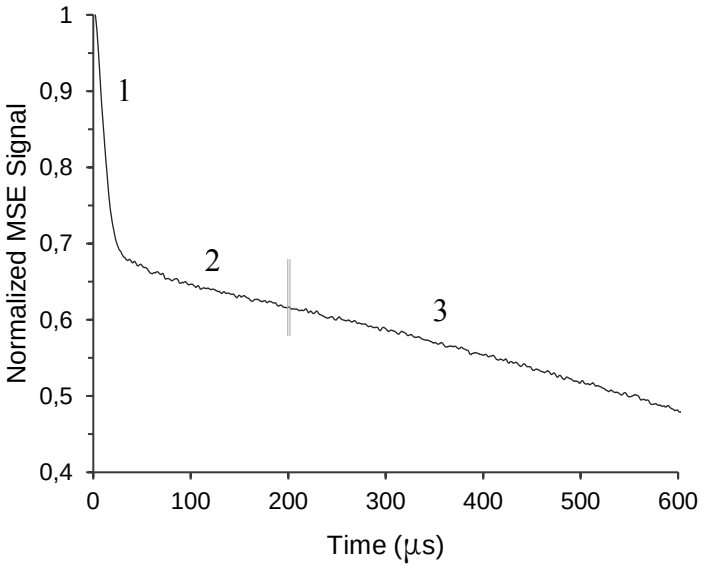

Figure 3.13. Representative MSE signal for whole fat cheese powder at 40% relative humidity. The signal in region 1 represents the solid signal while region 2 and 3 belonged to amorphous and long component (water), respectively.

Semicrystalline model (Equation 2.2) which has been applied in another study to model dispersion of microfibrils of cellulose by water uptake (L. Y. Grunin et al., 2017) was applied to detect the changes in the fraction of amorphous and crystalline regions due to moisture adsorption. Results were shown in . Free induction decay curve taken by an MSE sequence gives accurate information on different phases within the sample. The signal could be assigned to the components with different mobility in the solid sample, thus enable estimation of crystallite, and more mobile amorphous components (L. Y. Grunin et al., 2017; Hertlein et al., 2006; Maus et al., 2006). In our samples, the crystalline contribution was mainly attributed to the fat and lactose in the structure. Since the method was already confirmed in previously

published studies (Berk et al., 2021; L. Grunin et al., 2019; Guner et al., 2021), no further analyses were required for confirmation.

Crystallinity of the samples decreased as the relative humidity or moisture content of the samples increased (L. Y. Grunin et al., 2017). One of the reasons of this behavior could be attributed to the plasticizing effect of water, which increases with adsorption (Gorska, 2022). By the analysis that cover the crystallinity results for all conditions and all samples, our results suggested that the crystallinity of LF milk was significantly higher than WF milk, following Light cheese and WF cheese, respectively. When we look at moisture adsorption behavior of our samples, we see that the order was different for only Light cheese and WF cheese, while the other samples ranked the same in the order of moisture adsorption tendency. We would have expect the crystallinity change to be in parallel with the moisture adsorption, but it was not the case. The reason behind this change was related to high surface and total fat content of the WF cheese sample. Although it did not adsorb as much moisture as Light cheese, the crystallinity was much lower, since the amount of fat on the surface of the WF cheese powder particles altered the mobility and the fluidity of the overall powder.

On the other hand, the highest crystallinity belonged to the LF milk, which had the lowest hygroscopicity. The reasoning had been explained in Section 3.3.2. Although relative humidity and temperature are the two factors that have control over caking, crystallinity of the lactose becomes one of the most important parameters for milk powders. Approximate lactose content of dried whole milk and skim milk referenced from literature were around 38% and 50%, respectively (Y. D. Listiohadi et al., 2005), while the amount is really very low for cheese products. The effect of lactose was dominant on the milk powders while the cheese powders were hypothesized to be affected from the salt in their composition. Formation of the crystalline lactose is desirable in the manufacturing stage so when the crystalline lactose content is higher, powder is known to have less tendency to cake (Y. Listiohadi et al., 2009). Since the crystallinity of the milk powders mainly depended on the lactose crystallization, their

crystallinities were higher and dominated the effect of fat content. The approach used here based on calculation of average second moments and the amplitude values of the samples (Equation 2.2 & Equation 2.3). Second moment is a very informative parameter on the internal dynamics of solid systems, which can be calculated from a definite formula described by quantum mechanics (Goc, 1998b, 2001). The second moments as well as the crystallinity by the MSE sequence of the milk powders were significantly higher than cheese powder samples, while there was no significant difference between high fat and low fat samples. This result showed that the presence of lactose in the formulation was more distinctive to understand crystallinity. Moreover, one other conclusion that could be drawn from this scenario is that, as the literature allows for the comparison of the effect of fat vs lactose content, when salt content was present as another variable in the system, its effect on crystallinity became much higher than lactose and fat content for our samples. Increasing the moisture adsorption, the amount of salt significantly decreased the crystallinity of cheese powders (Horng, 1990; F. Li et al., 2019).

In this perspective, crystallinity results were categorized according to their fat content, and the presence of salt (milk powders, and cheese powders) and analyzed separately for each RH condition (Table 3.4, lowercase letters). Crystallinity of the cheese powders were significantly lower than milk powders at each relative humidity. On the other hand, moisture content started to have a powerful impact on the samples after a limit of 60% relative humidity. Although the structures were also different, the presence of high salt content was considered as the largest contributor and caused higher moisture adsorption for cheese products at 70% RH. There emerged a significant difference between cheese samples at that relative humidity.

When we make a comparison between WF and light cheese to understand the effect of fat content at elevated moisture content, we saw that the crystallinity of light cheese decreased after 50% RH and remained constant. On the other hand, WF cheese showed a smoother decrease in crystallinity with increasing moisture content. This change could be attributed to the effect of fat content on the crystallinity of

cheese powders. Combining the change of surface fat content and the crystallinity for cheese powders around 50-60% relative humidity, the presence of fat in the case of WF cheese elongated the moisture adsorption process so the crystallinity was only affected significantly after 60% RH, rather than 50% RH in the case of LF cheese powder sample. Moisture adsorption trend was also in parallel with this interpretation (Table 3.5).

Another interesting result that was inferred from Table 1 was the disappearance of the significant difference between crystallinity of the milk powders at 60% RH. The crystallinity of LF milk powder did not show a regular trend. There was a significant increase in crystallinity at 50% RH, then the crystallinity started to decrease as does the other samples. When we look at the surface fat content results of that sample, it was seen that there was an unexpected decrease at the very same conditions, which was hardly a coincidence for the LF milk powder at 60% RH. As discussed in Section 3.3.1, the surface fat content of WF milk unexpectedly increased at 60% RH (Table 3.4), which was related to the lactose crystallization since the moisture content corresponds to a certain limit reported in the literature for milk powders (Buma, 1971). NMR crystallinity results also changed in coordination with this information.

Table 3.5. Results of MSE crystallinity, water activity and moisture content of samples with different fat contents stored at different relative humidity (RH) environments*.

Sample	RH (%)	MSE Crystallinity		Water Activity		Moisture Content	
Low Fat Milk Powder	40	0.968 ± 0.005	Aba	0.427 ± 0.007	D	5.059 ± 0.268	C
	50	0.975 ± 0.003	Aa	0.525 ± 0.011	C	6.475 ± 0.557	B
	60	0.957 ± 0.004	Ba	0.620 ± 0.014	B	8.441 ± 0.142	A
	70	0.938 ± 0.009	Ca	0.743 ± 0.012	A	9.472 ± 0.842	A
Whole Fat Milk Powder	40	0.947 ± 0.007	Ab	0.439 ± 0.003	D	5.836 ± 1.272	C
	50	0.931 ± 0.006	Bb	0.536 ± 0.008	C	7.172 ± 0.133	CB
	60	0.920 ± 0.005	Ba	0.636 ± 0.013	B	9.107 ± 0.597	B
	70	0.887 ± 0.006	Cb	0.757 ± 0.001	A	12.820 ± 0.472	A
Light Cheese Powder	40	0.898 ± 0.002	Ac	0.447 ± 0.006	D	8.649 ± 0.259	D
	50	0.869 ± 0.005	Bc	0.547 ± 0.003	C	10.494 ± 0.168	C
	60	0.816 ± 0.029	Cb	0.638 ± 0.010	B	13.468 ± 1.345	B
	70	0.783 ± 0.009	Cc	0.735 ± 0.015	A	20.691 ± 0.959	A
Whole Fat Cheese Powder	40	0.884 ± 0.013	Ac	0.444 ± 0.002	D	5.981 ± 0.215	C
	50	0.851 ± 0.017	Abc	0.545 ± 0.009	C	6.387 ± 0.721	C
	60	0.817 ± 0.002	Bb	0.642 ± 0.003	B	9.794 ± 0.528	B
	70	0.744 ± 0.020	Cd	0.731 ± 0.014	A	19.444 ± 1.126	A

*Results were analyzed by using Tukey's multiple comparison test at 5% confidence interval, average of 3 replicates were reported with standard deviations. Comparison tests were made for each response separately and the effect of relative humidity for each type of sample were indicated by uppercase letters. Lowercase letter denoted the significant difference between samples, the analyses were made separately for each RH.

CHAPTER 4

CONCLUSION

As the powder adsorbs moisture, the mobility and the fraction of its components change. The amount of the change depends on the environmental conditions such as temperature, relative humidity or the intrinsic factors such as the components of the original powder, particle size, amount of compression…etc. Caking could be correlated to the degree of crystallinity since the stickiness behavior is affected from liquid and solid bridges formed between particles. Crystallinity is commonly measured by X-ray diffraction tools to detect crystalline entities of the food matrixes. The presence of those crystals on the surface of the food products is considered as a quality parameter for cheese. In this study, our aim was to come up with an easy to use method so that the caking tendency and the present stickiness behavior could be quantitatively measured. Crystallinity term was used to refer the solid and less mobile component fraction for NMR analyses and correlated to caking properties of the powders. SE and MSE sequences were run on the sugar samples (glucose, sucrose, and lactose) and the results were compared with the XRD results. Their correlation were found to be really high (0.944 and 0.964 for SE and MSE, respectively). The results suggested that the caking tendency and the instant quality of the powders could be predicted in a short time without extra interpretation/sample preparation by NMR, which will be an easy to use, low cost, quick measurement technique alternative.

After the applicability of the method was confirmed, the development of the crystallinity increase triggered by decreasing the temperature was studied in the second part of the study. The aim of the kinetic measurements were to provide a quantitatively comparable data for crystallization rate of simple sugars and to explain the underlying chemistry behind their well-known behavior in the applications. Temperature dependent crystallinity increase of glucose, fructose, allulose, lactose,

and sucrose were successfully monitored by the applied SE sequence. R-square values changed between 0.929-0.996. Since MSE analysis took much longer than both SE and FID, it was not appropriate for a kinetic analysis, as suspected at the beginning. Simple FID analysis results were not as accurate as the results of SE analysis.

Results showed that although the structure of the sugars were identical (glucose, fructose and allulose), crystallization rate could be drastically different. The competence of the anomers in the solution and the relative comparison between different isomers was explained by the conformation and equilibrium concentration of different anomers. To be specific, glucose mutarotation rate restricted the crystallization rate while for fructose, crystallization at the stable beta form was hypothesized to be the reason for retarding crystallization. On the other hand, another isomer of fructose, popular rare sugar of the last decade, allulose, had neither of those restrictions and enabled easy conversion for both mutarotation and crystallization reactions by possessing all four isomers at the comparable concentration at the same time in the solution.

In the last section of the study, crystallinity approach by MSE sequence was applied to complex food powders. Samples were stored at different relative humidities and the effect of the composition on their caking behavior was investigated. This time, method was improved and the acquired signal was fitted to a semicrystalline model to calculate crystallinity. The liquid bridges formed on the particle surface due to moisture absorption caused a general decrease in the crystallinities for all samples. The caking tendency increased by decreasing crystallinity. Although the free fat content decreased by moisture adsorption, there was seen only the effect of moisture content on the crystallinity of WF cheese since the cohesion of the milk powders were not affected from surface fat after 20% fat content. This information leads to a conclusion that although moisture adsorption steadily increase stickiness, surface fat content will not affect the sample after a certain limit. One should prevent the fat migration on the powder surface before the mentioned range to maintain high quality.

For milk powders, the decrease in surface fat content was interfered around 50-60% RH. The reason behind was attributed to the crystallization of lactose, which was triggered at a moisture content range around 10% for WF milk while it was around 7% for LF milk powders. As the lactose absorb water and crystallize, it resulted in a sudden increase in free fat content. That was why whole fat milk powder samples' moisture absorption were not perfectly correlated to their free fat content and the lactose crystallization required more moisture absorption than LF milk.

The hygroscopicity of the milk samples were lower than cheese powders due to presence of casein micelles and lack of salt. The most hygroscopic sample was Light cheese, due to high salt content, however the caking tendency was found to be higher for WF cheese. The presence of salt in the formula of cheese products significantly affected the crystallinity, thus caking behavior of the food powders.

The mobility and the fraction change of a powders's components change by moisture uptake. This could be either by adsorption on all over the particle surfaces (which changes the surface morphology) or due to condensation on the contact surfaces, which are both strongly related to caking properties. In both cases, the mobility of the surface components or the contact points will incorporate water in their structure. In this study, the starting point of the research was detection of this mobility change by TD-NMR tools, which will provide an understanding of the caking phenomena.

In summary, the suggested method was succesfully applied to detect crystallinity amount and the crystal growth on model food samples. Furthermore, combined effect of moisture adsorption and fat content on the crystallinity of cheese and milk powders were also explained by the analysis of MSE signals, which gave information on the caking tendency of the powders. As a consequence, the method was suggested as a user friendly alternative to XRD crystallinity measurement.

REFERENCES

Adhikari, B., Howes, T., Bhandari, B. R., & Truong, V. (2001). Stickiness in foods: A review of mechanisms and test methods. *International Journal of Food Properties*, *4*(1), 1–33. https://doi.org/10.1081/JFP-100002186

Adhikari, B. M., Truong, T., Bansal, N., & Bhandari, B. (2018). Influence of gas addition on crystallisation behaviour of lactose from supersaturated solution. *Food and Bioproducts Processing*, *109*, 86–97. https://doi.org/10.1016/j.fbp.2018.03.003

Afrassiabian, Z., Leturia, M., Benali, M., Guessasmac, M., & Saleh, K. (2016). An overview of the role of capillary condensation in wet caking of powders. *Chemical Engineering Research and Design*, *110*, 245–254.

Aguilera, J. M., del Valle, J. M., & Karel, M. (1995). Caking phenomena in amorphous food powders. *Trends in Food Science and Technology*, *6*(5), 149–155. https://doi.org/10.1016/S0924-2244(00)89023-8

Al-Muhtaseb, A. H., McMinn, W. A. M., & Magee, T. R. A. (2002). Moisture sorption isotherm characteristics of food products: A review. *Food and Bioproducts Processing: Transactions of the Institution of of Chemical Engineers, Part C*, *80*(2), 118–128. https://doi.org/10.1205/09603080252938753

Altamimi, M. J., Royall, P. G., Wolff, K., & Martin, G. P. (2017). An Investigation of the Anomeric Stability of Lactose Powder Stored Under High Stress Conditions. *Pharmaceutical Technology*, *41*(3), 36–45. https://doi.org/10.1128/9781683670179.ch2

Atsukawa, K., Kudo, S., Amari, S., & Takiyama, H. (2020). Increase of solidification rate to improve quality of productivity for xylitol/sorbitol crystalline candy products. *Journal of Food Engineering*, *268*(September 2019), 109738.

https://doi.org/10.1016/j.jfoodeng.2019.109738

Baranowska, H. M., Sikora, M., Krystyjan, M., & Tomasik, P. (2012). Evaluation of the time-dependent stability of starch-hydrocolloid binary gels involving NMR relaxation time measurements. *Journal of Food Engineering*, *109*(4), 685–690. https://doi.org/10.1016/j.jfoodeng.2011.11.025

Bates, F. J. (1942). Polarimetry, Saccharimetry, and the Sugars. In *U.S. Government Printing Office* (Vol. 440).

Belcourt, L. A., & Labuza, T. P. (2007). Effect of raffinose on sucrose recrystallization and textural changes in soft cookies. *Journal of Food Science*, *72*(1). https://doi.org/10.1111/j.1750-3841.2006.00218.x

Belitz, H. D., Grosch, W., & Schieberle, P. (2009). Food chemistry. In *Food Chemistry*. https://doi.org/10.1007/978-3-540-69934-7

Berk, B., Grunin, L., & Oztop, M. H. (2021). A non-conventional TD-NMR approach to monitor honey crystallization and melting. *Journal of Food Engineering*, *292*(August 2020), 110292. https://doi.org/10.1016/j.jfoodeng.2020.110292

Besghini, D., Mauri, M., & Simonutti, R. (2019). Time domain NMR in polymer science: From the laboratory to the industry. *Applied Sciences (Switzerland)*, *9*(9). https://doi.org/10.3390/app9091801

Bhandari, B., & Howes, T. (2005). Relating the stickiness property of foods undergoing drying and dried products to their surface energetics. *Drying Technology*, *23*(4), 781–797. https://doi.org/10.1081/DRT-200054194

Bhandari, B. R. (2007). Stickiness and Caking in Food Preservation. *Handbook of Food Engineering*, 387–400. https://doi.org/10.1201/9781420017373.ch17

Billings, S. W., Bronlund, J. E., & Paterson, A. H. J. (2006). Effects of capillary condensation on the caking of bulk sucrose. In *Journal of Food Engineering* (Vol. 77, Issue 4, pp. 887–895). https://doi.org/10.1016/j.jfoodeng.2005.08.031

Bock, K., & Lemieux, R. U. (1982). The conformational properties of sucrose in aqueous solution: intramolecular hydrogen-bonding. *Carbohydrate Research*, *100*(1), 63–74. https://doi.org/10.1016/S0008-6215(00)81026-5

Boutis, G. S., & Kausik, R. (2017). Comparing the efficacy of solid and magic-echo refocusing sequences: Applications to 1H NMR echo spectroscopy of shale rock. *Solid State Nuclear Magnetic Resonance*, *88*(October), 22–28. https://doi.org/10.1016/j.ssnmr.2017.10.005

Branca, C., Magazù, S., Maisano, G., & Migliardo, P. (1999). Anomalous cryoprotective effectiveness of trehalose: Raman scattering evidences. *Journal of Chemical Physics*, *111*(1), 281–287. https://doi.org/10.1063/1.479288

Bressan, C., Mathlouthi, M., & Sugar Proc Res Inst, I. N. C. (1994). Thermodynamic Activity of Water and Sucrose and the Stability of Crystalline Sugar. *Zuckerindustrie*, *119*(8), 190–209.

Britannica, T. E. of E. (n.d.). *Bragg law*. Encyclopedia Britannicae. Retrieved December 7, 2022, from https://www.britannica.com/science/Bragg-law

Brown, A. (2008). *Understanding Food: Principles and Preparation* (3rd ed.). Thomson Learning, Inc.

Buda, A., Demco, D. E., Bertmer, M., Blümich, B., Reining, B., Keul, H., & Höcker, H. (2003). Domain sizes in heterogeneous polymers by spin diffusion using single-quantum and double-quantum dipolar filters. *Solid State Nuclear Magnetic Resonance*, *24*(1), 39–67. https://doi.org/10.1016/S0926-2040(03)00020-1

Buma, T. J. (1971). Free fat and physical structure of spray-dried whole milk. *Netherland Milk Dairy Journal*, *25*, 33–121.

Butt, H. J., & Kappl, M. (2009). Normal capillary forces. *Advances in Colloid and Interface Science*, *146*(1–2), 48–60. https://doi.org/10.1016/j.cis.2008.10.002

Capes, C. E. (1980). Agglomerate bonding. In J. C. Williams & T. Allen (Eds.),

Handbook of Powder Technology (Vol. 1, Issue C, pp. 23–51). Elsevier Science Publishers B.V. https://doi.org/10.1016/B978-1-4832-5666-5.50007-4

Chen, M., Wu, S., Tang, W., & Gong, J. (2015). Caking and adhesion free energy of maltitol: Studying of mechanism in adhesion process. *Powder Technology*, *272*, 235–240. https://doi.org/10.1016/j.powtec.2014.12.012 0032-5910/©

Chen, M., Wu, S., Xu, S., Yu, B., Shilbayeh, M., Liu, Y., Zhu, X., Wang, J., & Gong, J. (2018). Caking of crystals: Characterization, mechanisms and prevention. *Powder Technology*, *337*, 51–67. https://doi.org/10.1016/j.powtec.2017.04.052

Chen, X. D., & Özkan, N. (2007). Stickiness, functionality, and microstructure of food powders. *Drying Technology*, *25*(6), 959–969. https://doi.org/10.1080/07373930701397400

Chianese, A., & Kramer, H. J. M. (Eds.). (2012). *Industrial Crystallization Process Monitoring and Control*. Wiley-VCH Verlag & Co. KGaA.

Chiou, D., & Langrish, T. A. G. (2007). Development and characterisation of novel nutraceuticals with spray drying technology. *Journal of Food Engineering*, *82*(1), 84–91. https://doi.org/10.1016/j.jfoodeng.2007.01.021

Choi, R. P., Tatter, C. W., & O'Malley, C. M. (1951). Lactose Crystallization in Dry Products of Milk. II. The Effects of Moisture and Alcohol. *Journal of Dairy Science*, *34*(9), 850–854. https://doi.org/10.3168/jds.S0022-0302(51)91792-4

Christakis, N., Wang, J., Patel, M. K., & Bradley, M. S. A. (2006). Aggregation and caking processes of granular materials : continuum model and numerical simulation with. *Advanced Powder Technology*, *17*(5), 543–565. https://doi.org/10.1163/156855206778440480

Chung, M.-S., Ruan, R., Chen, P., Chung, S.-H., Ahn, T.-H., & Lee, K.-H. (2000). Study of Caking in Powdered Foods Using Nuclear Magnetic Resonance Spectroscopy. *Journal of Food Science*, *65*(1), 134–138.

Chung, M.-S., Ruan, R., Chen, P., Lee, Y.-G., Ahn, T.-H., & Baik, C.-K. (2008).

Formulation of Caking-Resistant Powdered Soups Based on NMR Analysis. *Journal of Food Science*, *66*(8), 1147–1151. https://doi.org/10.1111/j.1365-2621.2001.tb16096.x

Cockman, M., Kubler, D. G., Oswald, A. S., & Wilson, L. (1987). The mutarolatlon of fructose the invertase hydrolysis of sucrose. *Journal of Carbohydrate Chemistry*, *6*(2), 181–201. https://doi.org/10.1080/07328308708058870

Cubillas, P., & Anderson, M. W. (2010). Synthesis Mechanism: Crystal Growth and Nucleation. In J. Cejka, A. Corma, & S. Zones (Eds.), *Zeolites and Catalysis: Synthesis, Reactions and Applications* (1st ed., p. 86). WILEY-VCH Verlag GmbH & Co. KGaA. https://doi.org/https://doi.org/10.1002/9783527630295.ch1

Cucinelli Neto, R. P., da Rocha Rodrigues, E. J., & Bruno Tavares, M. I. (2018). Proton NMR relaxometry as probe of gelatinization, plasticization and montmorillonite-loading effects on starch-based materials. *Carbohydrate Polymers*, *182*(August 2017), 123–131. https://doi.org/10.1016/j.carbpol.2017.11.021

Dejong, A. E., & Hartel, R. W. (2016). Determination of sorbitol crystal content and crystallization rate using TD-NMR. *Journal of Food Engineering*, *178*, 117–123. https://doi.org/10.1016/j.jfoodeng.2016.01.012

Determination of Solid Fat Content (SFC) in Oils and Fats by pulsed- NMR Analyzer [Brochure]. (2017). Resonance Systems.

Downton, G. E., Flores-Luna, J. L., & King, C. J. (1982). Mechanism of Stickiness in Hygroscopic, Amorphous Powders. *Industrial and Engineering Chemistry Fundamentals*, *21*(4), 447–451. https://doi.org/10.1021/i100008a023

Earle, R. L. (2004). *Unit Operations in Food Processing* (web editio). The New Zealand Institute of Food Science & Technology (Inc.).

Engelsen, S. B., Monteiro, C., Hervé De Penhoat, C., & Pérez, S. (2001). The diluted

aqueous solvation of carbohydrates as inferred from molecular dynamics simulations and NMR spectroscopy. *Biophysical Chemistry*, *93*(2–3), 103–127. https://doi.org/10.1016/S0301-4622(01)00215-0

Erdemir, D., Lee, A. Y., & Myerson, A. S. (2009). Nucleation of crystals from solution: Classical and two-step models. *Accounts of Chemical Research*, *42*(5), 621–629. https://doi.org/10.1021/ar800217x

Ergun, R., Lietha, R., & Hartel, R. W. (2010). Moisture and shelf life in sugar confections. *Critical Reviews in Food Science and Nutrition*, *50*(2), 162–192. https://doi.org/10.1080/10408390802248833

Fanchi, J. R. (2002). Measures of Rock-Fluid Interactions. In *Shared Earth Modeling* (pp. 108–132). Elsevier Science. https://doi.org/10.1016/B978-0-7506-7522-2.50007-0

FDA. (2014). *Water Activity (aw) in Foods*. https://www.fda.gov/inspections-compliance-enforcement-and-criminal-investigations/inspection-technical-guides/water-activity-aw-foods

FDA. (2017). GRAS Notice (GRN) No. 693. *Encyclopedia of Toxicology*, *693*, 417–420. https://doi.org/10.1016/b0-12-369400-0/00448-8

Felix da Silva, D., Ahrné, L., Larsen, F. H., Hougaard, A. B., & Ipsen, R. (2018). Physical and functional properties of cheese powders affected by sweet whey powder addition before or after spray drying. *Powder Technology*, *323*, 139–148. https://doi.org/10.1016/j.powtec.2017.10.014

Fitzpatrick, J. J. (2007). Particle properties and the design of solid food particle processing operations. *Food and Bioproducts Processing*, *85*(4 C), 308–314. https://doi.org/10.1205/fbp07056

Fitzpatrick, J. J., Hodnett, M., Twomey, M., Cerqueira, P. S. M., O'Flynn, J., & Roos, Y. H. (2007). Glass transition and the flowability and caking of powders containing amorphous lactose. *Powder Technology*, *178*(2), 119–128.

https://doi.org/10.1016/j.powtec.2007.04.017

Fitzpatrick, J. J., O'Connor, J., Cudmore, M., & Dos Santos, D. (2017). Caking behaviour of food powder binary mixes containing sticky and non-sticky powders. *Journal of Food Engineering*, *204*, 73–79. https://doi.org/10.1016/j.jfoodeng.2017.02.021

Fitzpatrick, John J., & Ahrné, L. (2005). Food powder handling and processing: Industry problems, knowledge barriers and research opportunities. *Chemical Engineering and Processing: Process Intensification*, *44*(2), 209–214. https://doi.org/10.1016/j.cep.2004.03.014

Foster, K. D., Bronlund, J. E., & Paterson, A. H. J. (2005). The contribution of milk fat towards the caking of dairy powders. *International Dairy Journal*, *15*(1), 85–91. https://doi.org/10.1016/j.idairyj.2004.05.005

Freeman, T., Brockbank, K., & Armstrong, B. (2015). Measurement and quantification of caking in powders. *Procedia Engineering*, *102*(December), 35–44. https://doi.org/10.1016/j.proeng.2015.01.104

French, A. D., & Santiago Cintrón, M. (2013). Cellulose polymorphy, crystallite size, and the Segal Crystallinity Index. *Cellulose*, *20*(1), 583–588. https://doi.org/10.1007/s10570-012-9833-y

Fukada, K., Ishii, T., Tanaka, K., Masatsugu, Y., Yamaoka, Y., Kobashi, K., & Izomuri, K. (2010). Crystal Structure, Solubility, and Mutarotation of the Rare Monosaccharide D-Psicose CH2OHCH2OH. *Bulletin of the Chemical Society of Japan*, *83*(10), 1193–1197.

Garvey, C. J., Parker, I. H., & Simon, G. P. (2005). On the interpretation of X-ray diffraction powder patterns in terms of the nanostructure of cellulose I fibres. *Macromolecular Chemistry and Physics*, *206*(15), 1568–1575. https://doi.org/10.1002/macp.200500008

Gay, C., & Leibler, L. (1999). On Stickiness. *Physics Today*, *52*(11), 48–52.

https://doi.org/10.1063/1.882884

Gharsallaoui, A., Rogé, B., Génotelle, J., & Mathlouthi, M. (2008). Relationships between hydration number, water activity and density of aqueous sugar solutions. *Food Chemistry*, *106*(4 SPEC. ISS.), 1443–1453. https://doi.org/10.1016/j.foodchem.2007.02.047

Girlich, D., & Lüdemann, H. D. (1994). Molecular Mobility of the Water Molecules in Aqueous Sucrose Solutions, Studied by 2H-NMR Relaxation. *Zeitschrift Fur Naturforschung - Section C Journal of Biosciences*, *49*(3–4), 250–257. https://doi.org/10.1515/znc-1994-3-414

Goc, R. (1998a). Calculation of the NMR second moment for materials with different types of internal rotation. *Solid State Nuclear Magnetic Resonance*, *13*(1–2), 55–61. https://doi.org/10.1016/S0926-2040(98)00082-4

Goc, R. (1998b). Calculation of the NMR second moment for materials with different types of internal rotation. *Solid State Nuclear Magnetic Resonance*, *13*(1–2), 55–61. https://doi.org/10.1016/S0926-2040(98)00082-4

Goc, R. (2001). Simulation of the NMR Second Moment as a Function of Temperature in the Presence of Molecular Motion. Application to (CH3)3NBH3. *Zeitschrift Fur Naturforschung*, *57*(a), 29–35.

Gorska, A. (2022). Applications of Instrumental Methods for Food and Food By-Products Analysis. In *Applications of Instrumental Methods for Food and Food By-Products Analysis*. https://doi.org/10.3390/books978-3-0365-4522-6

Griffith, E. J. (1991). *Cake formation in particulate systems*. Wiley-VCH.

Grunin, L., Oztop, M. H., Guner, S., & Baltaci, S. F. (2019). Exploring the crystallinity of different powder sugars through solid echo and magic sandwich echo sequences. *Magnetic Resonance in Chemistry*, *March*, 607–615. https://doi.org/10.1002/mrc.4866

Grunin, L. Y., Grunin, Y. B., Nikolskaya, E. A., Sheveleva, N. N., & Nikolaev, I. A.

(2017). An NMR relaxation and spin diffusion study of cellulose structure during water adsorption. *Biophysics*, *62*(2), 198–206. https://doi.org/10.1134/S0006350917020087

Guner, S., Grunin, L., Sumnu, S. G., & Halil, M. (2021). Use of Solid Echo Sequence to Monitor Crystallization Kinetics of Mono and Di-Saccharides. *Food Biophysics*, *0123456789*. https://doi.org/10.1007/s11483-021-09688-6

Hansen, E. W., Kristiansen, P. E., & Pedersen, B. (1998). Crystallinity of Polyethylene Derived from Solid-State Proton NMR Free Induction Decay. *J. Phys. Chem. B*, *102*(98), 5444–5450. https://doi.org/10.1021/jp981753z

Harnkarnsujarit, N., & Charoenrein, S. (2011). Effect of water activity on sugar crystallization and β-carotene stability of freeze-dried mango powder. *Journal of Food Engineering*, *105*(4), 592–598. https://doi.org/10.1016/j.jfoodeng.2011.03.026

Hartel, R. W. (2002). Crystallization in Foods. In A. S. Myerson (Ed.), *Handbook of Industrial Crystallization* (2nd ed., pp. 287–304). https://doi.org/10.1016/B978-0-7506-7012-8.X5000-9

Hartel, R. W., & Shastry, A. V. (1991). Sugar crystallization in food products. *Critical Reviews in Food Science and Nutrition*, *30*(1), 49–112. https://doi.org/10.1080/10408399109527541

Hertlein, C., Saalwächter, K., & Strobl, G. (2006). Low-field NMR studies of polymer crystallization kinetics: Changes in the melt dynamics. *Polymer*, *47*(20), 7216–7221. https://doi.org/10.1016/j.polymer.2006.03.117

Horng, P. (1990). *Effect of inorganic salts on adsorption process*. New Jersey Institute of Technology.

Horton, D. (2004). *Advances in Crbohydrate Chemistry and Biochemistry* (Vol. 59). Elsevier.

Huppertz, T., & Gazi, I. (2016). Lactose in dairy ingredients: Effect on processing

and storage stability. *Journal of Dairy Science*, *99*(8), 6842–6851. https://doi.org/10.3168/jds.2015-10033

Ikeda, S., Furuta, C., Fujita, Y., & Gohtani, S. (2014). Effects of D-psicose on gelatinization and retrogradation of rice flour. *Standardization News*, *66*(9–10), 773–779. https://doi.org/10.1002/star.201300259

Ilhan, E., Pocan, P., Ogawa, M., & Oztop, M. H. (2020). Role of 'D-allulose' in a starch based composite gel matrix. *Carbohydrate Polymers*, *228*(September 2019), 115373. https://doi.org/10.1016/j.carbpol.2019.115373

Jackson, R. F., & Silsbee, C. G. (1922). THE solubility of dextrose in water. *Journal of the Franklin Institute*, *194*(1), 95–96. https://doi.org/10.1016/S0016-0032(22)90021-3

Jawad, R., Elleman, C., Martin, G. P., & Royall, P. G. (2018). Crystallisation of freeze-dried sucrose in model mixtures that represent the amorphous sugar matrices present in confectionery. *Food and Function*, *9*(9), 4621–4634. https://doi.org/10.1039/c8fo00729b

Jiang, S., Xiao, W., Zhu, X., Yang, P., Zheng, Z., Lu, S., Jiang, S., Zhang, G., & Liu, J. (2020). Review on D-Allulose: In vivo Metabolism, Catalytic Mechanism, Engineering Strain Construction, Bio-Production Technology. *Frontiers in Bioengineering and Biotechnology*, *8*(February). https://doi.org/10.3389/fbioe.2020.00026

Keda, S. I., Ohtani, S. G., Ukada, K. F., & Mo, Y. A. (2011). *Dielectric Relaxation and Water Activity in Aqueous Solution of D -Psicose*. *12*(2), 67–74.

Kelly, G. M., O'Mahony, J. A., Kelly, A. L., Huppertz, T., Kennedy, D., & O'Callaghan, D. J. (2015). Influence of protein concentration on surface composition and physico-chemical properties of spray-dried milk protein concentrate powders. *International Dairy Journal*, *51*, 34–40. https://doi.org/10.1016/j.idairyj.2015.07.001

Khalfaoui, M., Knani, S., Hachicha, M. A., & Lamine, A. Ben. (2003). New theoretical expressions for the five adsorption type isotherms classified by BET based on statistical physics treatment. *Journal of Colloid and Interface Science*, *263*(2), 350–356. https://doi.org/10.1016/S0021-9797(03)00139-5

Khvorova, L. S., Lukin, N. D., & Baranova, L. V. (2018). Glucose nucleation in the presence of surface active agents. *Foods and Raw Materials*, *6*(1), 219–229. https://doi.org/10.21603/2308-4057-2018-1-219-229

Kidder, K., & Lyu, X. (2020). *X-ray diffraction (XRD) basics and application*. LibreTexts. https://chem.libretexts.org/Courses/Franklin_and_Marshall_College/Introduction_to_Materials_Characterization__CHM_412_Collaborative_Text/Diffraction_Techniques/X-ray_diffraction_(XRD)_basics_and_application

Kim, E. H. J., Chen, X. D., & Pearce, D. (2005). Melting characteristics of fat present on the surface of industrial spray-dried dairy powders. *Colloids and Surfaces B: Biointerfaces*, *42*(1), 1–8. https://doi.org/10.1016/j.colsurfb.2005.01.004

Kinetics and Mass Transfer in Crystallization. (n.d.). Retrieved May 9, 2020, from https://www.cheric.org/files/education/cyberlecture/d201501/d201501-1601.pdf

Kirtil, E., & Oztop, M. H. (2015). 1H Nuclear Magnetic Resonance Relaxometry and Magnetic Resonance Imaging and Applications in Food Science and Processing. *Food Engineering Reviews*, *JANUARY 2015*. https://doi.org/10.1007/s12393-015-9118-y

Laine, P., Kylli, P., Heinonen, M., & Jouppila, K. (2008). Storage stability of microencapsulated cloudberry (Rubus chamaemorus) phenolics. *Journal of Agricultural and Food Chemistry*, *56*(23), 11251–11261. https://doi.org/10.1021/jf801868h

Lans, A. M. (2016). *Evaluation of Water Sorption and Thermal Properties of Galacto-oligosaccharides, and Application in Glassy Confections* [The Ohio

State University]. https://etd.ohiolink.edu/apexprod/rws_etd/send_file/send?accession=osu1460764786&disposition=inline

Le Botlan, D., Casseron, F., & Lantier, F. (1998). Polymorphism of sugars studied by time domain NMR. *Analusis*, *26*(5), 198–204. https://doi.org/10.1051/analusis:1998135

Lee, D. S., & Robertson, G. L. (2022). Shelf-life estimation of packaged dried foods as affected by choice of moisture sorption isotherm models. *Journal of Food Processing and Preservation*, *46*(3), 1–9. https://doi.org/10.1111/jfpp.16335

Lee, S. L., Debenedetti, P. G., & Errington, J. R. (2005). A computational study of hydration, solution structure, and dynamics in dilute carbohydrate solutions. *Journal of Chemical Physics*, *122*(20). https://doi.org/10.1063/1.1917745

Li, A., Cai, L., Chen, Z., Wang, M., Wang, N., Nakanishi, H., Gao, X. D., & Li, Z. (2017). Recent advances in the synthesis of rare sugars using DHAP-dependent aldolases. *Carbohydrate Research*, *452*, 108–115. https://doi.org/10.1016/j.carres.2017.10.009

Li, F., Wang, X., Guo, Q., Zhang, B., Pei, Q., & Yang, S. (2019). Moisture Adsorption Mechanism of Earthen Plaster Containing Soluble Salts in the Mogao Grottoes of China. *Studies in Conservation*, *64*(3), 159–173. https://doi.org/10.1080/00393630.2018.1537351

Lipasek, R. A., Ortiz, J. C., Taylor, L. S., & Mauer, L. J. (2012). Effects of anticaking agents and storage conditions on the moisture sorption, caking,and flowability of deliquescent ingredients. *Food Research International Journal*, *45*, 369–380.

Listiohadi, Y. D., Hourigan, J. A., Sleigh, R. W., & Steele, R. J. (2005). Properties of Lactose and its caking behavior. *The Australian Journal of Dairy Technology*, *60*(1), 33–52. http://dx.doi.org/10.1016/j.jaci.2012.05.050

Listiohadi, Y., Hourigan, J. A., Sleigh, R. W., & Steele, R. J. (2009). Thermal

analysis of amorphous lactose and σ-lactose monohydrate. *Dairy Science and Technology*, *89*(1), 43–67. https://doi.org/10.1051/dst:2008027

Litvinov, V. M., & Penning, J. P. (2004). Phase composition and molecular mobility in nylon 6 fibers as studied by proton NMR transverse magnetization relaxation. *Macromolecular Chemistry and Physics*, *205*(13), 1721–1734. https://doi.org/10.1002/macp.200400089

Lu, Y., Thomas, L., & Schmidt, S. (2017). Differences in the thermal behavior of beet and cane sucrose sources. *Journal of Food Engineering*, *201*, 57–70. https://doi.org/10.1016/j.jfoodeng.2017.01.005

Maeng, H. J., Yoon, J. H., Chun, K. H., Kim, S. T., Jang, D. J., Park, J. E., Kim, Y. H., Kim, S. B., & Kim, Y. C. (2019). Metabolic stability of D-allulose in biorelevant media and hepatocytes: Comparison with fructose and erythritol. *Foods*, *8*(10), 1–13. https://doi.org/10.3390/foods8100448

Martins, P. M., Rocha, F. A., & Rein, P. (2005). Modeling sucrose evaporative crystallization. Part 1. Vacuum pan monitoring by mass balance and image analysis methods. *Industrial and Engineering Chemistry Research*, *44*(23), 8858–8864. https://doi.org/10.1021/ie050639h

Mathlouthi, M., & Rogé, B. (2003). Water vapour sorption isotherms and the caking of food powders. *Food Chemistry*, *82*(1), 61–71. https://doi.org/10.1016/S0308-8146(02)00534-4

Mathlouthi, M, & Genotelle, J. (1998). *Role of water in sucrose crystallization 1*. *37*, 335–342.

Mathlouthi, Mohamed. (1981). X-ray diffraction study of the molecular association in aqueous solutions of d-fructose, d-glucose, and sucrose. *Carbohydrate Research*, *91*(2), 113–123. https://doi.org/10.1016/S0008-6215(00)86024-3

Maus, A., Hertlein, C., & Saalwächter, K. (2006). A robust proton NMR method to investigate hard/soft ratios, crystallinity, and component mobility in polymers.

Macromolecular Chemistry and Physics, *207*(13), 1150–1158. https://doi.org/10.1002/macp.200600169

Michalski, M. C., Desobry, S., & Hardy, J. (1997). Food materials adhesion: A review. *Critical Reviews in Food Science and Nutrition*, *37*(7), 591–619. https://doi.org/10.1080/10408399709527791

Miller, E., & Hartel, R. W. (2015). Sucrose crystallization in caramel. *Journal of Food Engineering*, *153*(November), 28–38. https://doi.org/10.1016/j.jfoodeng.2014.11.028

Minor, H., & Murthy, N. S. (1989). General procedure for evaluating amorphous scattering and crystallinity from X-ray diffraction scans of semicrystalline polymers. *Polymer*, *31*, 996–1002.

Moraga, N. O., & Barraza, H. G. (2003). Predicting heat conduction during solidification of a food inside a freezer due to natural convection. *Journal of Food Engineering*, *56*(1), 17–26. https://doi.org/10.1016/S0260-8774(02)00135-8

Muller, C. R. (2017). *Caking considerations: causes, mechanisms, quantification*. https://www.foodprocessing.com.au/content/materials-handling-storage-and-supply-chain/article/caking-considerations-causes-mechanisms-quantification-42795435

Muzaffar, K., Nayik, G. A., & Kumar, P. (2015). Stickiness Problem Associated with Spray Drying of Sugar and Acid Rich Foods: A Mini Review. *Nutrition and Food Science*, *S12:003*, 11–13. https://doi.org/10.4172/2155-9600.1000S12003

Nagy, Z. K., Fevotte, G., Kramer, H., & Simon, L. L. (2013). Recent advances in the monitoring, modelling and control of crystallization systems. *Chemical Engineering Research and Design*, *91*(10), 1903–1922. https://doi.org/10.1016/j.cherd.2013.07.018

Nam, S., French, A. D., Condon, B. D., & Concha, M. (2016). Segal crystallinity index revisited by the simulation of X-ray diffraction patterns of cotton cellulose Iβ and cellulose II. *Carbohydrate Polymers*, *135*, 1–9. https://doi.org/10.1016/j.carbpol.2015.08.035

Nestl, S. P., Universit, S. T., Science, F., & View, T. (2011). *Food Engineering Interfaces* (Issue January). https://doi.org/10.1007/978-1-4419-7475-4

Nurhadi, B., & Roos, Y. H. (2017). Influence of anti-caking agent on the water sorption isotherm and flow-ability properties of vacuum dried honey powder. *Journal of Food Engineering*, *210*, 76–82. https://doi.org/10.1016/j.jfoodeng.2017.04.020

Olsson, C., & Swenson, J. (2020). Structural Comparison between Sucrose and Trehalose in Aqueous Solution. *Journal of Physical Chemistry B*, *124*(15), 3074–3082. https://doi.org/10.1021/acs.jpcb.9b09701

Özkan, N., Walisinghe, N., & Chen, X. D. (2002). Characterization of stickiness and cake formation in whole and skim milk powders. *Journal of Food Engineering*, *55*(4), 293–303. https://doi.org/10.1016/S0260-8774(02)00104-8

Park, S., Baker, J. O., Himmel, Michael, E., Parilla, P. A., & Johnson, D. K. (2010). Research Cellulose crystallinity index: measurement techniques and their impact on interpreting cellulase performance. *Biotechnology for Biofuels*, *3*(10), 1–10.

Partini, M., & Pantani, R. (2007). Determination of crystallinity of an aliphatic polyester by FTIR spectroscopy. *Polymer Bulletin*, *59*(3), 403–412. https://doi.org/10.1007/s00289-007-0782-9

Paterson, A. H. J., Brooks, G. F., Bronlund, J. E., & Foster, K. D. (2005). Development of stickiness in amorphous lactose at constant T-Tg levels. *International Dairy Journal*, *15*(5), 513–519. https://doi.org/10.1016/j.idairyj.2004.08.012

Peleg, M., & Mannheim, C. H. (1977). The Mechanism of Caking of Powdered Onion. *Journal of Food Processing and Preservation*, *1*(1), 3–11. https://doi.org/10.1111/j.1745-4549.1977.tb00309.x

Porter, T., & Hartel, R. W. (2013). Quantifying Sucrose Crystal Content in Fondant. *The Manufacturing Confectioner*, *January*, 61–64.

Post, A. E., Arnold, B., Weiss, J., & Hinrichs, J. (2012). Effect of temperature and pH on the solubility of caseins: Environmental influences on the dissociation of α S- and β-casein. *Journal of Dairy Science*, *95*(4), 1603–1616. https://doi.org/10.3168/jds.2011-4641

Pyne, C. H. (1961). *Reconstitution of Dry Milk Products*. University of Minnesota.

Richardson, S. J., Baianu, I. C., & Steinberg, M. P. (1987). Mobility of Water in Sucrose Solutions Determined by Deuterium and Oxygen-l7 Nuclear Magnetic Resonance Measurements. *Journal of Food Science*, *52*(3), 806–809. https://doi.org/10.1111/j.1365-2621.1987.tb06732.x

Roos, Y. (1993). Melting and glass transitions of low molecular weight carbohydrates. *Carbohydrate Research*, *238*, 39–48. http://www.sciencedirect.com/science/article/pii/000862159387004C%5Cnpapers2://publication/uuid/F2F3CE37-AC6E-470B-9416-9940080A6584

Roos, Yrjö H., Karel, M., Labuza, T. P., Levine, H., Mathlouthi, M., Reid, D., Shalaev, E., & Slade, L. (2013). Melting and crystallization of sugars in high-solids systems. *Journal of Agricultural and Food Chemistry*, *61*(13), 3167–3178. https://doi.org/10.1021/jf305419y

Roos, Yrö H. (1995). Physical State and Molecular Mobility. *Phase Transitions in Foods*, 19–48. https://doi.org/10.1016/b978-012595340-5/50002-x

Rotaru, R., Savin, M., Tudorachi, N., Peptu, C., Samoila, P., Sacarescu, L., & Harabagiu, V. (2018). Ferromagnetic iron oxide–cellulose nanocomposites prepared by ultrasonication. *Polymer Chemistry*, *9*(7), 860–868.

https://doi.org/10.1039/C7PY01587A

Sander, A., & Kardum, J. P. (2012). Pentaerythritol crystallization - Influence of the process conditions on the granulometric properties of crystals. *Advanced Powder Technology*, *23*(2), 191–198. https://doi.org/10.1016/j.apt.2011.02.001

Saxena, J., Adhikari, B., Brkljaca, R., Huppertz, T., Chandrapala, J., & Zisu, B. (2020). Inter-relationship between lactose crystallization and surface free fat during storage of infant formula. *Food Chemistry*, *322*(March), 126636. https://doi.org/10.1016/j.foodchem.2020.126636

Schmidt-Rohr, K., & Spiess, H. W. (1994). Introduction. *Multidimensional Solid-State NMR and Polymers*, 1–12. https://doi.org/10.1016/b978-0-08-092562-2.50006-0

Schuck, P., Mejean, S., Dolivet, A., Jeantet, R., Renseign, N., Schuck, P., Mejean, S., Dolivet, A., Jeantet, R., & Renseign, N. (2007). *Keeping quality of dairy ingredients*. *87*, 481–488.

Schwartz, A. M., & Myerson, A. S. (2002). Solutions and Solution Properties. In A. S. Myerson (Ed.), *Handbook of Industrial Crystallization* (2nd ed., pp. 1–32). Butterworth-Heinemann.

Serrano Nava, M. E., Hernández Morelos, J. L., Reséndiz González, M. C., Guardian Tapia, R., Vlasova, M., & Márquez Aguilar, P. A. (2022). Analysis of wide diffuse halo formation in the x-ray diffraction spectrum during the reduction of Fe2O3 by waste-activated sludge (WAS). *Materials Research Express*, *9*(9). https://doi.org/10.1088/2053-1591/ac8ccf

Shallenberger, R. S., & Birch, G. G. (1975). *Sugar Chemistry*. The Avi Publishing Comapny, Inc.

Shalu, R. K. S. (2018). Effect of ionic liquids on the crystallization kinetics of various polymers and polymer electrolytes. In *Crystallization in Multiphase Polymer Systems* (Issue 1). Elsevier Inc. https://doi.org/10.1016/B978-0-12-

809453-2.00016-5

Shenoy, P., Xanthakis, E., Innings, F., Jonsson, C., Fitzpatrick, J., & Ahrné, L. (2015). Dry mixing of food powders: Effect of water content and composition on mixture quality of binary mixtures. *Journal of Food Engineering*, *149*, 229–236. https://doi.org/10.1016/j.jfoodeng.2014.10.019

Shintani, T., Yamada, T., Hayashi, N., Iida, T., Nagata, Y., Ozaki, N., & Toyoda, Y. (2017). Rare Sugar Syrup Containing d -Allulose but Not High-Fructose Corn Syrup Maintains Glucose Tolerance and Insulin Sensitivity Partly via Hepatic Glucokinase Translocation in Wistar Rats. *Journal of Agricultural and Food Chemistry*, *65*(13), 2888–2894. https://doi.org/10.1021/acs.jafc.6b05627

Simperler, A., Kornherr, A., Chopra, R., Bonnet, P. A., Jones, W., Motherwell, W. D. S., & Zifferer, G. (2006). Glass transition temperature of glucose, sucrose, and trehalose: An experimental and in silico study. *Journal of Physical Chemistry B*, *110*(39), 19678–19684. https://doi.org/10.1021/jp063134t

Sing, K. S. W., Everett, D. H., Haul, R. A. W., Moscou, L., Pierotti, R. A., Rouquerol, J., & Siemieniewska, T. (1985). Reporting Physisoprtion Data for Gas/Solid Systems with Special Reference to the Determination of Surface Area and Porosity. *Pure and Applied Chemistry*, *57*(4), 603–619. https://doi.org/10.1002/pola.26338

Srisa-nga, S., & Flood, A. E. (2004). Mutarotation Rates and Equilibrium of Simple Carbohydrates. *Asian Pacific Confederation of Chemical Engineering Congress Program and Abstracts*, *113*(133), 1–10. https://doi.org/10.11491/apcche.2004.0.110.0

Srisa-Nga, S., Flood, A. E., & White, E. T. (2006). The secondary nucleation threshold and crystal growth of α-glucose monohydrate in aqueous solution. *Crystal Growth and Design*, *6*(3), 795–801. https://doi.org/10.1021/cg050432r

Starzak, M., & Mathlouthi, M. (2002). Water activity in concentrated sucrose solutions and its consequences for the availability of water in the film of syrup

surrounding the sugar crystal. *Zuckerindustrie*, *127*(3), 175–185.

Starzak, M., Peacock, S. D., & Mathlouthi, M. (2000). Hydration number and water activity models for the sucrose-water system: A critical review. In *Critical Reviews in Food Science and Nutrition* (Vol. 40, Issue 4). https://doi.org/10.1080/10408690091189185

Teixeira, G. A., Brito, A. M., Alves, M. R., Finzer, J. R. D., & Malagoni, R. A. (2013). Study of supersaturation, vibration intensity and time of crystallization variables in the vibrated bed lactose monohydrate production process. *Chemical Engineering Transactions*, *32*, 2191–2196. https://doi.org/10.3303/CET1332366

Torii, A., Sasaki, M., Hane, K., & Okuma, S. (1994). *Adhesive force distribution on microstructures investigated by an atomic force microscope*. *44*, 153–158.

Uehara, H., Yamanobe, T., & Komoto, T. (2000). Relationship between solid-state molecular motion and morphology for ultrahigh molecular weight polyethylene crystallized under different conditions. *Macromolecules*, *33*(13), 4861–4870. https://doi.org/10.1021/ma9918957

Urso, M. E. D., Lawrence, C. J., & Adams, M. J. (1999). Pendular, funicular, and capillary bridges: Results for two dimensions. *Journal of Colloid and Interface Science*, *220*(1), 42–56. https://doi.org/10.1006/jcis.1999.6512

Wang, R., & Hartel, R. W. (2020). Effects of moisture content and saccharide distribution on the stickiness of syrups. *Journal of Food Engineering*, *284*(February), 110067. https://doi.org/10.1016/j.jfoodeng.2020.110067

Widlak, N., Hartel, R. W., & Narine, S. (2001). *Crystallization and Solidification Properties of Lipids*. AOCS Press. https://books.google.com.tr/books?id=Dm4%5C_moxDMH4C

Willart, J. F., Caron, V., Lefort, R., Danède, F., Prévost, D., & Descamps, M. (2004). Athermal character of the solid state amorphization of lactose induced by ball

milling. *Solid State Communications*, *132*(10), 693–696. https://doi.org/10.1016/j.ssc.2004.09.007

Xiao, C., Shi, P., Yan, W., Chen, L., Qian, L., & Kim, S. H. (2019). Thickness and Structure of Adsorbed Water Layer and Effects on Adhesion and Friction at Nanoasperity Contact. In *Colloids and Interfaces* (Vol. 3, Issue 3). https://doi.org/10.3390/colloids3030055

Zafar, U., Vivacqua, V., Calvert, G., Ghadiri, M., & Cleaver, J. A. S. (2017). A review of bulk powder caking. *Powder Technology*, *313*, 389–401. https://doi.org/10.1016/j.powtec.2017.02.024

Zhang, W., Yu, S., Zhang, T., Jiang, B., & Mu, W. (2016). Recent advances in d-allulose: Physiological functionalities, applications, and biological production. *Trends in Food Science and Technology*, *54*, 127–137. https://doi.org/10.1016/j.tifs.2016.06.004

Zhang, W., Zhang, T., Jiang, B., & Mu, W. (2017). Enzymatic approaches to rare sugar production. *Biotechnology Advances*, *35*(2), 267–274. https://doi.org/10.1016/j.biotechadv.2017.01.004

Zhang, W., Zhang, Y., Huang, J., Chen, Z., Zhang, T., Guang, C., & Mu, W. (2018). Thermostability Improvement of the d -Allulose 3-Epimerase from Dorea sp. CAG317 by Site-Directed Mutagenesis at the Interface Regions. *Journal of Agricultural and Food Chemistry*, *66*(22), 5593–5601. https://doi.org/10.1021/acs.jafc.8b01200

Zouari, A., Briard-Bion, V., Schuck, P., Gaucheron, F., Delaplace, G., Attia, H., & Ayadi, M. A. (2020). Changes in physical and biochemical properties of spray dried camel and bovine milk powders. *Lwt*, *128*(March), 109437. https://doi.org/10.1016/j.lwt.2020.109437

APPENDICES

A. Applicability of the Method by the Crystallinity Analysis of Sugars Statistical Analyses

Table A 1. Pearson correlation analysis between SE and MSE sequence crystallinity results.

Method

Correlation type	Pearson
Rows used	18

Correlations

	MSE_Crystallinity
SE_Crystallinity	0.970

Table A 2. Analysis of Varience for MSE crystallinity of control and freezed-ried (FD) sugar samples.

Method

Null hypothesis	All means are equal
Alternative hypothesis	Not all means are equal
Significance level	$\alpha = 0.05$

Equal variances were assumed for the analysis.

Factor Information

Factor	Levels	Values
Sample	6	FD Glucose, FD Lactose, FD Sucrose, Glucose, Lactose, Sucrose

Analysis of Variance

Source	DF	Adj SS	Adj MS	F-Value	P-Value
Sample	5	7.32875	1.46575	501.06	0.000
Error	12	0.03510	0.00293		
Total	17	7.36385			

Model Summary

S	R-sq	R-sq(adj)	R-sq(pred)
0.0540858	99.52%	99.32%	98.93%

Means

Sample	N	Mean	StDev	95% CI
FD Glucose	3	1.3476	0.0616	(1.2795, 1.4156)
FD Lactose	3	1.1265	0.0848	(1.0584, 1.1945)
FD Sucrose	3	-0.3829	0.0505	(-0.4510, -0.3149)
Glucose	3	1.3408	0.0499	(1.2727, 1.4088)
Lactose	3	0.9825	0.0356	(0.9144, 1.0505)
Sucrose	3	1.52702	0.01571	(1.45898, 1.59506)

Pooled StDev = 0.0540858

Tukey Pairwise Comparisons

Grouping Information Using the Tukey Method and 95% Confidence

Sample	N	Mean	Grouping			
Sucrose	3	1.52702	A			
FD Glucose	3	1.3476		B		
Glucose	3	1.3408		B		
FD Lactose	3	1.1265			C	
Lactose	3	0.9825			C	
FD Sucrose	3	-0.3829				D

Means that do not share a letter are significantly different.

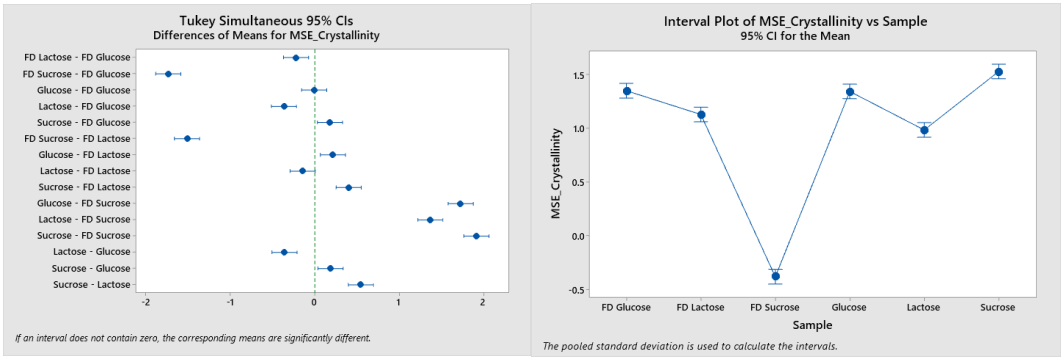

Table A 3. Normality and Equal variance tests for MSE crystallinity of control and freezed-ried (FD) sugar samples.

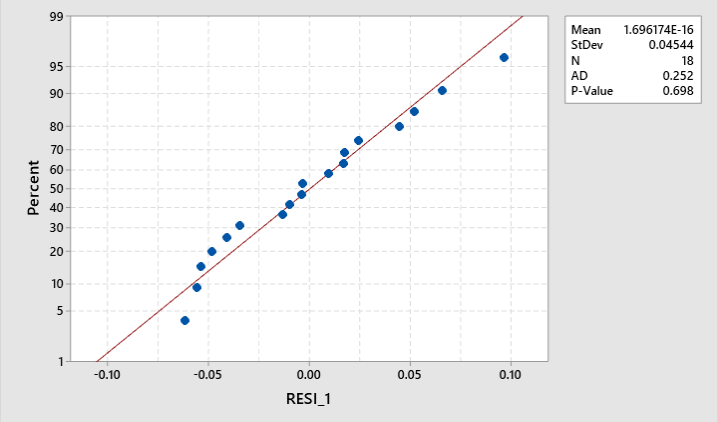

Method

Null hypothesis	All variances are equal
Alternative hypothesis	At least one variance is different
Significance level	α = 0.05

95% Bonferroni Confidence Intervals for Standard Deviations

Sample	N	StDev	CI
FD Glucose	3	0.0616312	(0.0000136, 2310.59)
FD Lactose	3	0.0848338	(0.0000188, 3180.47)
FD Sucrose	3	0.0505393	(0.0000112, 1894.75)
Glucose	3	0.0498517	(0.0000110, 1868.97)
Lactose	3	0.0356403	(0.0000079, 1336.18)
Sucrose	3	0.0157102	(0.0000035, 588.99)

Individual confidence level = 99.1667%

Method	Test Statistic	P-Value
Multiple comparisons	—	0.330
Levene	0.43	0.820

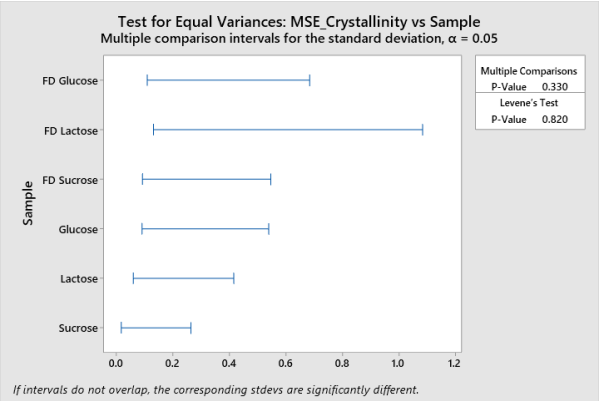

Table A 4. Analysis of Varience for SE crystallinity of control and freezed-ried (FD) sugar samples.

Method

Null hypothesis	All means are equal
Alternative hypothesis	Not all means are equal
Significance level	α = 0.05

Equal variances were assumed for the analysis.

Factor Information

Factor	Levels	Values
Sample	6	FD Glucose, FD Lactose, FD Sucrose, Glucose, Lactose, Sucrose

Analysis of Variance

Source	DF	Adj SS	Adj MS	F-Value	P-Value
Sample	5	7.69195	1.53839	242.30	0.000
Error	12	0.07619	0.00635		
Total	17	7.76814			

Model Summary

S	R-sq	R-sq(adj)	R-sq(pred)
0.0796810	99.02%	98.61%	97.79%

Means

Sample	N	Mean	StDev	95% CI
FD Glucose	3	1.2751	0.0198	(1.1749, 1.3754)
FD Lactose	3	0.8711	0.0708	(0.7709, 0.9713)
FD Sucrose	3	-0.6728	0.0596	(-0.7730, -0.5726)
Glucose	3	1.1246	0.1519	(1.0244, 1.2249)
Lactose	3	0.89486	0.01440	(0.79463, 0.99509)
Sucrose	3	1.0469	0.0766	(0.9467, 1.1471)

Pooled StDev = 0.0796810

Tukey Pairwise Comparisons

Grouping Information Using the Tukey Method and 95% Confidence

Sample	N	Mean	Grouping			
FD Glucose	3	1.2751	A			
Glucose	3	1.1246	A	B		
Sucrose	3	1.0469		B	C	
Lactose	3	0.89486			C	
FD Lactose	3	0.8711			C	
FD Sucrose	3	-0.6728				D

Means that do not share a letter are significantly different.

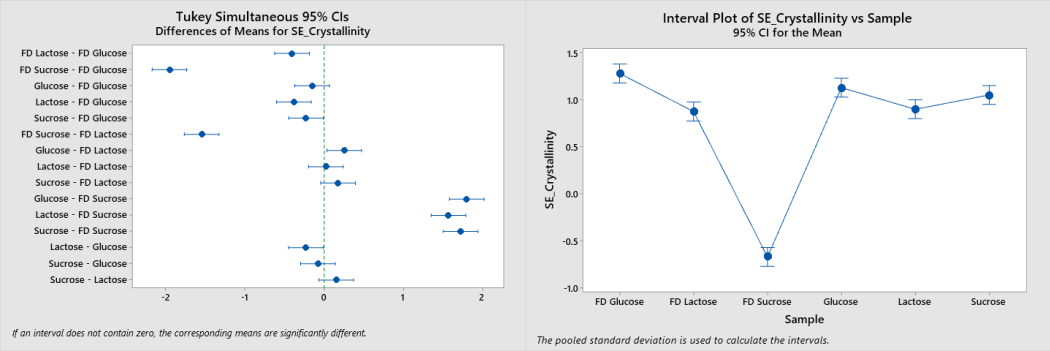

Table A 5. Normality and Equal variance tests for SE crystallinity of control and freezed-ried (FD) sugar samples.

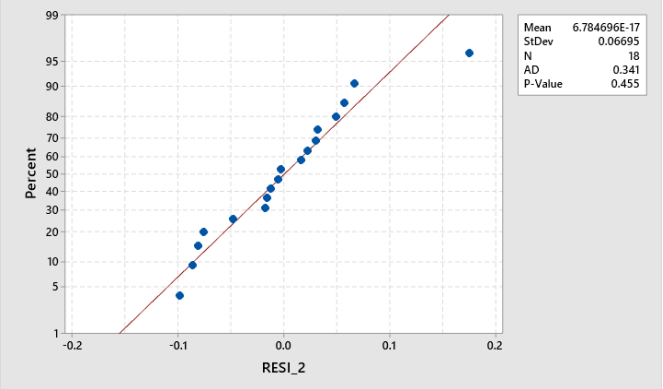

Method

Null hypothesis	All variances are equal
Alternative hypothesis	At least one variance is different
Significance level	α = 0.05

95% Bonferroni Confidence Intervals for Standard Deviations

Sample	N	StDev	CI
FD Glucose	3	0.019779	(0.0000044, 741.54)
FD Lactose	3	0.070825	(0.0000157, 2655.26)
FD Sucrose	3	0.059585	(0.0000132, 2233.87)
Glucose	3	0.151879	(0.0000336, 5694.05)
Lactose	3	0.014395	(0.0000032, 539.68)
Sucrose	3	0.076564	(0.0000169, 2870.44)

Individual confidence level = 99.1667%

Method	Test Statistic	P-Value
Multiple comparisons	—	0.058
Levene	0.54	0.740

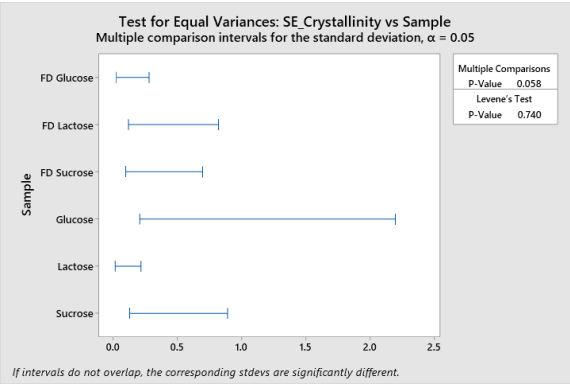

B. Use of Crystallinity Measurement Approach on Model Food Systems Statistical Analyses

Table A 6. Analysis of Varience for kinetic rate constant (k) of allulose and lactose.

Method

Null hypothesis	All means are equal
Alternative hypothesis	Not all means are equal
Significance level	$\alpha = 0.05$

Equal variances were assumed for the analysis.

Factor Information

Factor	Levels	Values
Sugar Type_AL	2	Allulose, Lactose

Analysis of Variance

Source	DF	Adj SS	Adj MS	F-Value	P-Value
Sugar Type_AL	1	0.000012	0.000012	8.17	0.046
Error	4	0.000006	0.000001		
Total	5	0.000017			

Model Summary

S	R-sq	R-sq(adj)	R-sq(pred)
0.0011900	67.12%	58.90%	26.03%

Means

Sugar Type_AL	N	Mean	StDev	95% CI
Allulose	3	0.006650	0.000920	(0.004742, 0.008558)
Lactose	3	0.009427	0.001409	(0.007519, 0.011334)

Pooled StDev = 0.00119003

Tukey Pairwise Comparisons

Grouping Information Using the Tukey Method and 95% Confidence

Sugar Type_AL	N	Mean	Grouping
Lactose	3	0.009427	A
Allulose	3	0.006650	B

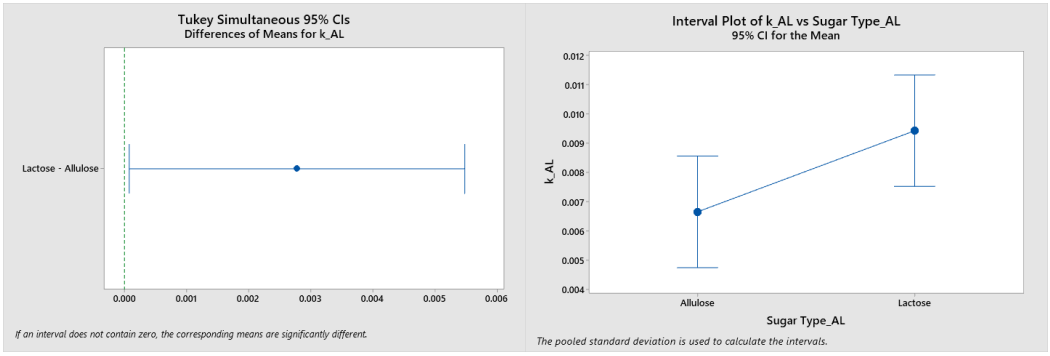

Table A 7. Normality and Equal variance tests for kinetic rate constant (k) of allulose and lactose.

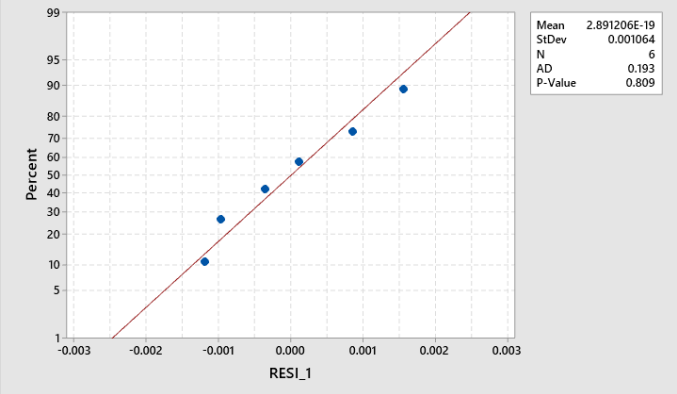

Method

Null hypothesis	All variances are equal
Alternative hypothesis	At least one variance is different
Significance level	α = 0.05

95% Bonferroni Confidence Intervals for Standard Deviations

Sugar Type_AL	N	StDev	CI
Allulose	3	0.0009199	(0.0000394, 0.084964)
Lactose	3	0.0014093	(0.0000603, 0.130157)

Individual confidence level = 97.5%

Method	Test Statistic	P-Value
Multiple comparisons	0.42	0.518
Levene	0.23	0.656

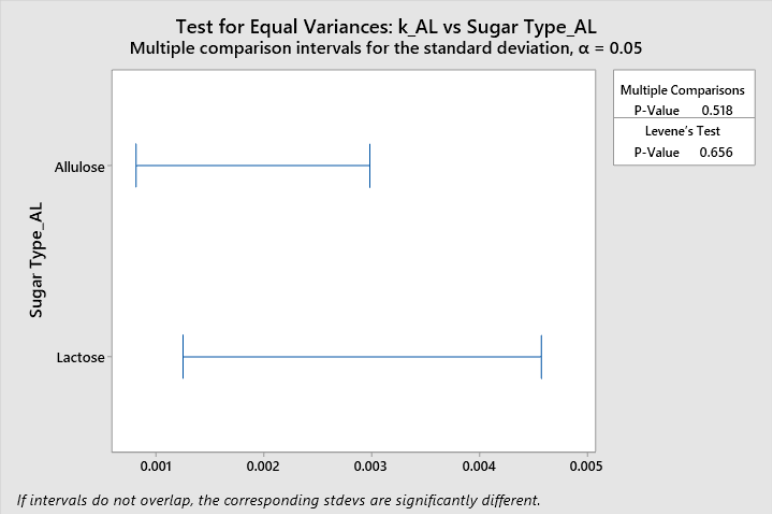

Table A 8. Analysis of Varience for kinetic rate constant (k) of fructose and glucose.

Method

Null hypothesis	All means are equal
Alternative hypothesis	Not all means are equal
Significance level	α = 0.05

Equal variances were assumed for the analysis.

Factor Information

Factor	Levels	Values
Sugar Type_FG	2	Fructose, Glucose

Analysis of Variance

Source	DF	Adj SS	Adj MS	F-Value	P-Value
Sugar Type_FG	1	0.000000	0.000000	1.41	0.301
Error	4	0.000000	0.000000		
Total	5	0.000000			

Model Summary

S	R-sq	R-sq(adj)	R-sq(pred)
0.0000203	26.07%	7.58%	0.00%

Means

Sugar Type_FG	N	Mean	StDev	95% CI
Fructose	3	0.000106	0.000020	(0.000073, 0.000138)
Glucose	3	0.000086	0.000020	(0.000053, 0.000119)

Pooled StDev = 0.0000203158

Tukey Pairwise Comparisons

Grouping Information Using the Tukey Method and 95% Confidence

Sugar Type_FG	N	Mean	Grouping
Fructose	3	0.000106	A
Glucose	3	0.000086	A

Means that do not share a letter are significantly different.

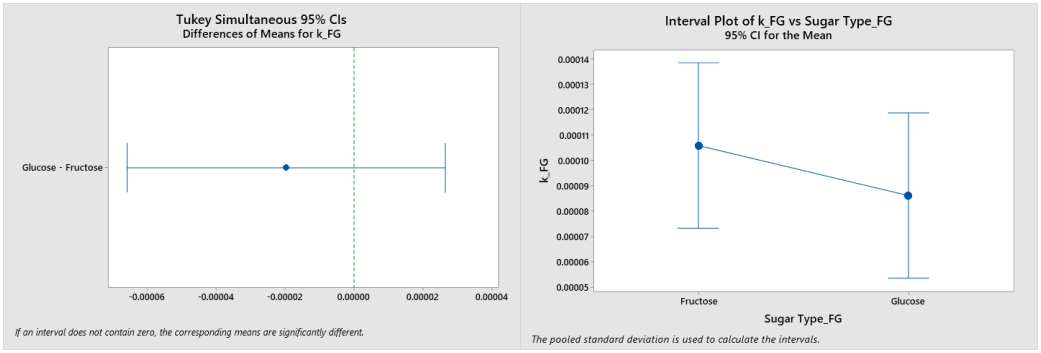

Table A 9. Normality and Equal Varience tests for kinetic rate constant (k) of fructose and glucose.

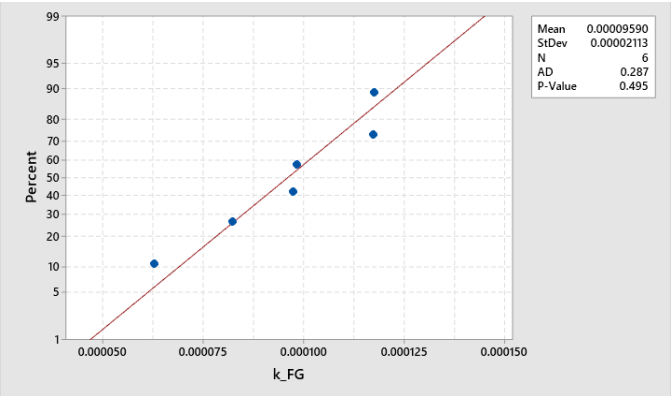

Method

Null hypothesis	All variances are equal
Alternative hypothesis	At least one variance is different
Significance level	α = 0.05

95% Bonferroni Confidence Intervals for Standard Deviations

Sugar Type_FG	N	StDev	CI
Fructose	3	0.0000203	(0.0000009, 0.0018754)
Glucose	3	0.0000203	(0.0000009, 0.0018773)

Individual confidence level = 97.5%

Method	Test Statistic	P-Value
Multiple comparisons	0.00	0.999
Levene	0.00	0.994

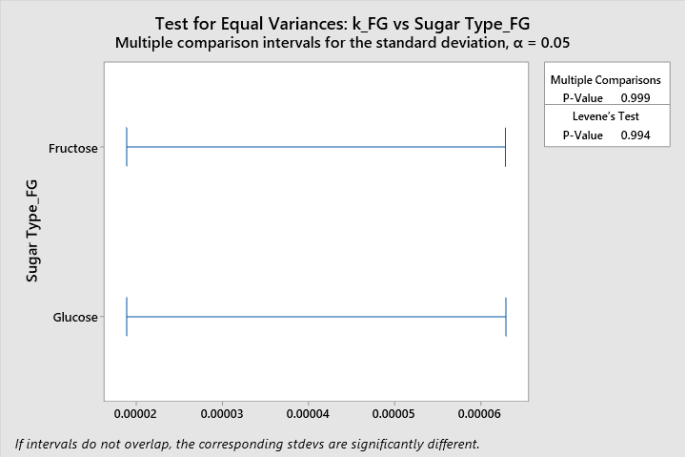

Table A 10. Analysis of Varience for A2 value of sugars.

Method

Null hypothesis	All means are equal
Alternative hypothesis	Not all means are equal
Significance level	α = 0.05

Equal variances were assumed for the analysis.

Factor Information

Factor	Levels	Values
Sugar Type	5	Allulose, Fructose, Glucose, Lactose, Sucrose

Analysis of Variance

Source	DF	Adj SS	Adj MS	F-Value	P-Value
Sugar Type	4	240.271	60.0678	359.02	0.000
Error	10	1.673	0.1673		
Total	14	241.944			

Model Summary

S	R-sq	R-sq(adj)	R-sq(pred)
0.409038	99.31%	99.03%	98.44%

Means

Sugar Type	N	Mean	StDev	95% CI
Allulose	3	12.121	0.450	(11.595, 12.647)
Fructose	3	7.132	0.247	(6.606, 7.658)
Glucose	3	9.502	0.699	(8.975, 10.028)
Lactose	3	2.2277	0.1336	(1.7015, 2.7539)
Sucrose	3	1.932	0.257	(1.405, 2.458)

Pooled StDev = 0.409038

Tukey Pairwise Comparisons

Grouping Information Using the Tukey Method and 95% Confidence

Sugar Type	N	Mean	Grouping
Allulose	3	12.121	A
Glucose	3	9.502	B
Fructose	3	7.132	C
Lactose	3	2.2277	D
Sucrose	3	1.932	D

Means that do not share a letter are significantly different.

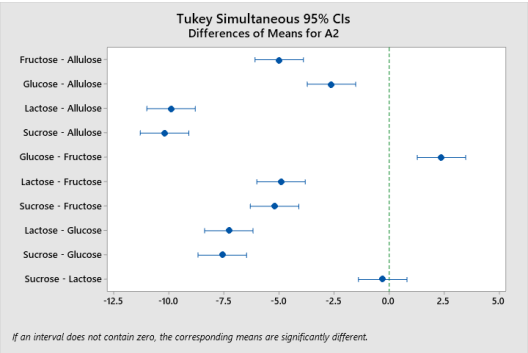

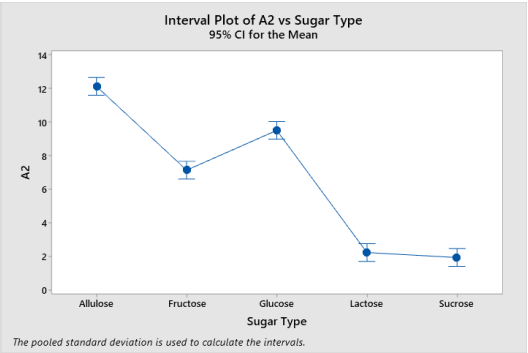

Table A 11. Normality and Equal Varience tests for A2 value of sugars.

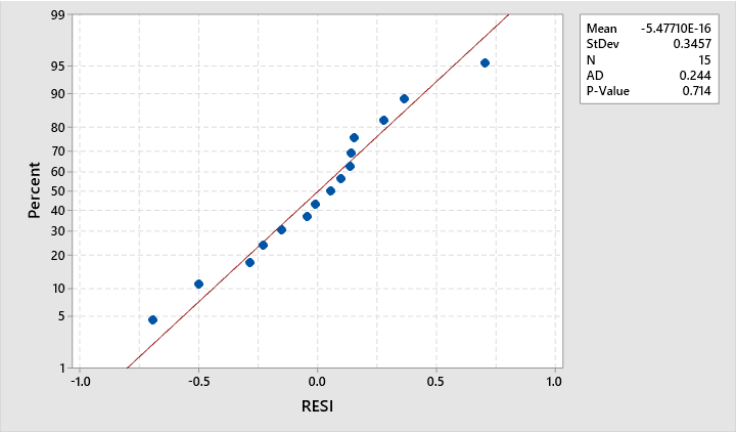

Method

Null hypothesis	All variances are equal
Alternative hypothesis	At least one variance is different
Significance level	α = 0.05

95% Bonferroni Confidence Intervals for Standard Deviations

Sugar Type	N	StDev	CI
Allulose	3	0.450031	(0.0004488, 3191.51)
Fructose	3	0.246874	(0.0002462, 1750.77)
Glucose	3	0.699353	(0.0006975, 4959.63)
Lactose	3	0.133559	(0.0001332, 947.17)
Sucrose	3	0.257204	(0.0002565, 1824.02)

Individual confidence level = 99%

Tests

Method	Test Statistic	P-Value
Multiple comparisons	—	0.258
Levene	0.95	0.477

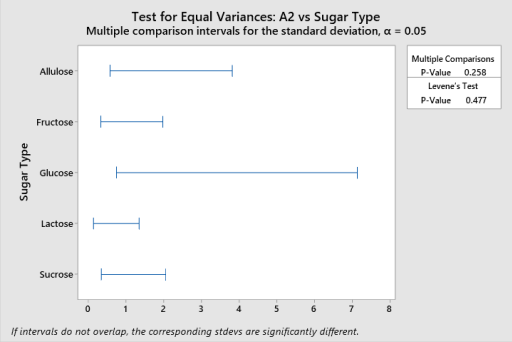

Table A 12. Analysis of Varience test for A1 value of sugars.

Method

Null hypothesis	All means are equal
Alternative hypothesis	Not all means are equal
Significance level	α = 0.05

Equal variances were assumed for the analysis.

Factor Information

Factor	Levels	Values
Sugar Type	5	Allulose, Fructose, Glucose, Lactose, Sucrose

Analysis of Variance

Source	DF	Adj SS	Adj MS	F-Value	P-Value
Sugar Type	4	910.58	227.646	69.33	0.000
Error	10	32.83	3.283		
Total	14	943.42			

Model Summary

S	R-sq	R-sq(adj)	R-sq(pred)
1.81201	96.52%	95.13%	92.17%

Means

Sugar Type	N	Mean	StDev	95% CI
Allulose	3	49.625	0.946	(47.294, 51.956)
Fructose	3	61.34	3.25	(59.01, 63.67)
Glucose	3	48.694	1.713	(46.363, 51.025)
Lactose	3	36.760	0.186	(34.429, 39.091)
Sucrose	3	50.203	1.402	(47.872, 52.534)

Pooled StDev = 1.81201

Tukey Pairwise Comparisons

Grouping Information Using the Tukey Method and 95% Confidence

Sugar Type	N	Mean	Grouping		
Fructose	3	61.34	A		
Sucrose	3	50.203		B	
Allulose	3	49.625		B	
Glucose	3	48.694		B	
Lactose	3	36.760			C

Means that do not share a letter are significantly different.

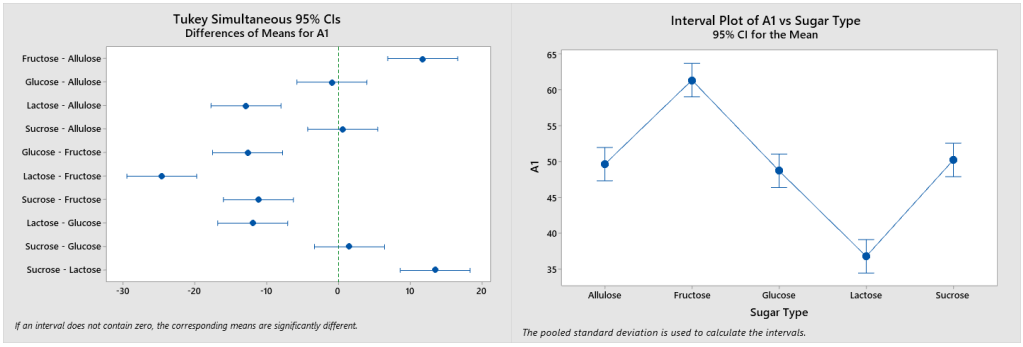

Table A 13. Normality Equal Varience tests for A1 value of sugars.

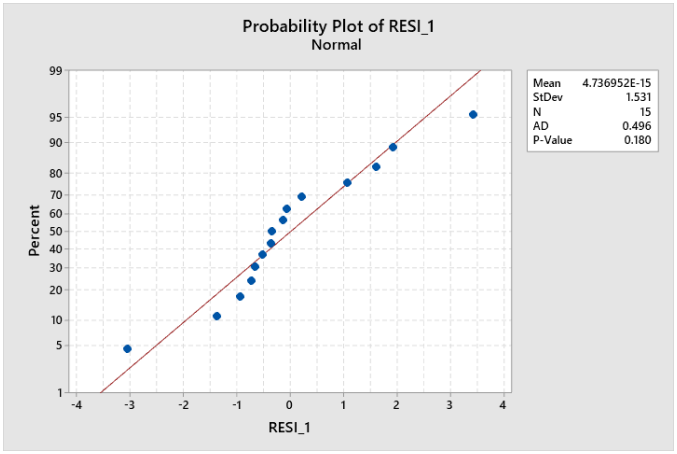

Method

Null hypothesis	All variances are equal
Alternative hypothesis	At least one variance is different
Significance level	α = 0.05

95% Bonferroni Confidence Intervals for Standard Deviations

Sugar Type	N	StDev	CI
Allulose	3	0.94570	(0.0009432, 6706.7)
Fructose	3	3.25379	(0.0032450, 23075.1)
Glucose	3	1.71323	(0.0017086, 12149.8)
Lactose	3	0.18602	(0.0001855, 1319.2)
Sucrose	3	1.40200	(0.0013982, 9942.6)

Individual confidence level = 99%

Method	Test Statistic	P-Value
Multiple comparisons	—	0.013
Levene	1.17	0.381

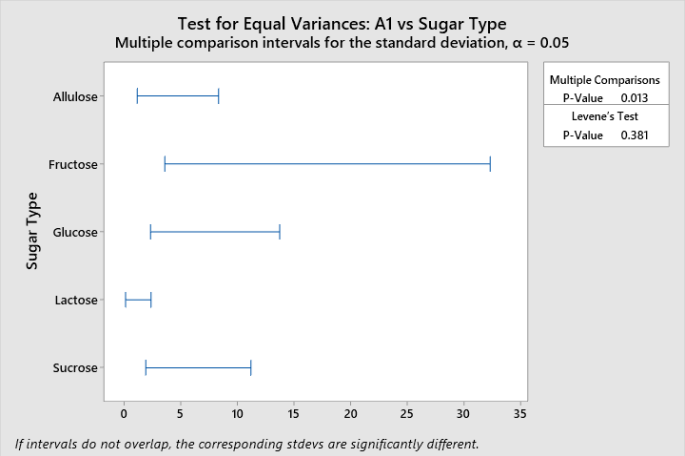

Table A 14. Analysis of Variance test for (A1-A2) value of sugars.

Method

Null hypothesis	All means are equal
Alternative hypothesis	Not all means are equal
Significance level	α = 0.05

Equal variances were assumed for the analysis.

Factor Information

Factor	Levels	Values
Sugar Type	5	Allulose, Fructose, Glucose, Lactose, Sucrose

Analysis of Variance

Source	DF	Adj SS	Adj MS	F-Value	P-Value
Sugar Type	4	808.52	202.130	53.67	0.000
Error	10	37.66	3.766		
Total	14	846.18			

Model Summary

S	R-sq	R-sq(adj)	R-sq(pred)
1.94062	95.55%	93.77%	89.99%

Means

Sugar Type	N	Mean	StDev	95% CI
Allulose	3	37.504	0.840	(35.008, 40.001)
Fructose	3	54.21	3.23	(51.71, 56.71)
Glucose	3	39.19	2.26	(36.70, 41.69)
Lactose	3	34.5326	0.1655	(32.0361, 37.0290)
Sucrose	3	48.271	1.596	(45.775, 50.768)

Pooled StDev = 1.94062

Grouping Information Using the Tukey Method and 95% Confidence

Sugar Type	N	Mean	Grouping		
Fructose	3	54.21	A		
Sucrose	3	48.271		B	
Glucose	3	39.19			C
Allulose	3	37.504			C
Lactose	3	34.5326			C

Means that do not share a letter are significantly different.

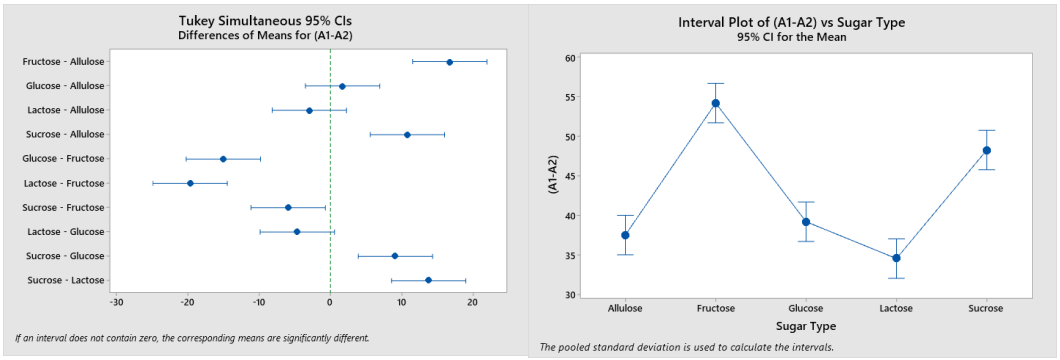

Table A 15. Normality and Equal Varience tests for (A1-A2) value of sugars.

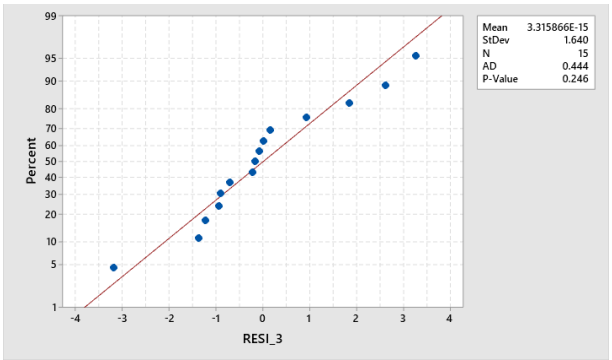

Method

Null hypothesis	All variances are equal
Alternative hypothesis	At least one variance is different
Significance level	α = 0.05

95% Bonferroni Confidence Intervals for Standard Deviations

Sugar Type	N	StDev	CI
Allulose	3	0.84035	(0.0008381, 5959.6)
Fructose	3	3.23047	(0.0032218, 22909.7)
Glucose	3	2.26096	(0.0022549, 16034.1)
Lactose	3	0.16549	(0.0001650, 1173.6)
Sucrose	3	1.59641	(0.0015921, 11321.3)

Individual confidence level = 99%

Method	Test Statistic	P-Value
Multiple comparisons	—	0.006
Levene	0.83	0.536

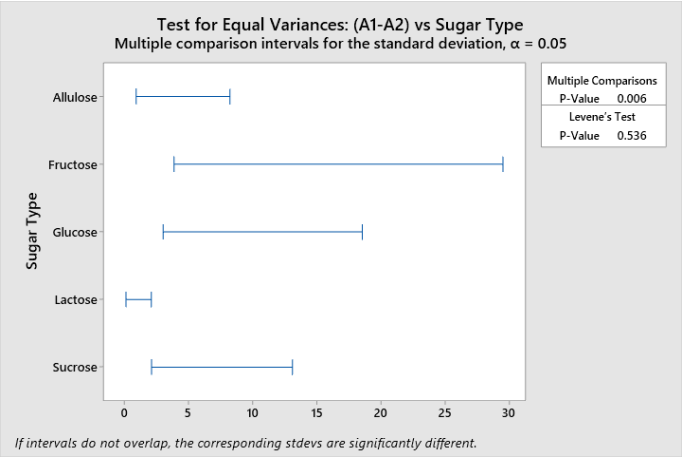

C. Use of Crystallinity Measurement Approach on Real Food Systems Statistical Analyses

Table A 16. Analysis of Variance test for surface fat content of the samples at 40% relative humidity.

Method

Null hypothesis	All means are equal
Alternative hypothesis	Not all means are equal
Significance level	$\alpha = 0.05$

Equal variances were assumed for the analysis.

Factor Information

Factor	Levels	Values
Sample	4	LF Milk Powder, Light Cheese Powder, WF Cheese Powder, WF Milk Powder

Analysis of Variance

Source	DF	Adj SS	Adj MS	F-Value	P-Value
Sample	3	0.184052	0.061351	4577.94	0.000
Error	8	0.000107	0.000013		
Total	11	0.184160			

Model Summary

S	R-sq	R-sq(adj)	R-sq(pred)
0.0036608	99.94%	99.92%	99.87%

Means

Sample	N	Mean	StDev	95% CI
LF Milk Powder	3	0.15223	0.00359	(0.14735, 0.15710)
Light Cheese Powder	3	0.014687	0.000510	(0.009813, 0.019560)
WF Cheese Powder	3	0.36243	0.00512	(0.35756, 0.36730)
WF Milk Powder	3	0.17972	0.00378	(0.17485, 0.18459)

Pooled StDev = 0.00366079

Tukey Pairwise Comparisons

Grouping Information Using the Tukey Method and 95% Confidence

Sample	N	Mean	Grouping
WF Cheese Powder	3	0.36243	A
WF Milk Powder	3	0.17972	B
LF Milk Powder	3	0.15223	C
Light Cheese Powder	3	0.014687	D

Means that do not share a letter are significantly different.

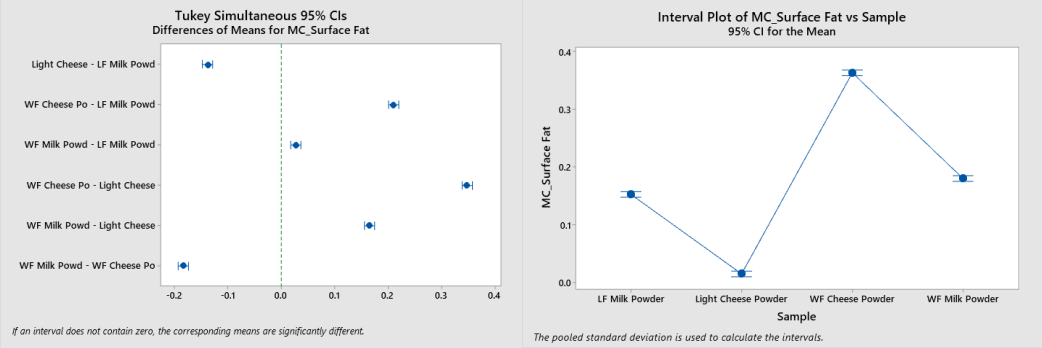

Table A 17. Normality and Equal Varience tests for surface fat content of the samples at 40% relative humidity.

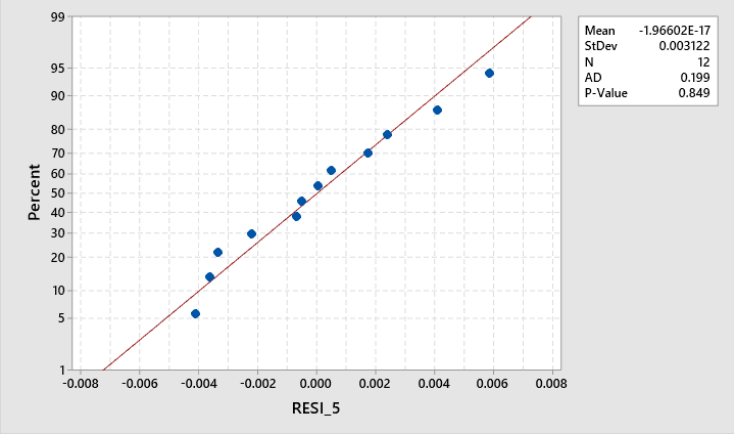

Method

Null hypothesis	All variances are equal
Alternative hypothesis	At least one variance is different
Significance level	α = 0.05

95% Bonferroni Confidence Intervals for Standard Deviations

Sample	N	StDev	CI
LF Milk Powder	3	0.0035887	(0.0000137, 5.60244)
Light Cheese Powder	3	0.0005103	(0.0000020, 0.79669)
WF Cheese Powder	3	0.0051178	(0.0000196, 7.98968)
WF Milk Powder	3	0.0037782	(0.0000145, 5.89826)

Individual confidence level = 98.75%

Method	Test Statistic	P-Value
Multiple comparisons	—	0.038
Levene	0.50	0.692

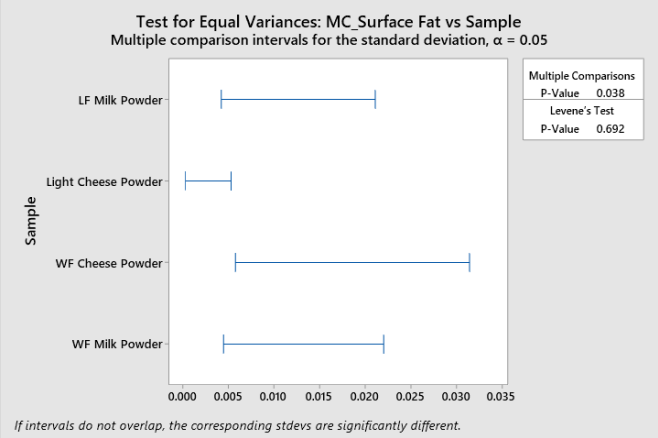

Table A 18. Analysis of Variance test for surface fat content of the samples at 50% relative humidity.

Method

Null hypothesis	All means are equal
Alternative hypothesis	Not all means are equal
Significance level	α = 0.05

Equal variances were assumed for the analysis.

Factor Information

Factor	Levels	Values
Sample	4	LF Milk Powder, Light Cheese Powder, WF Cheese Powder, WF Milk Powder

Analysis of Variance

Source	DF	Adj SS	Adj MS	F-Value	P-Value
Sample	3	0.176839	0.058946	1661.88	0.000
Error	8	0.000284	0.000035		
Total	11	0.177123			

Model Summary

S	R-sq	R-sq(adj)	R-sq(pred)
0.0059556	99.84%	99.78%	99.64%

Means

Sample	N	Mean	StDev	95% CI
LF Milk Powder	3	0.14604	0.00320	(0.13811, 0.15397)
Light Cheese Powder	3	0.014339	0.000873	(0.006410, 0.022268)
WF Cheese Powder	3	0.35479	0.01133	(0.34686, 0.36272)
WF Milk Powder	3	0.174066	0.001557	(0.166137, 0.181995)

Pooled StDev = 0.00595563

Tukey Pairwise Comparisons

Grouping Information Using the Tukey Method and 95% Confidence

Sample	N	Mean	Grouping
WF Cheese Powder	3	0.35479	A
WF Milk Powder	3	0.174066	B
LF Milk Powder	3	0.14604	C
Light Cheese Powder	3	0.014339	D

Means that do not share a letter are significantly different.

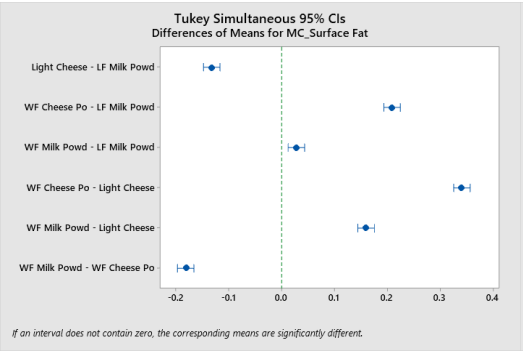

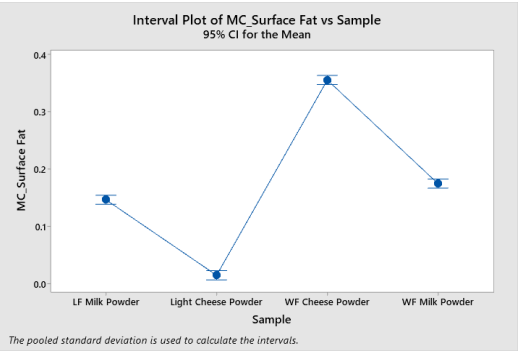

Table A 19. Normality and Equal Varience tests for surface fat content of the samples at 50% relative humidity.

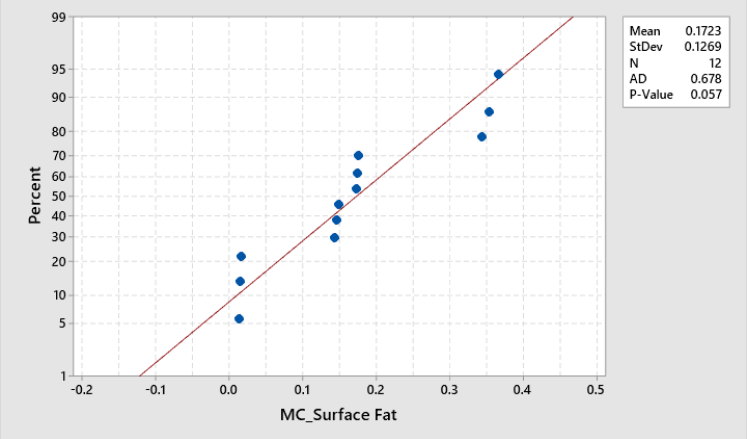

Method

Null hypothesis	All variances are equal
Alternative hypothesis	At least one variance is different
Significance level	α = 0.05

95% Bonferroni Confidence Intervals for Standard Deviations

Sample	N	StDev	CI
LF Milk Powder	3	0.0031973	(0.0000122, 4.9915)
Light Cheese Powder	3	0.0008727	(0.0000033, 1.3625)
WF Cheese Powder	3	0.0113345	(0.0000434, 17.6947)
WF Milk Powder	3	0.0015569	(0.0000060, 2.4306)

Individual confidence level = 98.75%

Method	Test Statistic	P-Value
Multiple comparisons	—	0.015
Levene	2.50	0.134

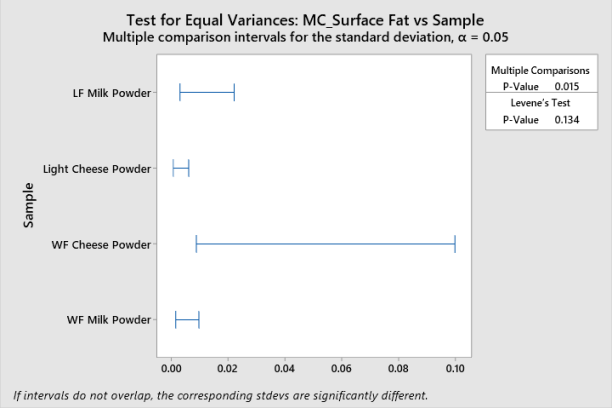

Table A 20. Analysis of Variance test for surface fat content of the samples at 60% relative humidity.

Method

Null hypothesis	All means are equal
Alternative hypothesis	Not all means are equal
Significance level	α = 0.05

Equal variances were assumed for the analysis.

Factor Information

Factor	Levels	Values
Sample	4	LF Milk Powder, Light Cheese Powder, WF Cheese Powder, WF Milk Powder

Analysis of Variance

Source	DF	Adj SS	Adj MS	F-Value	P-Value
Sample	3	0.183966	0.061322	843.44	0.000
Error	8	0.000582	0.000073		
Total	11	0.184547			

Model Summary

S	R-sq	R-sq(adj)	R-sq(pred)
0.0085267	99.68%	99.57%	99.29%

Means

Sample	N	Mean	StDev	95% CI
LF Milk Powder	3	0.14745	0.01135	(0.13610, 0.15880)
Light Cheese Powder	3	0.011451	0.001592	(0.000099, 0.022803)
WF Cheese Powder	3	0.35808	0.01242	(0.34672, 0.36943)
WF Milk Powder	3	0.19296	0.00229	(0.18161, 0.20432)

Pooled StDev = 0.00852670

Grouping Information Using the Tukey Method and 95% Confidence

Sample	N	Mean	Grouping			
WF Cheese Powder	3	0.35808	A			
WF Milk Powder	3	0.19296		B		
LF Milk Powder	3	0.14745			C	
Light Cheese Powder	3	0.011451				D

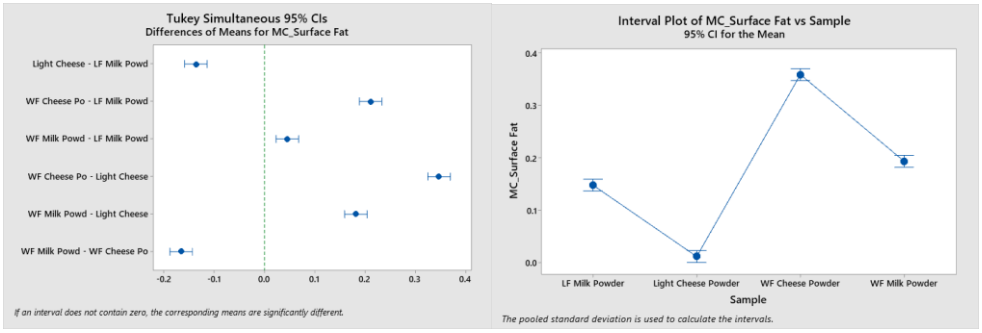

Table A 21. Normality and Equal Varience tests for surface fat content of the samples at 60% relative humidity.

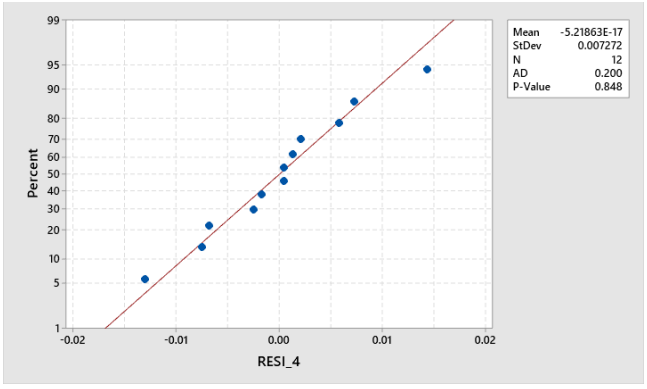

Method

Null hypothesis	All variances are equal
Alternative hypothesis	At least one variance is different
Significance level	α = 0.05

95% Bonferroni Confidence Intervals for Standard Deviations

Sample	N	StDev	CI
LF Milk Powder	3	0.0113516	(0.0000434, 17.7215)
Light Cheese Powder	3	0.0015920	(0.0000061, 2.4853)
WF Cheese Powder	3	0.0124179	(0.0000475, 19.3861)
WF Milk Powder	3	0.0022851	(0.0000087, 3.5673)

Individual confidence level = 98.75%

Method	Test Statistic	P-Value
Multiple comparisons	—	0.043
Levene	0.52	0.680

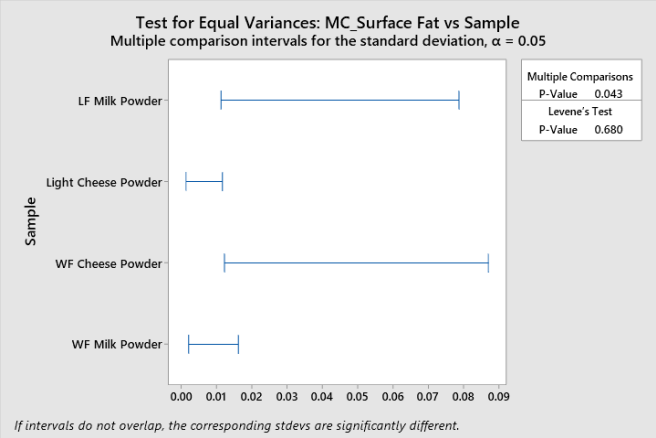

Table A 22. Analysis of Variance test for surface fat content of the samples at 70% relative humidity.

Method

Null hypothesis	All means are equal
Alternative hypothesis	Not all means are equal
Significance level	α = 0.05

Equal variances were assumed for the analysis.

Factor Information

Factor	Levels	Values
Sample	4	LF Milk Powder, Light Cheese Powder, WF Cheese Powder, WF Milk Powder

Analysis of Variance

Source	DF	Adj SS	Adj MS	F-Value	P-Value
Sample	3	0.149905	0.049968	855.61	0.000
Error	8	0.000467	0.000058		
Total	11	0.150372			

Model Summary

S	R-sq	R-sq(adj)	R-sq(pred)
0.0076420	99.69%	99.57%	99.30%

Means

Sample	N	Mean	StDev	95% CI
LF Milk Powder	3	0.129923	0.001626	(0.119749, 0.140098)
Light Cheese Powder	3	0.008203	0.000990	(-0.001971, 0.018378)
WF Cheese Powder	3	0.32159	0.01507	(0.31141, 0.33176)
WF Milk Powder	3	0.161271	0.001661	(0.151097, 0.171445)

Pooled StDev = 0.00764201

Grouping Information Using the Tukey Method and 95% Confidence

Sample	N	Mean	Grouping
WF Cheese Powder	3	0.32159	A
WF Milk Powder	3	0.161271	B
LF Milk Powder	3	0.129923	C
Light Cheese Powder	3	0.008203	D

Means that do not share a letter are significantly different.

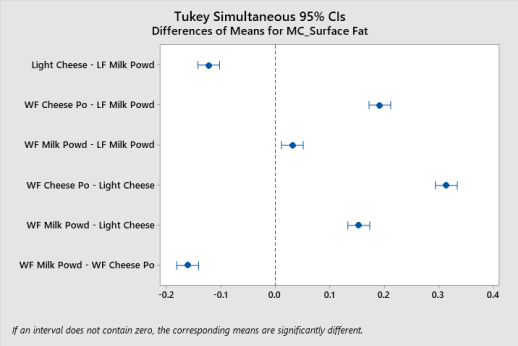

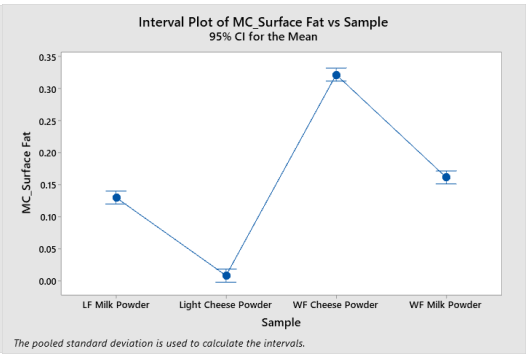

Table A 23. Normality and Equal Varience tests for surface fat content of the samples at 70% relative humidity.

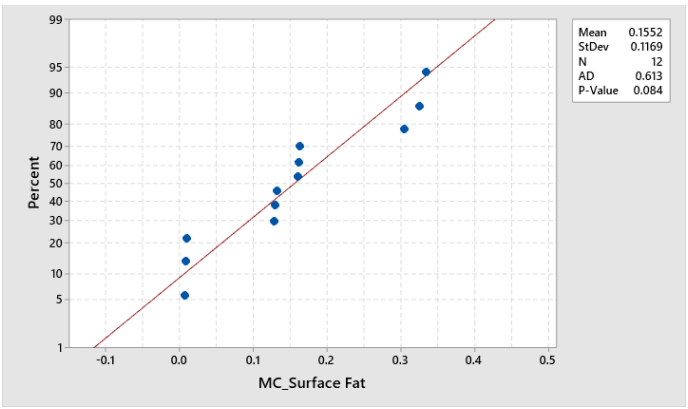

Method

Null hypothesis	All variances are equal
Alternative hypothesis	At least one variance is different
Significance level	α = 0.05

95% Bonferroni Confidence Intervals for Standard Deviations

Sample	N	StDev	CI
LF Milk Powder	3	0.0016261	(0.0000062, 2.5386)
Light Cheese Powder	3	0.0009896	(0.0000038, 1.5449)
WF Cheese Powder	3	0.0150738	(0.0000577, 23.5325)
WF Milk Powder	3	0.0016605	(0.0000064, 2.5924)

Individual confidence level = 98.75%

Method	Test Statistic	P-Value
Multiple comparisons	—	0.011
Levene	2.16	0.171

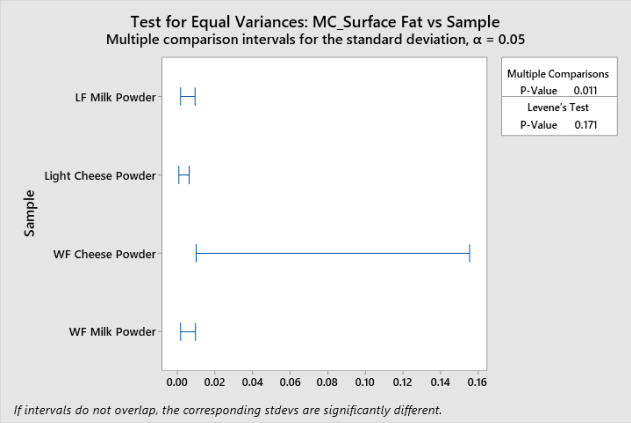

Table A 24. Analysis of Variance test for MSE crystallinity values of low fat milk powder at different relative humidity conditions.

Method

Null hypothesis	All means are equal
Alternative hypothesis	Not all means are equal
Significance level	α = 0.05

Equal variances were assumed for the analysis.

Factor Information

Factor	Levels	Values
Condition	4	40 RH, 50 RH, 60 RH, 70 RH

Analysis of Variance

Source	DF	Adj SS	Adj MS	F-Value	P-Value
Condition	3	0.002325	0.000775	23.49	0.000
Error	8	0.000264	0.000033		
Total	11	0.002589			

Model Summary

S	R-sq	R-sq(adj)	R-sq(pred)
0.0057450	89.80%	85.98%	77.06%

Means

Condition	N	Mean	StDev	95% CI
40 RH	3	0.96767	0.00477	(0.96002, 0.97532)
50 RH	3	0.97463	0.00278	(0.96698, 0.98228)
60 RH	3	0.95743	0.00439	(0.94978, 0.96508)
70 RH	3	0.93770	0.00907	(0.93005, 0.94535)

Pooled StDev = 0.00574500

Grouping Information Using the Tukey Method and 95% Confidence

Condition	N	Mean	Grouping		
50 RH	3	0.97463	A		
40 RH	3	0.96767	A	B	
60 RH	3	0.95743		B	
70 RH	3	0.93770			C

Means that do not share a letter are significantly different.

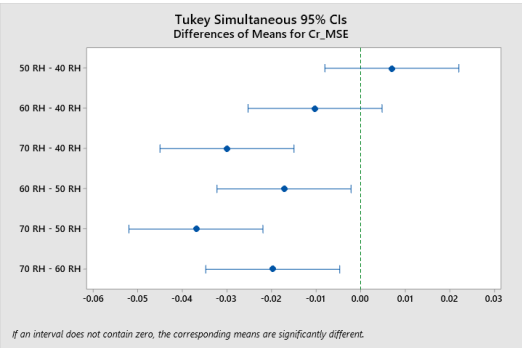

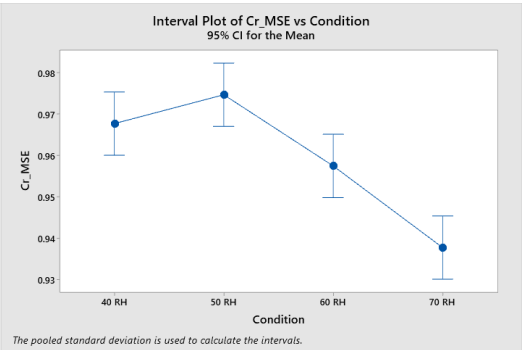

Table A 25. Normality and Equal Varience tests for MSE crystallinity values of low fat milk powder at different relative humidity conditions.

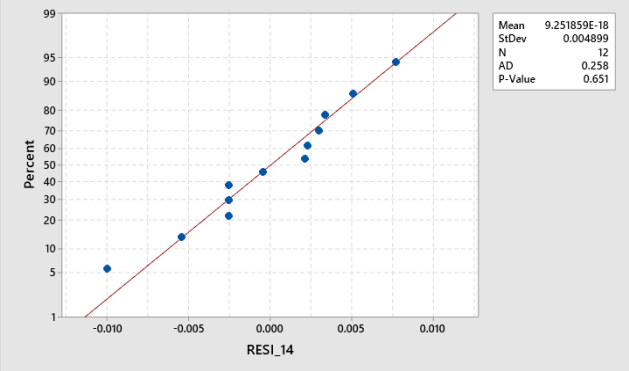

Method

Null hypothesis	All variances are equal
Alternative hypothesis	At least one variance is different
Significance level	α = 0.05

95% Bonferroni Confidence Intervals for Standard Deviations

Condition	N	StDev	CI
40 RH	3	0.0047721	(0.0000183, 7.4500)
50 RH	3	0.0027755	(0.0000106, 4.3329)
60 RH	3	0.0043879	(0.0000168, 6.8501)
70 RH	3	0.0090714	(0.0000347, 14.1618)

Individual confidence level = 98.75%

Tests

Method	Test Statistic	P-Value
Multiple comparisons	—	0.435
Levene	0.50	0.692

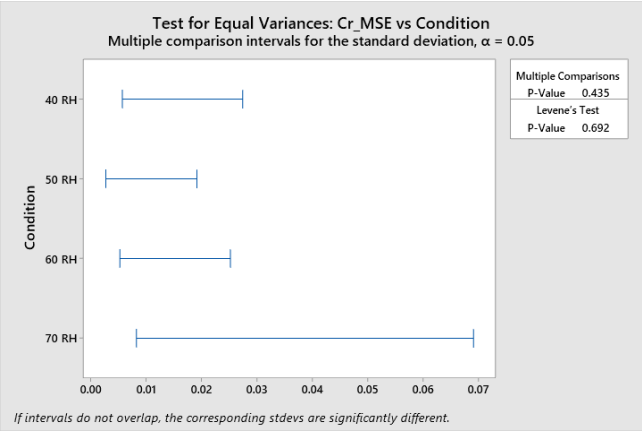

Table A 26. Analysis of Variance test for MSE crystallinity values of whole fat milk powder at different relative humidity conditions.

Method

Null hypothesis	All means are equal
Alternative hypothesis	Not all means are equal
Significance level	$\alpha = 0.05$

Equal variances were assumed for the analysis.

Factor Information

Factor	Levels	Values
Condition	4	40 RH, 50 RH, 60 RH, 70 RH

Analysis of Variance

Source	DF	Adj SS	Adj MS	F-Value	P-Value
Condition	3	0.005695	0.001898	50.73	0.000
Error	8	0.000299	0.000037		
Total	11	0.005995			

Model Summary

S	R-sq	R-sq(adj)	R-sq(pred)
0.0061175	95.01%	93.13%	88.76%

Means

Condition	N	Mean	StDev	95% CI
40 RH	3	0.94677	0.00691	(0.93862, 0.95491)
50 RH	3	0.93050	0.00649	(0.92236, 0.93864)
60 RH	3	0.91967	0.00497	(0.91152, 0.92781)
70 RH	3	0.88720	0.00593	(0.87906, 0.89534)

Pooled StDev = 0.00611753

Tukey Pairwise Comparisons

Grouping Information Using the Tukey Method and 95% Confidence

Condition	N	Mean	Grouping		
40 RH	3	0.94677	A		
50 RH	3	0.93050		B	
60 RH	3	0.91967		B	
70 RH	3	0.88720			C

Means that do not share a letter are significantly different.

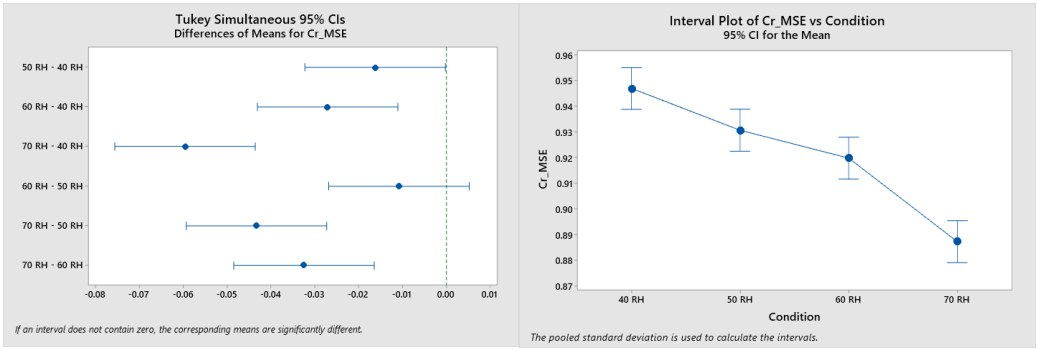

Table A 27. Normality and Equal Varience tests for MSE crystallinity values of whole fat milk powder at different relative humidity conditions.

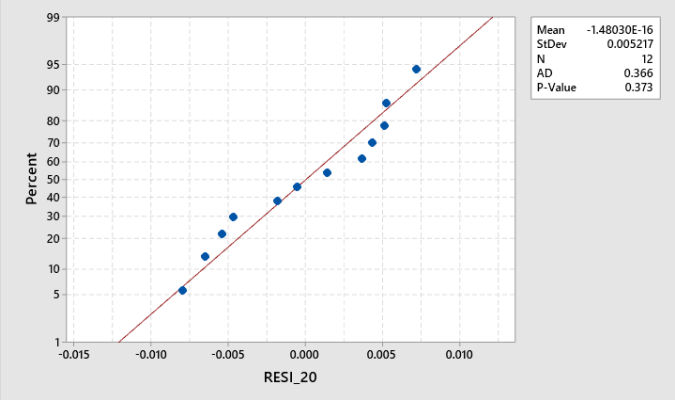

Method

Null hypothesis	All variances are equal
Alternative hypothesis	At least one variance is different
Significance level	α = 0.05

95% Bonferroni Confidence Intervals for Standard Deviations

Condition	N	StDev	CI
40 RH	3	0.0069082	(0.0000264, 10.7847)
50 RH	3	0.0064900	(0.0000248, 10.1318)
60 RH	3	0.0049743	(0.0000190, 7.7656)
70 RH	3	0.0059254	(0.0000227, 9.2504)

Individual confidence level = 98.75%

Method	Test Statistic	P-Value
Multiple comparisons	—	0.956
Levene	0.02	0.995

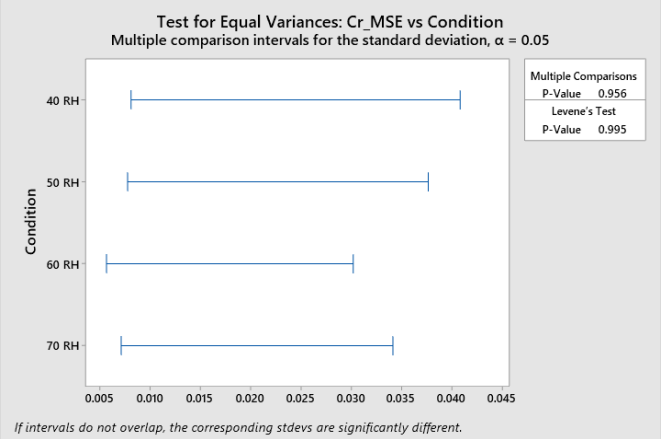

Table A 28. Analysis of Variance test for MSE crystallinity values of light cheese powder at different relative humidity conditions.

Method

Null hypothesis	All means are equal
Alternative hypothesis	Not all means are equal
Significance level	α = 0.05

Equal variances were assumed for the analysis.

Factor Information

Factor	Levels	Values
Condition	4	40 RH, 50 RH, 60 RH, 70 RH

Analysis of Variance

Source	DF	Adj SS	Adj MS	F-Value	P-Value
Condition	3	0.024041	0.008014	34.16	0.000
Error	8	0.001877	0.000235		
Total	11	0.025917			

Model Summary

S	R-sq	R-sq(adj)	R-sq(pred)
0.0153156	92.76%	90.04%	83.71%

Means

Condition	N	Mean	StDev	95% CI
40 RH	3	0.89757	0.00197	(0.87718, 0.91796)
50 RH	3	0.86913	0.00486	(0.84874, 0.88952)
60 RH	3	0.8163	0.0287	(0.7959, 0.8367)
70 RH	3	0.78257	0.00919	(0.76218, 0.80296)

Pooled StDev = 0.0153156

Tukey Pairwise Comparisons

Grouping Information Using the Tukey Method and 95% Confidence

Condition	N	Mean	Grouping
40 RH	3	0.89757	A
50 RH	3	0.86913	A
60 RH	3	0.8163	B
70 RH	3	0.78257	B

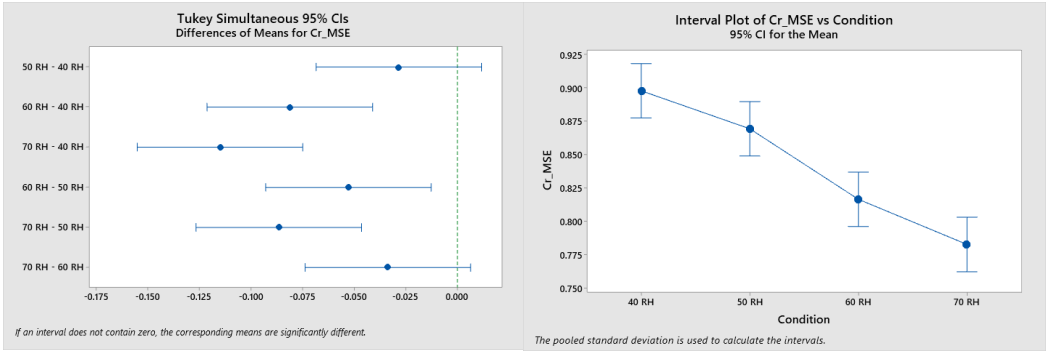

Table A 29. Normality and Equal Varience tests for MSE crystallinity values of light cheese powder at different relative humidity conditions.

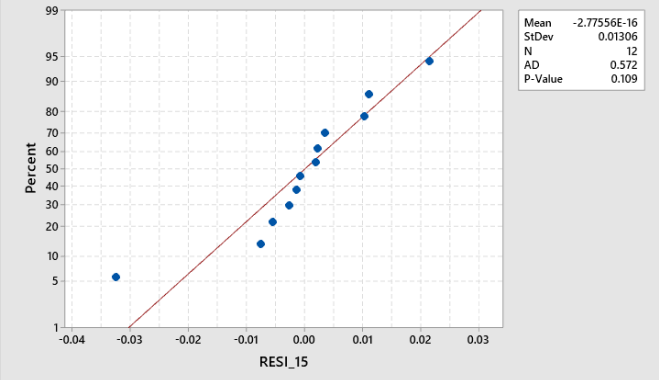

Method

Null hypothesis	All variances are equal
Alternative hypothesis	At least one variance is different
Significance level	α = 0.05

95% Bonferroni Confidence Intervals for Standard Deviations

Condition	N	StDev	CI
40 RH	3	0.0019655	(0.0000075, 3.0685)
50 RH	3	0.0048583	(0.0000186, 7.5846)
60 RH	3	0.0287448	(0.0001100, 44.8749)
70 RH	3	0.0091947	(0.0000352, 14.3544)

Individual confidence level = 98.75%

Tests

Method	Test Statistic	P-Value
Multiple comparisons	—	0.012
Levene	1.19	0.374

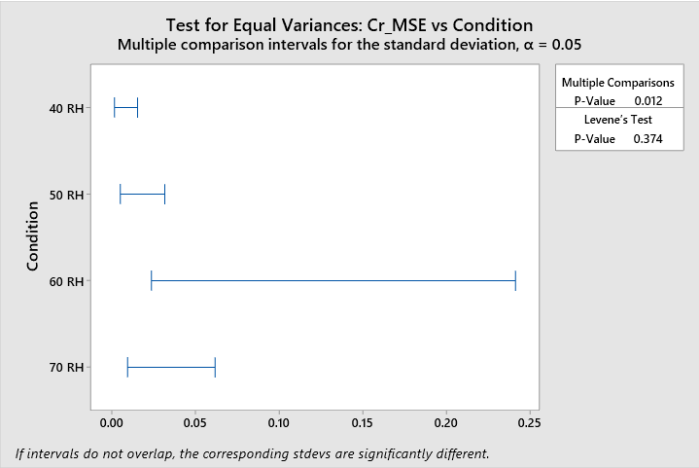

Table A 30. Analysis of Variance test for MSE crystallinity values of whole fat cheese powder at different relative humidity conditions.

Method

Null hypothesis	All means are equal
Alternative hypothesis	Not all means are equal
Significance level	α = 0.05

Equal variances were assumed for the analysis.

Factor Information

Factor	Levels	Values
Condition	4	40 RH, 50 RH, 60 RH, 70 RH

Analysis of Variance

Source	DF	Adj SS	Adj MS	F-Value	P-Value
Condition	3	0.032356	0.010785	50.75	0.000
Error	8	0.001700	0.000213		
Total	11	0.034056			

Model Summary

S	R-sq	R-sq(adj)	R-sq(pred)
0.0145780	95.01%	93.14%	88.77%

Means

Condition	N	Mean	StDev	95% CI
40 RH	3	0.88400	0.01324	(0.86459, 0.90341)
50 RH	3	0.85137	0.01651	(0.83196, 0.87078)
60 RH	3	0.81677	0.00249	(0.79736, 0.83618)
70 RH	3	0.7441	0.0199	(0.7247, 0.7635)

Pooled StDev = 0.0145780

Tukey Pairwise Comparisons

Grouping Information Using the Tukey Method and 95% Confidence

Condition	N	Mean	Grouping		
40 RH	3	0.88400	A		
50 RH	3	0.85137	A	B	
60 RH	3	0.81677		B	
70 RH	3	0.7441			C

Means that do not share a letter are significantly different.

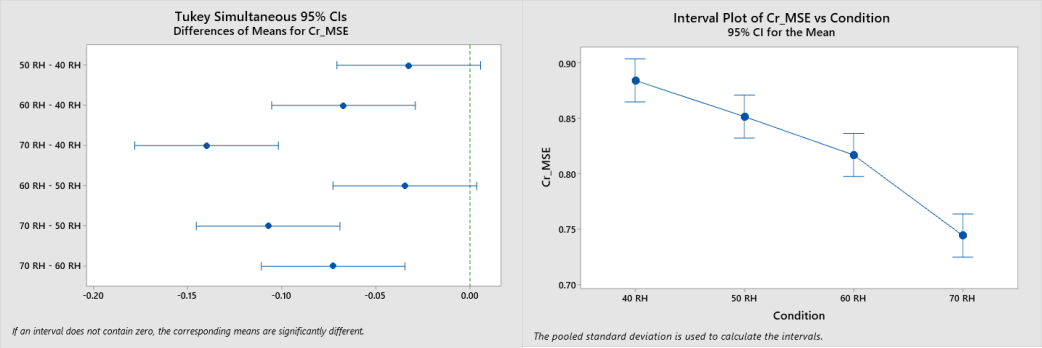

Table A 31. Normality and Equal Varience tests for MSE crystallinity values of whole fat cheese powder at different relative humidity conditions.

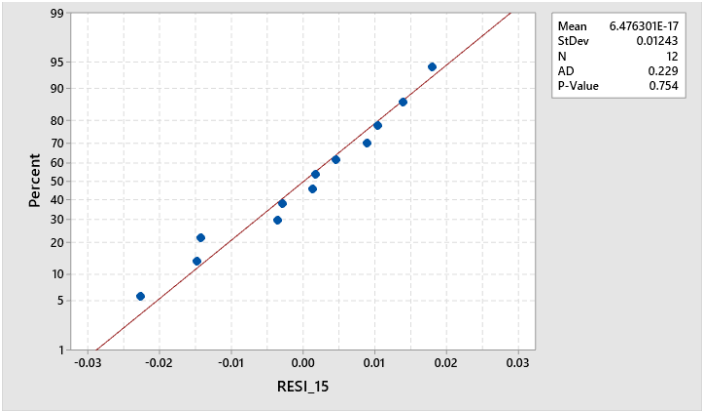

Method

Null hypothesis	All variances are equal
Alternative hypothesis	At least one variance is different
Significance level	α = 0.05

95% Bonferroni Confidence Intervals for Standard Deviations

Condition	N	StDev	CI
40 RH	3	0.0132367	(0.0000506, 20.6644)
50 RH	3	0.0165083	(0.0000632, 25.7719)
60 RH	3	0.0024906	(0.0000095, 3.8883)
70 RH	3	0.0199030	(0.0000761, 31.0715)

Individual confidence level = 98.75%

Method	Test Statistic	P-Value
Multiple comparisons	—	0.071
Levene	0.53	0.674

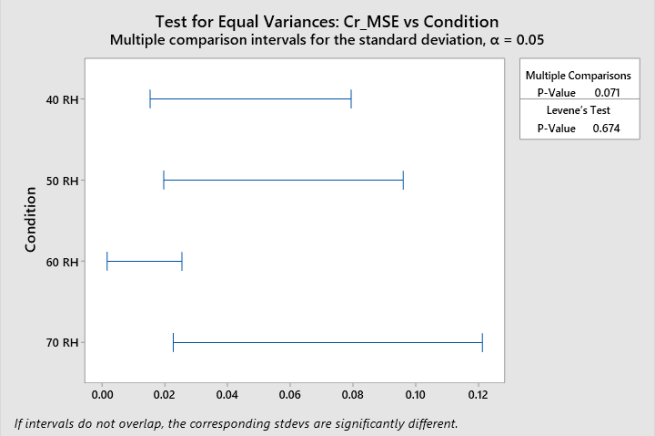

Table A 32. Analysis of Variance test for water activity values of low fat milk powder at different relative humidity conditions.

Method

Null hypothesis	All means are equal
Alternative hypothesis	Not all means are equal
Significance level	α = 0.05

Equal variances were assumed for the analysis.

Factor Information

Factor	Levels	Values
Condition	4	40 RH, 50 RH, 60 RH, 70 RH

Analysis of Variance

Source	DF	Adj SS	Adj MS	F-Value	P-Value
Condition	3	0.163772	0.054591	434.71	0.000
Error	8	0.001005	0.000126		
Total	11	0.164777			

Model Summary

S	R-sq	R-sq(adj)	R-sq(pred)
0.0112062	99.39%	99.16%	98.63%

Means

Condition	N	Mean	StDev	95% CI
40 RH	3	0.42703	0.00683	(0.41211, 0.44195)
50 RH	3	0.52517	0.01148	(0.51025, 0.54009)
60 RH	3	0.62000	0.01367	(0.60508, 0.63492)
70 RH	3	0.74307	0.01170	(0.72815, 0.75799)

Pooled StDev = 0.0112062

Grouping Information Using the Tukey Method and 95% Confidence

Condition	N	Mean	Grouping
70 RH	3	0.74307	A
60 RH	3	0.62000	B
50 RH	3	0.52517	C
40 RH	3	0.42703	D

Means that do not share a letter are significantly different.

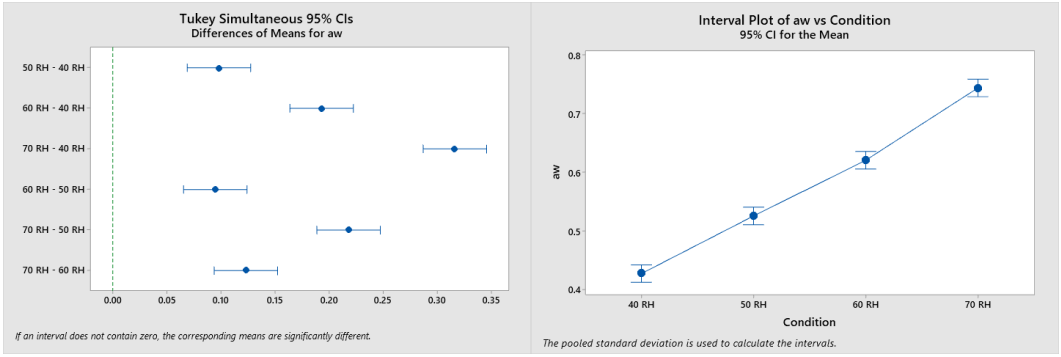

Table A 33. Normality and Equal Variance tests for water activity values of low fat milk powder at different relative humidity conditions.

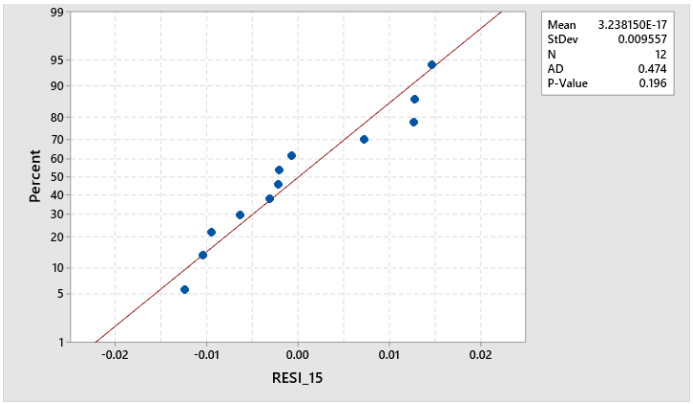

Method

Null hypothesis	All variances are equal
Alternative hypothesis	At least one variance is different
Significance level	α = 0.05

95% Bonferroni Confidence Intervals for Standard Deviations

Condition	N	StDev	CI
40 RH	3	0.0068296	(0.0000261, 10.6620)
50 RH	3	0.0114823	(0.0000439, 17.9256)
60 RH	3	0.0136715	(0.0000523, 21.3432)
70 RH	3	0.0117014	(0.0000448, 18.2676)

Individual confidence level = 98.75%

Tests

Method	Test Statistic	P-Value
Multiple comparisons	—	0.759
Levene	0.21	0.888

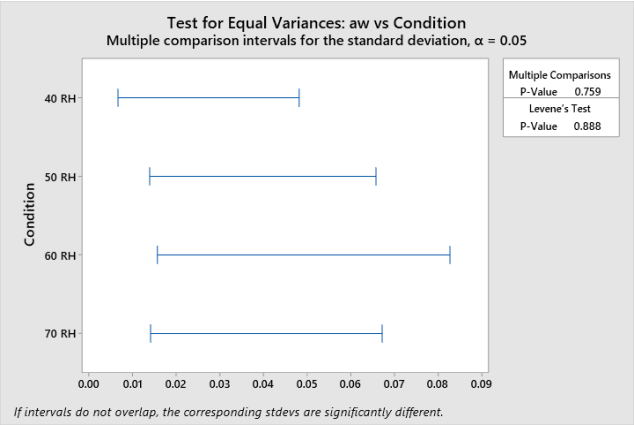

Table A 34. Analysis of Variance test for water activity values of whole fat milk powder at different relative humidity conditions.

Method

Null hypothesis	All means are equal
Alternative hypothesis	Not all means are equal
Significance level	α = 0.05

Equal variances were assumed for the analysis.

Factor Information

Factor	Levels	Values
Condition	4	40 RH, 50 RH, 60 RH, 70 RH

Analysis of Variance

Source	DF	Adj SS	Adj MS	F-Value	P-Value
Condition	3	0.166966	0.055655	942.55	0.000
Error	8	0.000472	0.000059		
Total	11	0.167438			

Model Summary

S	R-sq	R-sq(adj)	R-sq(pred)
0.0076842	99.72%	99.61%	99.37%

Means

Condition	N	Mean	StDev	95% CI
40 RH	3	0.43947	0.00320	(0.42924, 0.44970)
50 RH	3	0.53567	0.00800	(0.52544, 0.54590)
60 RH	3	0.63587	0.01264	(0.62564, 0.64610)
70 RH	3	0.757200	0.001473	(0.746969, 0.767431)

Pooled StDev = 0.00768424

Grouping Information Using the Tukey Method and 95% Confidence

Condition	N	Mean	Grouping
70 RH	3	0.757200	A
60 RH	3	0.63587	B
50 RH	3	0.53567	C
40 RH	3	0.43947	D

Means that do not share a letter are significantly different.

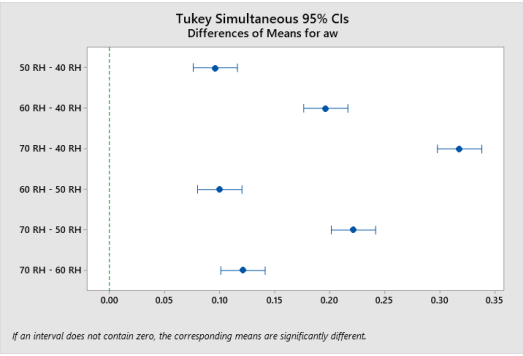

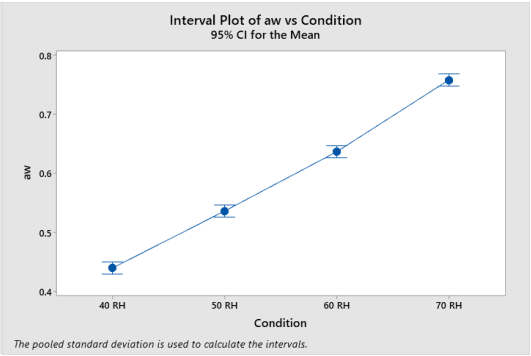

Table A 35. Normality and Equal Variance tests for water activity values of whole fat milk powder at different relative humidity conditions.

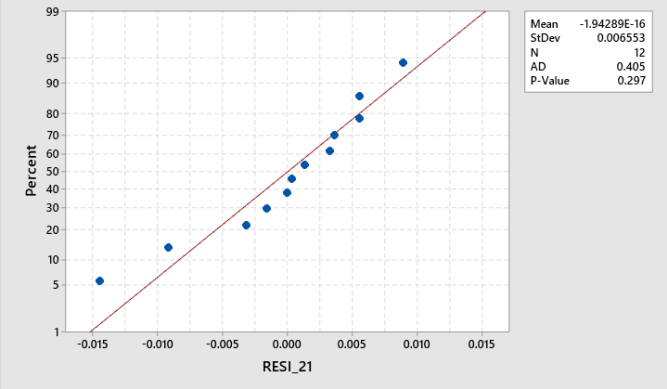

Method

Null hypothesis	All variances are equal
Alternative hypothesis	At least one variance is different
Significance level	α = 0.05

95% Bonferroni Confidence Intervals for Standard Deviations

Condition	N	StDev	CI
40 RH	3	0.0032005	(0.0000122, 4.9965)
50 RH	3	0.0079952	(0.0000306, 12.4817)
60 RH	3	0.0126433	(0.0000484, 19.7381)
70 RH	3	0.0014731	(0.0000056, 2.2997)

Individual confidence level = 98.75%

Method	Test Statistic	P-Value
Multiple comparisons	—	0.046
Levene	0.67	0.594

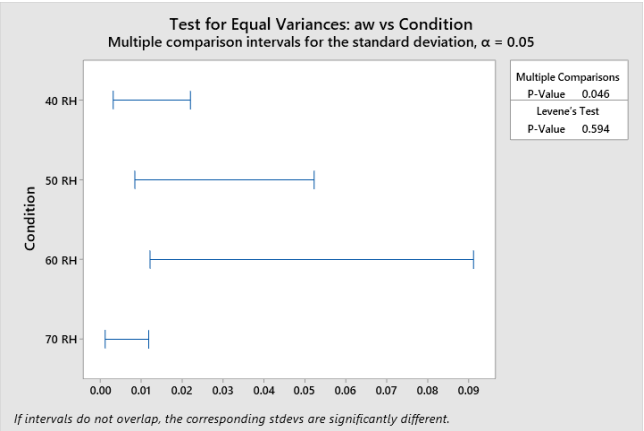

Table A 36. Analysis of Variance test for water activity values of light cheese powder at different relative humidity conditions.

Method

Null hypothesis	All means are equal
Alternative hypothesis	Not all means are equal
Significance level	$\alpha = 0.05$

Equal variances were assumed for the analysis.

Factor Information

Factor	Levels	Values
Condition	4	40 RH, 50 RH, 60 RH, 70 RH

Analysis of Variance

Source	DF	Adj SS	Adj MS	F-Value	P-Value
Condition	3	0.136749	0.045583	462.37	0.000
Error	8	0.000789	0.000099		
Total	11	0.137538			

Model Summary

S	R-sq	R-sq(adj)	R-sq(pred)
0.0099290	99.43%	99.21%	98.71%

Means

Condition	N	Mean	StDev	95% CI
40 RH	3	0.44687	0.00582	(0.43365, 0.46009)
50 RH	3	0.54707	0.00346	(0.53385, 0.56029)
60 RH	3	0.63833	0.01046	(0.62511, 0.65155)
70 RH	3	0.73467	0.01546	(0.72145, 0.74789)

Pooled StDev = 0.00992904

Grouping Information Using the Tukey Method and 95% Confidence

Condition	N	Mean	Grouping
70 RH	3	0.73467	A
60 RH	3	0.63833	B
50 RH	3	0.54707	C
40 RH	3	0.44687	D

Means that do not share a letter are significantly different.

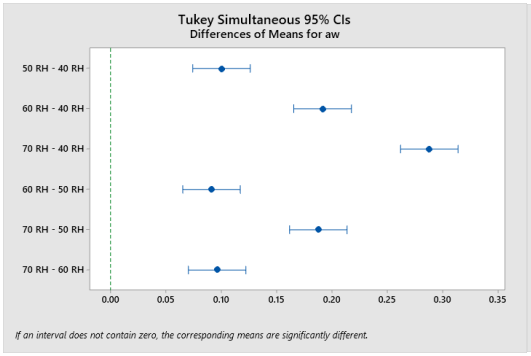

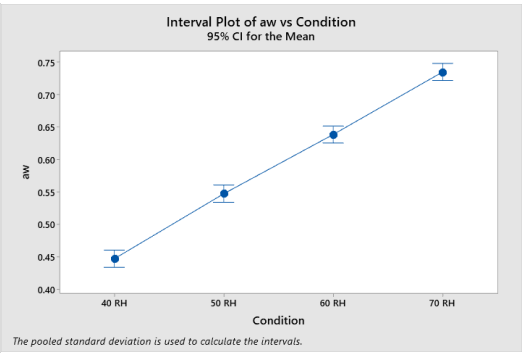

Table A 37. Normality and Equal Variance tests for water activity values of light cheese powder at different relative humidity conditions.

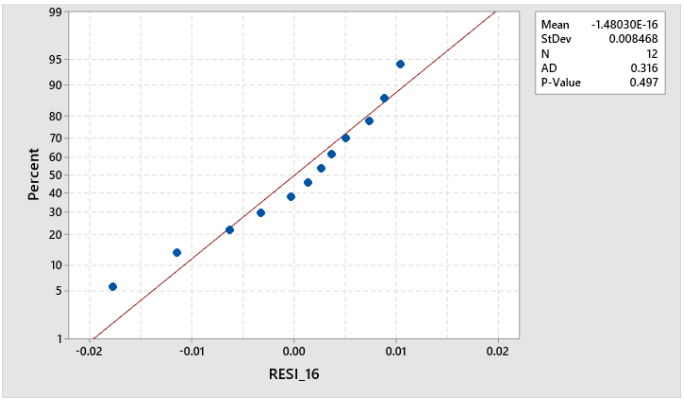

Method

Null hypothesis	All variances are equal
Alternative hypothesis	At least one variance is different
Significance level	α = 0.05

95% Bonferroni Confidence Intervals for Standard Deviations

Condition	N	StDev	CI
40 RH	3	0.0058158	(0.0000222, 9.0793)
50 RH	3	0.0034646	(0.0000133, 5.4087)
60 RH	3	0.0104582	(0.0000400, 16.3267)
70 RH	3	0.0154643	(0.0000592, 24.1420)

Individual confidence level = 98.75%

Tests

Method	Test Statistic	P-Value
Multiple comparisons	—	0.241
Levene	0.47	0.713

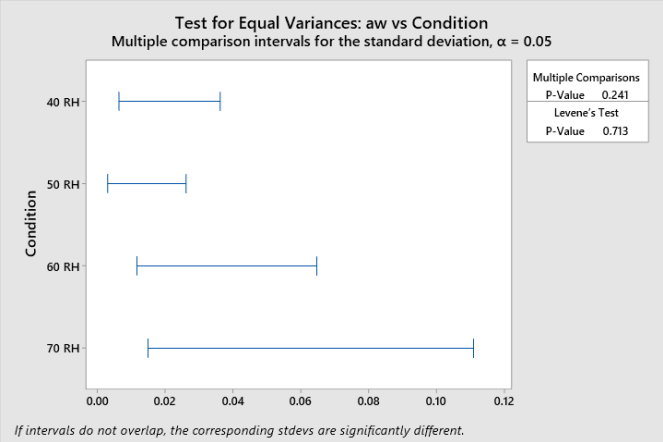

Table A 38. Analysis of Variance test for water activity values of whole fat cheese powder at different relative humidity conditions.

Method

Null hypothesis	All means are equal
Alternative hypothesis	Not all means are equal
Significance level	α = 0.05

Equal variances were assumed for the analysis.

Factor Information

Factor	Levels	Values
Condition	4	40 RH, 50 RH, 60 RH, 70 RH

Analysis of Variance

Source	DF	Adj SS	Adj MS	F-Value	P-Value
Condition	3	0.137203	0.045734	627.24	0.000
Error	8	0.000583	0.000073		
Total	11	0.137787			

Model Summary

S	R-sq	R-sq(adj)	R-sq(pred)
0.0085390	99.58%	99.42%	99.05%

Means

Condition	N	Mean	StDev	95% CI
40 RH	3	0.44410	0.00173	(0.43273, 0.45547)
50 RH	3	0.54497	0.00931	(0.53360, 0.55634)
60 RH	3	0.64177	0.00284	(0.63040, 0.65314)
70 RH	3	0.73050	0.01393	(0.71913, 0.74187)

Pooled StDev = 0.00853898

Tukey Pairwise Comparisons

Grouping Information Using the Tukey Method and 95% Confidence

Condition	N	Mean	Grouping
70 RH	3	0.73050	A
60 RH	3	0.64177	B
50 RH	3	0.54497	C
40 RH	3	0.44410	D

Means that do not share a letter are significantly different.

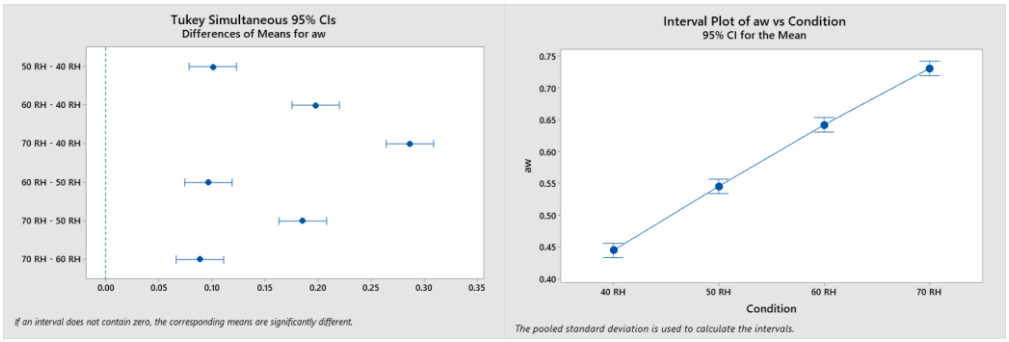

Table A 39. Normality and Equal Variance tests for water activity values of whole fat cheese powder at different relative humidity conditions.

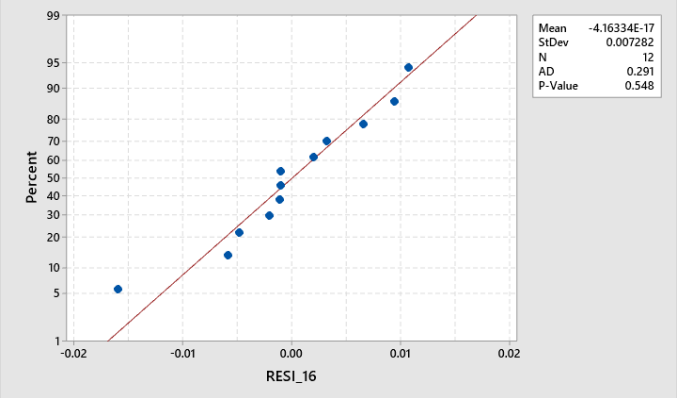

Method

Null hypothesis	All variances are equal
Alternative hypothesis	At least one variance is different
Significance level	α = 0.05

95% Bonferroni Confidence Intervals for Standard Deviations

Condition	N	StDev	CI
40 RH	3	0.0017321	(0.0000066, 2.7040)
50 RH	3	0.0093088	(0.0000356, 14.5324)
60 RH	3	0.0028361	(0.0000109, 4.4275)
70 RH	3	0.0139270	(0.0000533, 21.7420)

Individual confidence level = 98.75%

Method	Test Statistic	P-Value
Multiple comparisons	—	0.047
Levene	0.61	0.626

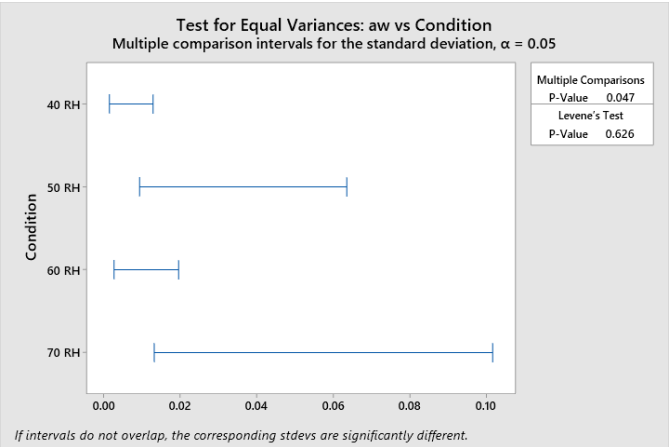

Table A 40. Analysis of Variance test for moisture content values of low fat milk powder at different relative humidity conditions.

Method

Null hypothesis	All means are equal
Alternative hypothesis	Not all means are equal
Significance level	$\alpha = 0.05$

Equal variances were assumed for the analysis.

Factor Information

Factor	Levels	Values
Condition	4	40 RH, 50 RH, 60 RH, 70 RH

Analysis of Variance

Source	DF	Adj SS	Adj MS	F-Value	P-Value
Condition	3	35.116	11.7053	42.16	0.000
Error	8	2.221	0.2776		
Total	11	37.337			

Model Summary

S	R-sq	R-sq(adj)	R-sq(pred)
0.526918	94.05%	91.82%	86.61%

Means

Condition	N	Mean	StDev	95% CI
40 RH	3	5.059	0.268	(4.358, 5.761)
50 RH	3	6.475	0.557	(5.773, 7.176)
60 RH	3	8.4407	0.1423	(7.7391, 9.1422)
70 RH	3	9.472	0.842	(8.770, 10.174)

Pooled StDev = 0.526918

Grouping Information Using the Tukey Method and 95% Confidence

Condition	N	Mean	Grouping		
70 RH	3	9.472	A		
60 RH	3	8.4407	A		
50 RH	3	6.475		B	
40 RH	3	5.059			C

Means that do not share a letter are significantly different.

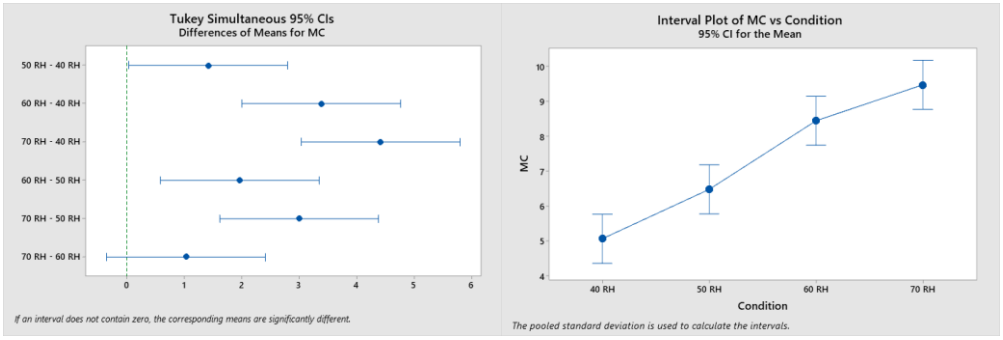

Table A 41. Normality and Equal Variance tests for moisture content values of low fat milk powder at different relative humidity conditions.

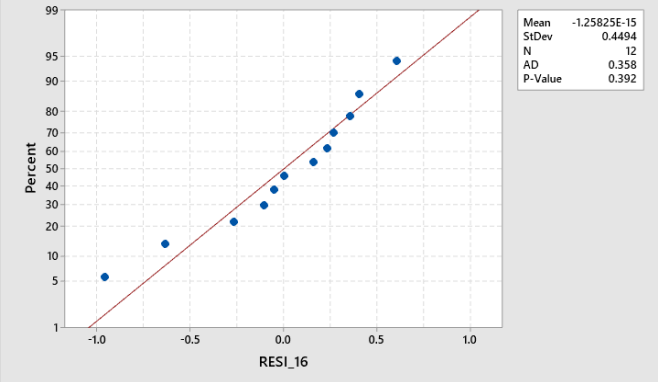

Method

Null hypothesis	All variances are equal
Alternative hypothesis	At least one variance is different
Significance level	α = 0.05

95% Bonferroni Confidence Intervals for Standard Deviations

Condition	N	StDev	CI
40 RH	3	0.267519	(0.0010235, 417.64)
50 RH	3	0.557104	(0.0021314, 869.72)
60 RH	3	0.142304	(0.0005444, 222.16)
70 RH	3	0.841660	(0.0032200, 1313.95)

Individual confidence level = 98.75%

Method	Test Statistic	P-Value
Multiple comparisons	—	0.128
Levene	0.60	0.635

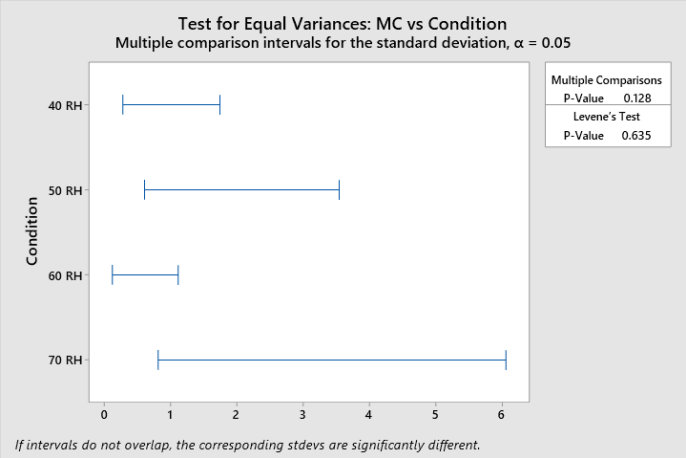

Table A 42. Analysis of Variance test for moisture content values of whole fat milk powder at different relative humidity conditions.

Method

Null hypothesis	All means are equal
Alternative hypothesis	Not all means are equal
Significance level	α = 0.05

Equal variances were assumed for the analysis.

Factor Information

Factor	Levels	Values
Condition	4	40 RH, 50 RH, 60 RH, 70 RH

Analysis of Variance

Source	DF	Adj SS	Adj MS	F-Value	P-Value
Condition	3	83.018	27.6728	49.99	0.000
Error	8	4.428	0.5536		
Total	11	87.447			

Model Summary

S	R-sq	R-sq(adj)	R-sq(pred)
0.744011	94.94%	93.04%	88.61%

Means

Condition	N	Mean	StDev	95% CI
40 RH	3	5.836	1.272	(4.845, 6.827)
50 RH	3	7.1720	0.1329	(6.1814, 8.1626)
60 RH	3	9.107	0.597	(8.116, 10.098)
70 RH	3	12.820	0.472	(11.829, 13.811)

Pooled StDev = 0.744011

Grouping Information Using the Tukey Method and 95% Confidence

Condition	N	Mean	Grouping		
70 RH	3	12.820	A		
60 RH	3	9.107		B	
50 RH	3	7.1720		B	C
40 RH	3	5.836			C

Means that do not share a letter are significantly different.

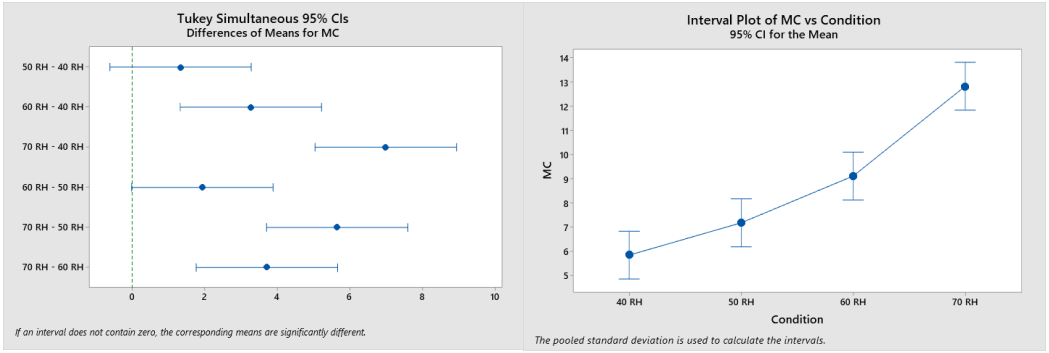

Table A 43. Normality and Equal Variance tests for moisture content values of whole fat milk powder at different relative humidity conditions.

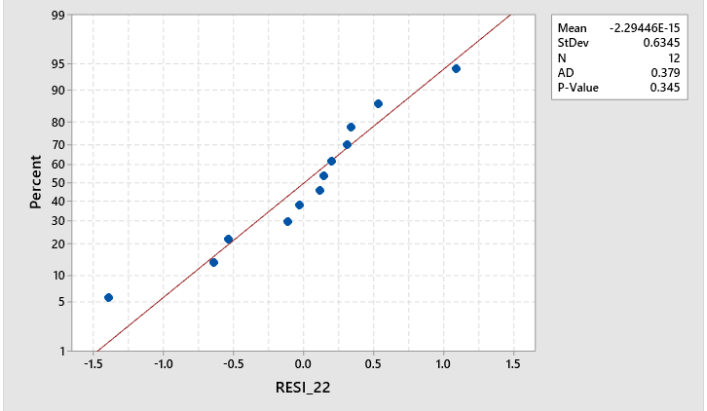

Method

Null hypothesis	All variances are equal
Alternative hypothesis	At least one variance is different
Significance level	α = 0.05

95% Bonferroni Confidence Intervals for Standard Deviations

Condition	N	StDev	CI
40 RH	3	1.27203	(0.0048665, 1985.82)
50 RH	3	0.13289	(0.0005084, 207.47)
60 RH	3	0.59658	(0.0022824, 931.35)
70 RH	3	0.47179	(0.0018049, 736.53)

Individual confidence level = 98.75%

Method	Test Statistic	P-Value
Multiple comparisons	—	0.051
Levene	1.13	0.394

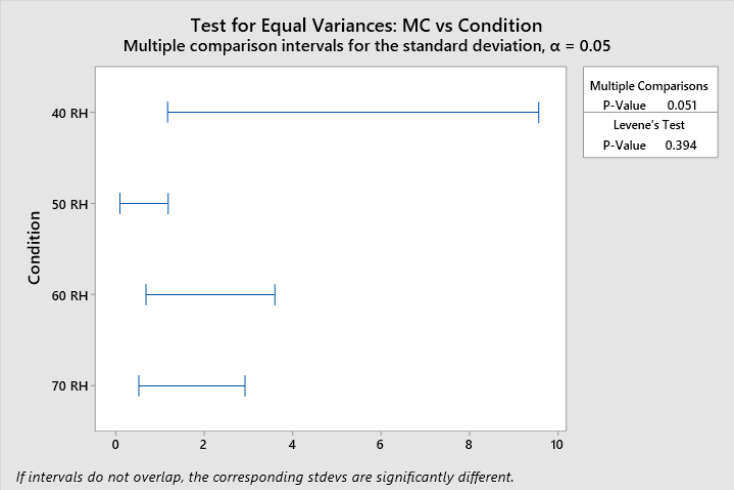

Table A 44. Analysis of Variance test for moisture content values of light cheese powder at different relative humidity conditions.

Method

Null hypothesis	All means are equal
Alternative hypothesis	Not all means are equal
Significance level	α = 0.05

Equal variances were assumed for the analysis.

Factor Information

Factor	Levels	Values
Condition	4	40 RH, 50 RH, 60 RH, 70 RH

Analysis of Variance

Source	DF	Adj SS	Adj MS	F-Value	P-Value
Condition	3	252.489	84.1629	119.22	0.000
Error	8	5.648	0.7059		
Total	11	258.136			

Model Summary

S	R-sq	R-sq(adj)	R-sq(pred)
0.840201	97.81%	96.99%	95.08%

Means

Condition	N	Mean	StDev	95% CI
40 RH	3	8.649	0.259	(7.530, 9.768)
50 RH	3	10.4940	0.1684	(9.3754, 11.6126)
60 RH	3	13.468	1.345	(12.350, 14.587)
70 RH	3	20.691	0.959	(19.573, 21.810)

Pooled StDev = 0.840201

Grouping Information Using the Tukey Method and 95% Confidence

Condition	N	Mean	Grouping		
70 RH	3	20.691	A		
60 RH	3	13.468		B	
50 RH	3	10.4940			C
40 RH	3	8.649			C

Means that do not share a letter are significantly different.

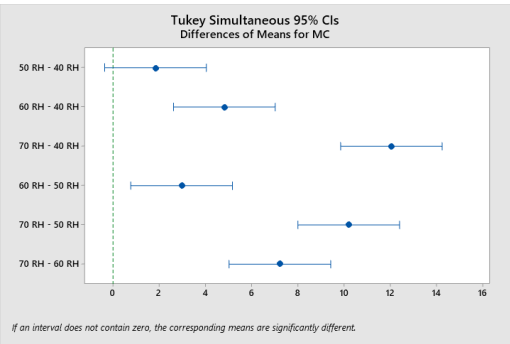

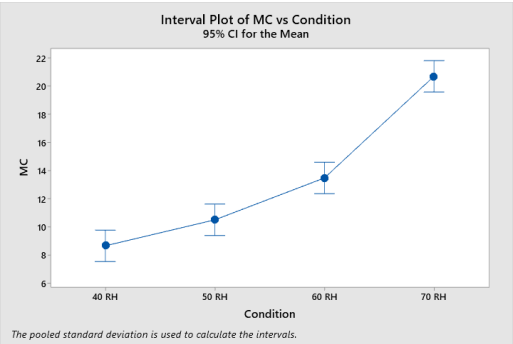

Table A 45. Normality and Equal Variance tests for moisture content values of light cheese powder at different relative humidity conditions.

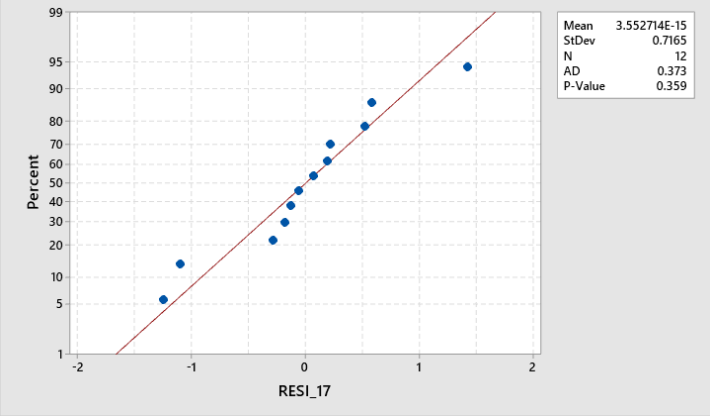

Method

Null hypothesis	All variances are equal
Alternative hypothesis	At least one variance is different
Significance level	α = 0.05

95% Bonferroni Confidence Intervals for Standard Deviations

Condition	N	StDev	CI
40 RH	3	0.25947	(0.0009927, 405.08)
50 RH	3	0.16844	(0.0006444, 262.95)
60 RH	3	1.34500	(0.0051456, 2099.74)
70 RH	3	0.95866	(0.0036676, 1496.62)

Individual confidence level = 98.75%

Tests

Method	Test Statistic	P-Value
Multiple comparisons	—	0.045
Levene	1.03	0.429

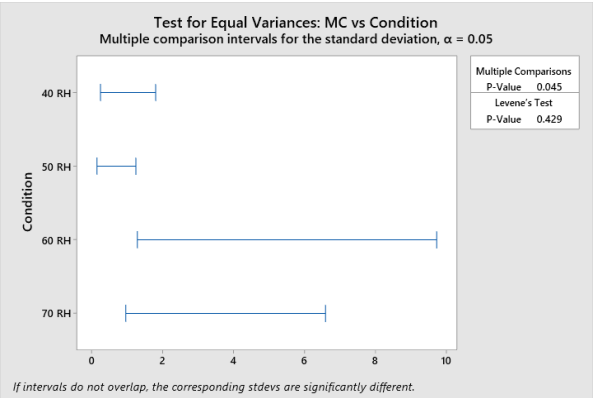

Table A 46. Analysis of Variance test for moisture content values of whole fat cheese powder at different relative humidity conditions.

Method

Null hypothesis	All means are equal
Alternative hypothesis	Not all means are equal
Significance level	$\alpha = 0.05$

Equal variances were assumed for the analysis.

Factor Information

Factor	Levels	Values
Condition	4	40 RH, 50 RH, 60 RH, 70 RH

Analysis of Variance

Source	DF	Adj SS	Adj MS	F-Value	P-Value
Condition	3	353.353	117.784	222.81	0.000
Error	8	4.229	0.529		
Total	11	357.582			

Model Summary

S	R-sq	R-sq(adj)	R-sq(pred)
0.727075	98.82%	98.37%	97.34%

Means

Condition	N	Mean	StDev	95% CI
40 RH	3	5.981	0.215	(5.013, 6.949)
50 RH	3	6.387	0.721	(5.419, 7.355)
60 RH	3	9.794	0.528	(8.826, 10.762)
70 RH	3	19.444	1.126	(18.476, 20.412)

Pooled StDev = 0.727075

Grouping Information Using the Tukey Method and 95% Confidence

Condition	N	Mean	Grouping		
70 RH	3	19.444	A		
60 RH	3	9.794		B	
50 RH	3	6.387			C
40 RH	3	5.981			C

Means that do not share a letter are significantly different.

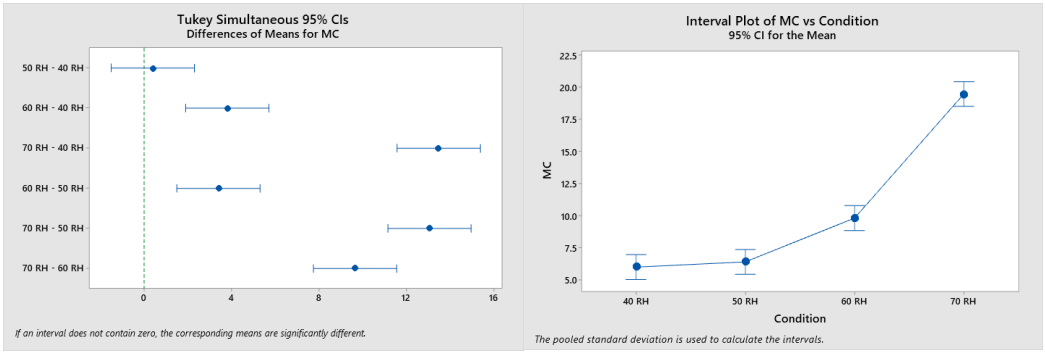

Table A 47. Normality and Equal Variance tests for moisture content values of whole fat cheese powder at different relative humidity conditions.

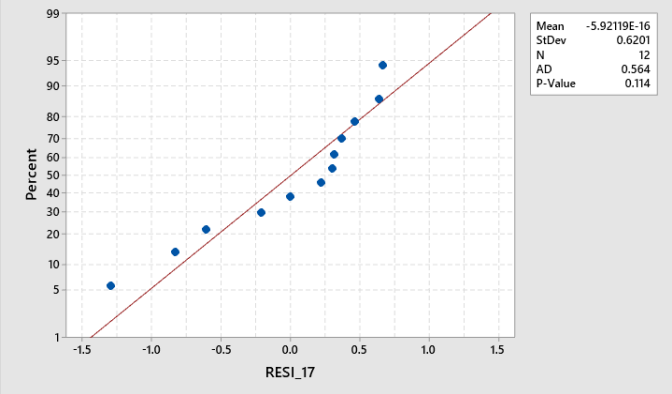

Method

Null hypothesis	All variances are equal
Alternative hypothesis	At least one variance is different
Significance level	α = 0.05

95% Bonferroni Confidence Intervals for Standard Deviations

Condition	N	StDev	CI
40 RH	3	0.21454	(0.0008208, 334.93)
50 RH	3	0.72142	(0.0027600, 1126.25)
60 RH	3	0.52832	(0.0020212, 824.79)
70 RH	3	1.12647	(0.0043096, 1758.59)

Individual confidence level = 98.75%

Method	Test Statistic	P-Value
Multiple comparisons	—	0.193
Levene	0.28	0.837

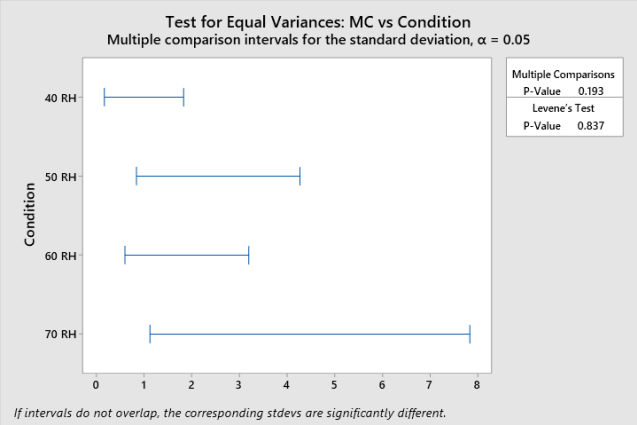

Table A 48. Analysis of Variance test for MSE crystallinity values of different samples at 40% relative humidity.

Method

Null hypothesis	All means are equal
Alternative hypothesis	Not all means are equal
Significance level	α = 0.05

Equal variances were assumed for the analysis.

Factor Information

Factor	Levels	Values
Sample	4	LF Milk Powder, Light Cheese Powder, WF Cheese Powder, WF Milk Powder

Analysis of Variance

Source	DF	Adj SS	Adj MS	F-Value	P-Value
Sample	3	0.014171	0.004724	75.71	0.000
Error	8	0.000499	0.000062		
Total	11	0.014671			

Model Summary

S	R-sq	R-sq(adj)	R-sq(pred)
0.0078989	96.60%	95.32%	92.34%

Means

Sample	N	Mean	StDev	95% CI
LF Milk Powder	3	0.96767	0.00477	(0.95715, 0.97818)
Light Cheese Powder	3	0.89757	0.00197	(0.88705, 0.90808)
WF Cheese Powder	3	0.88400	0.01324	(0.87348, 0.89452)
WF Milk Powder	3	0.94677	0.00691	(0.93625, 0.95728)

Pooled StDev = 0.00789889

Grouping Information Using the Tukey Method and 95% Confidence

Sample	N	Mean	Grouping		
LF Milk Powder	3	0.96767	A		
WF Milk Powder	3	0.94677		B	
Light Cheese Powder	3	0.89757			C
WF Cheese Powder	3	0.88400			C

Means that do not share a letter are significantly different.

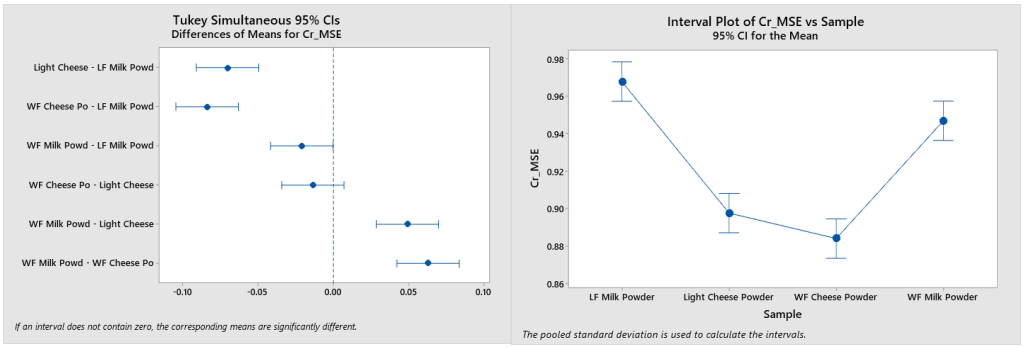

Table A 49. Normality and Equal Variance tests for MSE crystallinity values of different samples at 40% relative humidity.

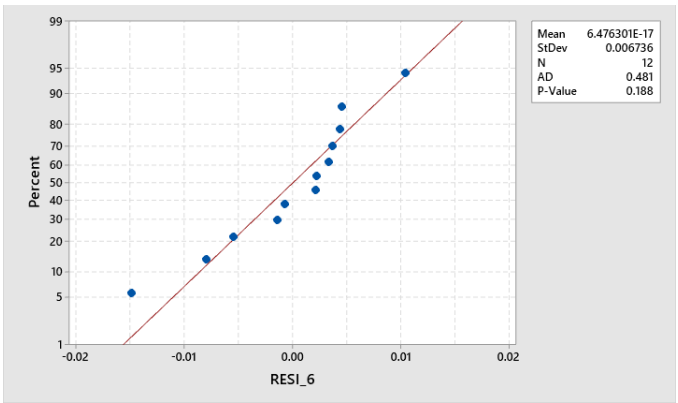

Method

Null hypothesis	All variances are equal
Alternative hypothesis	At least one variance is different
Significance level	α = 0.05

95% Bonferroni Confidence Intervals for Standard Deviations

Sample	N	StDev	CI
LF Milk Powder	3	0.0047721	(0.0000183, 7.4500)
Light Cheese Powder	3	0.0019655	(0.0000075, 3.0685)
WF Cheese Powder	3	0.0132367	(0.0000506, 20.6644)
WF Milk Powder	3	0.0069082	(0.0000264, 10.7847)

Individual confidence level = 98.75%

Method	Test Statistic	P-Value
Multiple comparisons	—	0.114
Levene	0.71	0.574

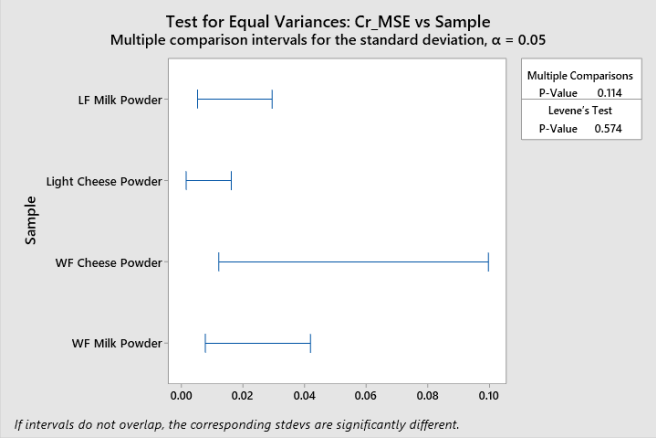

Table A 50. Analysis of Variance test for MSE crystallinity values of different samples at 50% relative humidity.

Method

Null hypothesis	All means are equal
Alternative hypothesis	Not all means are equal
Significance level	α = 0.05

Equal variances were assumed for the analysis.

Factor Information

Factor	Levels	Values
Sample	4	LF Milk Powder, Light Cheese Powder, WF Cheese Powder, WF Milk Powder

Analysis of Variance

Source	DF	Adj SS	Adj MS	F-Value	P-Value
Sample	3	0.028962	0.009654	111.62	0.000
Error	8	0.000692	0.000086		
Total	11	0.029654			

Model Summary

S	R-sq	R-sq(adj)	R-sq(pred)
0.0092999	97.67%	96.79%	94.75%

Means

Sample	N	Mean	StDev	95% CI
LF Milk Powder	3	0.97463	0.00278	(0.96225, 0.98701)
Light Cheese Powder	3	0.86913	0.00486	(0.85675, 0.88151)
WF Cheese Powder	3	0.85137	0.01651	(0.83899, 0.86375)
WF Milk Powder	3	0.93050	0.00649	(0.91812, 0.94288)

Pooled StDev = 0.00929987

Grouping Information Using the Tukey Method and 95% Confidence

Sample	N	Mean	Grouping		
LF Milk Powder	3	0.97463	A		
WF Milk Powder	3	0.93050		B	
Light Cheese Powder	3	0.86913			C
WF Cheese Powder	3	0.85137			C

Means that do not share a letter are significantly different.

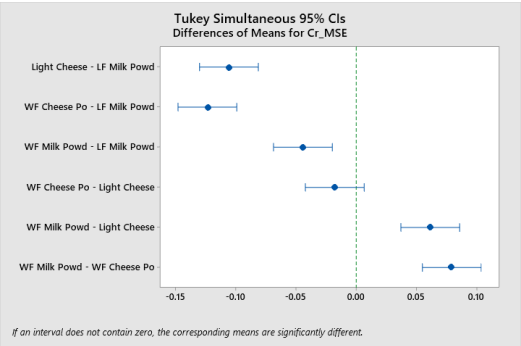

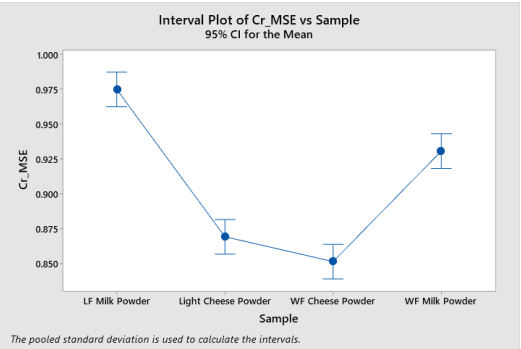

Table A 51. Normality and Equal Variance tests for MSE crystallinity values of different samples at 50% relative humidity.

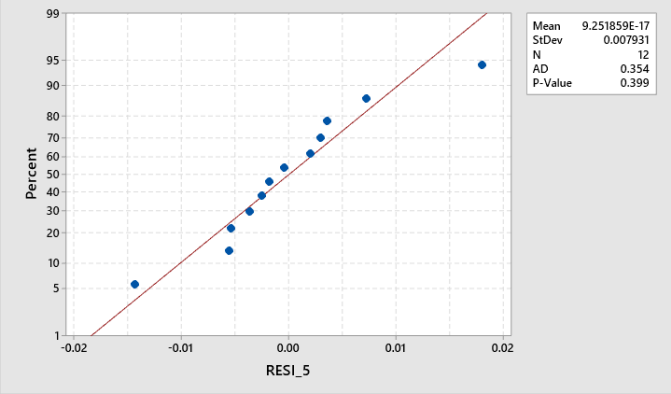

Method

Null hypothesis	All variances are equal
Alternative hypothesis	At least one variance is different
Significance level	α = 0.05

95% Bonferroni Confidence Intervals for Standard Deviations

Sample	N	StDev	CI
LF Milk Powder	3	0.0027755	(0.0000106, 4.3329)
Light Cheese Powder	3	0.0048583	(0.0000186, 7.5846)
WF Cheese Powder	3	0.0165083	(0.0000632, 25.7719)
WF Milk Powder	3	0.0064900	(0.0000248, 10.1318)

Individual confidence level = 98.75%

Method	Test Statistic	P-Value
Multiple comparisons	—	0.152
Levene	1.23	0.361

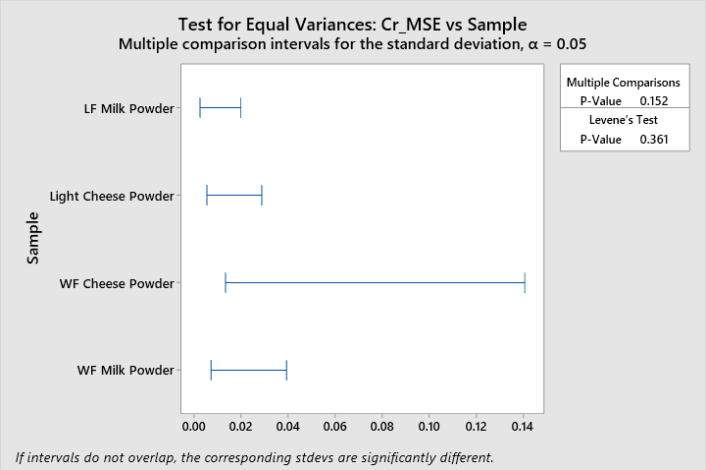

Table A 52. Analysis of Variance test for MSE crystallinity values of different samples at 60% relative humidity.

Method

Null hypothesis	All means are equal
Alternative hypothesis	Not all means are equal
Significance level	$\alpha = 0.05$

Equal variances were assumed for the analysis.

Factor Information

Factor	Levels	Values
Sample	3	Light Cheese Powder, WF Cheese Powder, WF Milk Powder

Analysis of Variance

Source	DF	Adj SS	Adj MS	F-Value	P-Value
Sample	2	0.021266	0.010633	37.21	0.000
Error	6	0.001714	0.000286		
Total	8	0.022981			

Model Summary

S	R-sq	R-sq(adj)	R-sq(pred)
0.0169037	92.54%	90.05%	83.21%

Means

Sample	N	Mean	StDev	95% CI
Light Cheese Powder	3	0.8163	0.0287	(0.7925, 0.8402)
WF Cheese Powder	3	0.81677	0.00249	(0.79289, 0.84065)
WF Milk Powder	3	0.91967	0.00497	(0.89579, 0.94355)

Pooled StDev = 0.0169037

Grouping Information Using the Tukey Method and 95% Confidence

Sample	N	Mean	Grouping	
WF Milk Powder	3	0.91967	A	
WF Cheese Powder	3	0.81677		B
Light Cheese Powder	3	0.8163		B

Means that do not share a letter are significantly different.

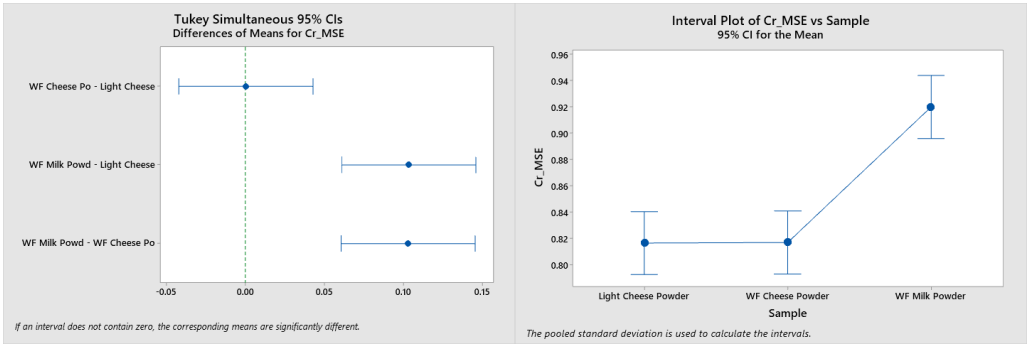

Table A 53. Normality and Equal Variance tests for MSE crystallinity values of different samples at 60% relative humidity.

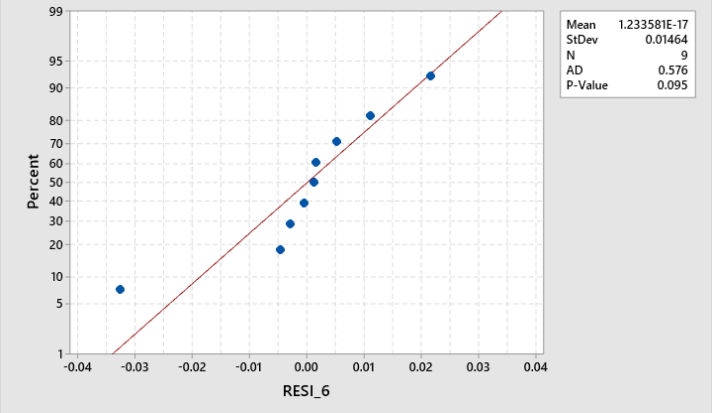

Method

Null hypothesis	All variances are equal
Alternative hypothesis	At least one variance is different
Significance level	α = 0.05

95% Bonferroni Confidence Intervals for Standard Deviations

Sample	N	StDev	CI
Light Cheese Powder	3	0.0287448	(0.0003778, 10.8272)
WF Cheese Powder	3	0.0024906	(0.0000327, 0.9381)
WF Milk Powder	3	0.0049743	(0.0000654, 1.8736)

Individual confidence level = 98.3333%

Tests

Method	Test Statistic	P-Value
Multiple comparisons	—	0.012
Levene	1.39	0.319

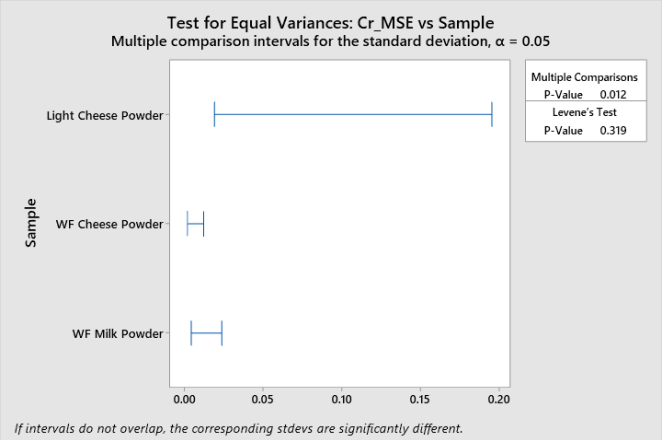

Table A 54. Analysis of Variance test for MSE crystallinity values of different samples at 70% relative humidity.

Method

Null hypothesis	All means are equal
Alternative hypothesis	Not all means are equal
Significance level	α = 0.05

Equal variances were assumed for the analysis.

Factor Information

Factor	Levels	Values
Sample	4	LF Milk Powder, Light Cheese Powder, WF Cheese Powder, WF Milk Powder

Analysis of Variance

Source	DF	Adj SS	Adj MS	F-Value	P-Value
Sample	3	0.072752	0.024251	162.19	0.000
Error	8	0.001196	0.000150		
Total	11	0.073948			

Model Summary

S	R-sq	R-sq(adj)	R-sq(pred)
0.0122278	98.38%	97.78%	96.36%

Means

Sample	N	Mean	StDev	95% CI
LF Milk Powder	3	0.93770	0.00907	(0.92142, 0.95398)
Light Cheese Powder	3	0.78257	0.00919	(0.76629, 0.79885)
WF Cheese Powder	3	0.7441	0.0199	(0.7278, 0.7604)
WF Milk Powder	3	0.88720	0.00593	(0.87092, 0.90348)

Pooled StDev = 0.0122278

Grouping Information Using the Tukey Method and 95% Confidence

Sample	N	Mean	Grouping
LF Milk Powder	3	0.93770	A
WF Milk Powder	3	0.88720	B
Light Cheese Powder	3	0.78257	C
WF Cheese Powder	3	0.7441	D

Means that do not share a letter are significantly different.

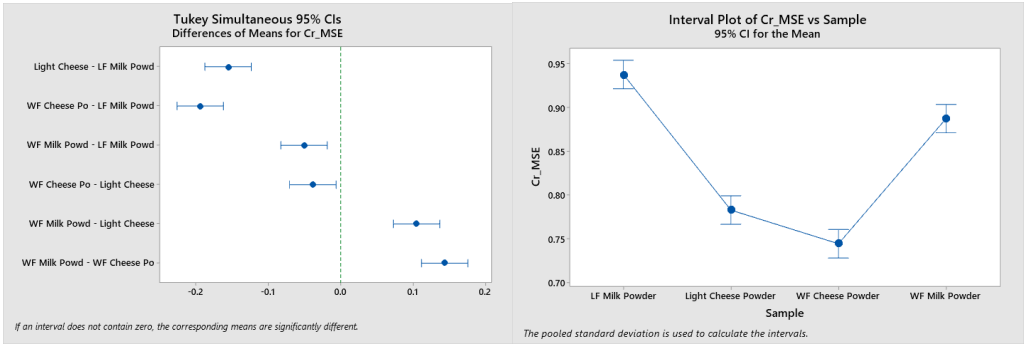

Table A 55. Normality and Equal Variance tests for MSE crystallinity values of different samples at 70% relative humidity.

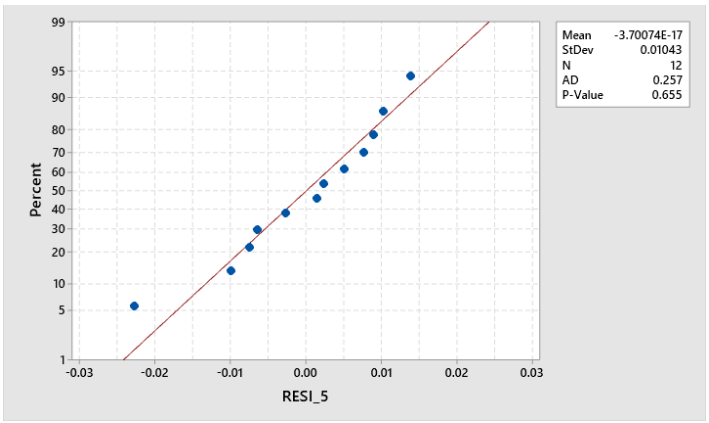

Method

Null hypothesis	All variances are equal
Alternative hypothesis	At least one variance is different
Significance level	α = 0.05

95% Bonferroni Confidence Intervals for Standard Deviations

Sample	N	StDev	CI
LF Milk Powder	3	0.0090714	(0.0000347, 14.1618)
Light Cheese Powder	3	0.0091947	(0.0000352, 14.3544)
WF Cheese Powder	3	0.0199030	(0.0000761, 31.0715)
WF Milk Powder	3	0.0059254	(0.0000227, 9.2504)

Individual confidence level = 98.75%

Tests

Method	Test Statistic	P-Value
Multiple comparisons	—	0.420
Levene	0.41	0.751

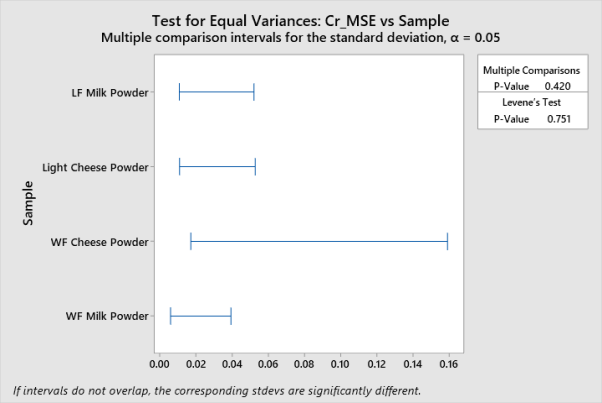

CURRICULUM VITAE (ONLY FOR DOCTORAL THESIS)

Surname, Name: Güner, Selen

EDUCATION

Degree	Institution	Year of Graduation
MS	METU Food Engineering	2016
BS	METU Food Engineering	2013
High School	Ankara Atatürk High School, Ankara	2007

FOREIGN LANGUAGES

Advanced English

PUBLICATIONS

Guner, S., & Oztop, M. H. (2017). Food grade liposome systems: Effect of solvent, homogenization types and storage conditions on oxidative and physical stability. Colloids and Surfaces A: Physicochemical and Engineering Aspects, 513. https://doi.org/10.1016/j.colsurfa.2016.11.022

Kirtil, E., Dag, D., Guner, S., Unal, K., & Oztop, M. H. (2017). Dynamics of unloaded and green tea extract loaded lecithin based liposomal dispersions investigated by nuclear magnetic resonance T2 relaxation. Food Research International. https://doi.org/10.1016/j.foodres.2017.06.064

Yildiz, E., Guner, S., Sumnu, G., Sahin, S., & Oztop, M. H. (2018). Monitoring the Effects of Ingredients and Baking Methods on Quality of Gluten-Free Cakes by Time-Domain (TD) NMR Relaxometry. Food and Bioprocess Technology, 11(10), 1923–1933. https://doi.org/10.1007/s11947-018-2152-z

Grunin, L., Oztop, M. H., Guner, S., & Baltaci, S. F. (2019). Exploring the crystallinity of different powder sugars through solid echo and magic sandwich echo sequences. Magnetic Resonance in Chemistry, 607–615. https://doi.org/10.1002/mrc.4866

Dag, D., Guner, S., & Oztop, M. H. (2019). Physicochemical mechanisms of different biopolymers' (lysozyme, gum arabic, whey protein, chitosan) adsorption on green tea extract loaded liposomes. International Journal of Biological Macromolecules, 138, 473–482. https://doi.org/10.1016/j.ijbiomac.2019.07.106

Guner, S., Grunin, L., Sumnu, S. G., & Halil, M. (2021). Use of Solid Echo Sequence to Monitor Crystallization Kinetics of Mono and Di-Saccharides. Food Biophysics, 0123456789. https://doi.org/10.1007/s11483-021-09688-6